THE UNIVERSITY OF HULL

An Investigation of Chemiluminescent Miniaturised Analytical Systems

Being a Thesis submitted for the Degree of

Doctor of Philosophy

In the University of Hull

by

Lorna Nelstrop BSc MSc

(June 2000)

ACKNOWLEDGEMENTS

I would like to thank my supervisor, Dr. Gillian Greenway, for her continued help, enthusiasm and encouragement throughout the development of this project and thesis. I would also like to acknowledge my industrial supervisor, Dr. Simon Port, BNFL Springfields, for his help and enthusiasm and Dr. Tom McCreedy, my study advisor, for his willingness to help and his constant stream of new and good ideas.

This project was supported by a SAC studentship from the RSC and a case award from BNFL.

Thanks must go to the technical staff, especially Terry Aspinall and Mike Bailey in the glass blowing workshop, John Clachananan and Nigel in the mechanical and electrical workshops respectively. I would especially like to thank members of the analytical research group at Hull, past and present, in particular Natalie Wilson, but also George Doku, Peter Petsul and Dr. Kalin Stoyanov for his help with experimental design.

Special thanks are due to Mum, Andrew and James for their encouragement and for believing in me. Finally to Tony Walmsley, Abi Webster, Sue Neville, Gareth Owen, Steve Todd, Emma Ironside, Steve Briggs and Katie Beverley: thanks for putting up with me!

CONTENTS

ABSTRACT

This thesis examines the feasibility of using chemiluminescence (CL) for detection in miniaturised analytical systems. The aim of this project was to design a miniaturised device that could potentially be used for the remote sensing of metal ions.

The development of miniaturised analytical devices for use with two well known chemiluminescent reactions; namely the tris(2,2'-bipyridyl)ruthenium (II) reaction and the luminol reaction, for the detection and quantification of codeine and cobalt (II) respectively are discussed.

Chapter 1 introduces the concept, the manufacture, operating principles and applications of miniaturised analytical systems, while the use of chemiluminescence, its requirements and applications as a sensitive, selective yet simple method of detection are reviewed in chapter 2.

Chapter 3 describes the manufacture and development of the robust and practical miniaturised analytical devices used for the analyses described in chapters 4 and 5.

Several novel developments are described in this chapter. These included the use of thicker top plates that enable the reservoirs to be contained within the single unit structure. This design was intended to prolong the lifetime of the chip system and increase the available reagent volumes. A microwave furnace for thermal bonding of the two glass plates was also used and the detection of the chemiluminesence produced in the chip system was carried out from underneath the chip base.

Chapter 4 details the application of the tris(2,2'-bipyridyl)ruthenium (II) (TBR) for analysis in a miniaturised analytical system. This reaction was selected as a model chemiluminescence reaction for the optimisation of the detection system in order to measure the very low levels of light produced. The incorporation of non-ionic surfactants into the analysis and their effect on the enhancement of the chemiluminescence emission intensity and the modification of electroosmotic flow is discussed.

A quantitative analysis of codeine was then successfully performed using this set-up. The points for the codeine concentrations of $5x10^{-7}$ to $1x10^{-4}$ mol l^{-1} were plotted to give a linear calibration plot. The equation of the line was $y = 6.0136x + 0.0949$, $R^2 = 0.9999$, where x was the codeine concentration in mol l^{-1} and y was the mean CL emission intensity in mV. A limit of detection for codeine was determined at the 95% confidence limits to be $8.3x10^{-7}$ mol l^{-1} codeine, with an RSD of 8% (n=5) at the $5x10^{-5}$ mol l^{-1} level. The sample throughput time including removal of products and water wash was found to be an average of 2 minutes.

The work described in chapter 5 builds on the findings of chapter 4 and examines the use of the luminol reaction in a miniaturised analysis system for the quantification of cobalt (II) ions.

A multivariate experimental design programme was carried out as part of the work described in this chapter to simultaneously optimise most of the reagent variables. The application of cationic surfactants to this reaction in the miniaturised analysis system is

also discussed, with particular emphasis on the observed enhancement of chemiluminescence emission intensity and lifetime, and the modification of the electroosmotic flow characteristics.

A quantitative determination of cobalt nitrate was successfully carried out with a calibration over six orders of magnitude. The equation of the linear portion of the graph (10^{-10} – 10^{-8} mol l^{-1}) was found to be $y = 64.625x + 735.71$ with $R^2 = 0.999$, where x (n=3) was the concentration in mol l^{-1} and y was the mean CL emission in mV. The limit of detection for cobalt nitrate at the 95% confidence limits was determined as ~$4x10^{-11}$ mol l^{-1} which equates to 0.01 ng ml^{-1} cobalt nitrate.

An RSD of 6.9% (n=3) was obtained for the $1x10^{-8}$ mol l^{-1} standard. The sample run time was approximately 12 minutes, which resulted in an average overall throughput time of 15 minutes.

The conclusions and ideas for future work are detailed in chapter 6.

1. Introduction to miniaturised analysis

1.1. Origins of miniaturisation in chemical systems: the concept for miniaturisation

The total analytical approach, which considers all steps in the analytical process and their ultimate affect on the quality of data produced, is now a very well established concept[1]. Although such a system is often fully automated and capable of producing reproducible analysis data, it is often lengthy, non-selective and can require high reagent consumption. The detector in a total analytical system (TAS) does not have to be very selective as potential matrix interferents are removed in the sample pre-treatment step. A sensor on the other hand usually exhibits good selectivity in a complex sample matrix for a single analyte or limited number of analytes.

It was proposed in 1990[2] by the group at Ciba-Geigy[2-5] that a total analytical system which carried out all sample handing steps close to the place of measurement be termed a μTAS (miniaturised total analysis system), a term which had been introduced at the Transducers '89 conference in Montreux[6]. The response time of a μTAS was deemed to be that of a sensor, though allowing the detection of more than one analyte. The ideal concept of a μTAS would include all the components contained in a conventional analytical instrument, but it would allow the user to take this technology virtually anywhere and perform analysis at the sample source[2].

1.1.1. History of the concept

Miniaturisation of chemical systems has become possible through technology developed in the microelectronics industry over the last 30 years[7]. Micromachining involves the

surface treatment of a solid material to obtain mechanical microstructures by film deposition, photolithography, etching and bonding[3,8]. The first reported use of this technology for analytical measurement was by Terry and Jarman[9] who devised a miniaturised gas chromatograph on a five inch, silicon wafer. Although Terry and co-workers were well ahead of their time, the trend did not take off until capillary electrophoresis (CE) and in particular, the potential of electroosmotic flow (EOF) was realised.

The main aims of miniaturised analysis technology are to provide equal analytical performance to conventional laboratory based equipment, while enabling rapid analysis away from the laboratory at the site of sample acquisition. In addition these devices should be essentially self-contained, requiring very little if any additional reagents or external equipment. Aside from the obvious advantages of reduced sample and reagent volumes and faster analysis times, there are other potential benefits associated with the high surface-to-volume ratio found in miniaturised chemical systems. Macro-scale processes limited by mass or heat transfer can be particularly efficient in narrow channels[10], in addition the laminar flow profile often observed in a miniaturised channel requires less energy which further increases cost saving. The net output can be increased, by combining multiple analysis or reactor systems in parallel, to produce a system that allows easy maintenance and with an output that can be tailored to suit required demand.

The eventual aim of miniaturised analysis systems is that these devices should be cost effective and disposable systems for rapid, accurate environmental, clinical and biochemical analysis. Current miniaturised analytical applications reported in the literature include environmental analysis of substances such as phosphates[11] and nitrites[12]

in water samples; clinical determination of amino acids[13], blood glucose[14,15], glucose and lactate[16] measurements; DNA analysis and PCR amplification[17-20], which are all described further in section 1.3.3.3.

1.1.2. Flow Injection Analysis (FIA)

Traditional FIA is a simple, low cost analytical method for sample mixing. A sample plug is injected into a flowing carrier stream, which then often merges with another reagent stream at a pre-determined point. Dispersion of the plug and chemical interaction of the sample and reagent(s) takes place as the fluid moves towards the detector. The mixing is usually very reproducible and good results are obtained.

The main disadvantages of macro scale FIA, such as high reagent volumes and large amounts of waste, are overcome by miniaturisation, thus many miniaturised chemical analysis systems quoted in the literature make use of a modified version of the FIA concept. These so called μFIA systems[11,12, 21-23] utilise either miniaturised pumps and valves for liquid manipulation, or dispense with moving parts altogether by propelling the reagents using electroosmotic flow (EOF). Electrophoresis is a related form of fluid manipulation also employed in miniaturised chemical analysis systems, whereby the ionic components are separated according to their charge and size as the sample plug migrates along a capillary. Electrophoresis and electroosmotic flow are defined and discussed fully in section 1.3.1.

1.2. Fabrication of miniaturised analysis systems

This section will focus on the methods of miniaturised analysis system fabrication, which lead to the production of a self-contained miniaturised unit for use in chemical synthesis or analysis. In particular, choices of substrate, fabrication methods and the type of designs commonly fabricated by specific methods will be discussed.

1.2.1. Substrates

The most widely used substrates for miniaturised chemical systems to date have been quartz, modified silicon and glass[11,12,24-30], however recently certain polymers, elastomers and plastics[31-33] have been utilised. The choice of substrate depends on many factors; cost, fabrication method, type of chemistry to be used in the finished system as well as the manifold design and the injection and detection systems to be employed. Although silicon would seem a good choice for the mass fabrication of nano and micrometer structures such as those used in integrated circuit technology, it is a conductor with a hydrophobic surface which therefore requires surface modification before it will support electroosmotic flow (EOF) as explained in section 1.3. Due to its relative low cost and good mechanical and chemical properties, silicon-coated surfaces (usually with SiO_2 or Si_3N_4) have been shown to support EOF in a miniaturised system[21,30]. However, the quality of the oxide film used was shown in both cases to be the limiting factor with respect to the voltage range that could be used in these systems.

Glass and silica are perhaps the most common choices as substrates in miniaturised chemical technology[11,12,21,24-28], due to their good optical properties, their ease of use for photolithography and wet-etch fabrication techniques and their ability to support EOF

without pre-treatment due to the presence of readily ionisable surface silanol groups. A range of glass types has been successfully used in chip production, including pyrex[27], sodalime[28] and Crown[11,12,27]. Miniaturised chemical systems manufactured from glass are generally robust and can be successfully used for both electroosmotic and electrophoretic driven systems. The miniaturised chemical systems can be sealed to form the channels using various bonding methods. Thermal bonding[11,12,21,25,26] is popular for glass-glass systems, although apparently the technique is not always reliable. Anodic bonding[30,34] can be used to covalently bond two surfaces (usually glass and silicon) together by means of electrostatic attraction, while silicon fusion bonding[35] can be employed to bond two slightly-oxidised silicon surfaces together at high temperatures. Using adhesives is also another option[36], although the types of suitable adhesives are limited when direct contact with chemical solutions is required. Thermal or anodic bonding techniques produce more robust structures.

Quartz (fused silica) is an alternative substrate to glass for use in miniaturised analysis systems. Conventional photolithography and wet-etching techniques can be employed for use with quartz substrates, although the etch rate for quartz is substantially slower than that observed in a glass substrate with the same etch dimensions[37], accompanied by significant undercutting of the metal etch mask. Higher temperatures of approximately 1000°C are required to successfully thermally bond quartz substrates. Quartz, however shows low thermal conductivity and does not absorb in the UV region, hence has the potential advantage, when used in optical detection systems, of much improved signal to noise ratios. This can be seen in miniaturised analytical systems employing fluorescence detection[37,38].

The polymer systems reported in the literature include two part elastomers such as polydimethyl siloxane (PDMS)[31,32] and single component plastics, for example polymethylmethacrylate (PMMA)[33,34], which can also be used as a positive photoresist, polycarbonate (PC)[35,36] and polystyrene (PS)[36,37].

1.2.2. Production methods

This section will be divided into the photolithography and wet-etching procedure used for glass, silica or quartz substrates and other fabrication techniques employed for use with different substrates.

1.2.2.1. Photolithography and wet-etching

This process is shown schematically in figure 1.1.

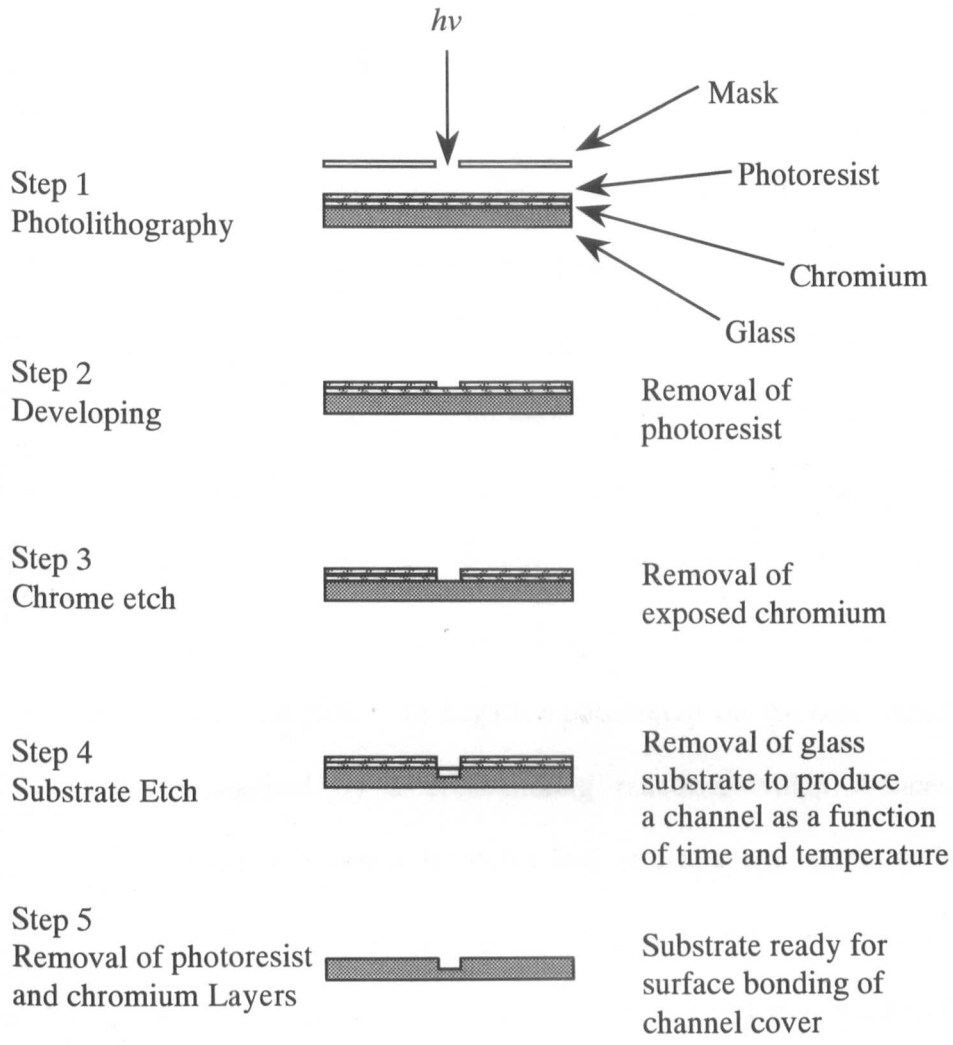

Figure 1.1. Chip production using photolithography and wet-etching procedures.

Preparation of substrate

Glass, silica and silicon substrates can be purchased from photomask producers, which will be pre-coated with a very thin metal layer (~0.1μm), often chromium or gold which is often achieved using sputtering or chemical vapour deposition. This metal layer is important as it helps to control the degree of surface etching that will occur when the substrate is exposed to the wet etch solution. The metal layer is then spin coated with a

layer of photoresist, (approx. 0.5- 2.0μm), which consists of a polymer base resin, a sensitizer and a casting solvent[35]. On exposure to radiation, there is a change in polymer structure; the presence of the solvent enables the application of very thin spin coated layers, while the sensitizer controls the chemical reactions that take place in the polymer when it is exposed to the light source. There are two types of photoresist; positive and negative. Exposure of positive photoresist results in a weakening of the polymer structure due to bond breakage of the main and side chains. The area of the resist that is exposed to light shows an increased development rate and hence becomes more soluble than the non-exposed areas and is thus able to be removed by basic media such as potassium hydroxide solution. In negative photoresist on the other hand, the exposed regions are strengthened by a cross-linking reaction, which reduces the rate of development and hence becomes insoluble and as a result is unable to be removed in solvent. However, the unexposed photoresist may be removed using acetone.

A positive photoresist was used to generate the channels that were produced as part of the work described later in this thesis. The channels created correspond to the negative of the design on the mask as described in the following section.

Photolithography

Photolithography is used to transfer the pattern of the channel design from the mask to the photoresist covered substrate surface. The mask is a stencil that on exposure to UV radiation produces the negative image on the surface of the chip, when a positive photoresist is used. Two high-resolution lenses are positioned between the light source and the mask and between the mask and the substrate surface in order to focus the UV light on the mask within ± 0.25 μm accuracy[35]. After the design has been transferred, the

plate should be baked for approximately 72 hours to harden the photoresist and remove any traces of solvents prior to the etching process[21].

Wet-etching procedures

Although various reagent mixtures have been used for wet etching of substrates, the most common mixture used for glass and silica substrates is hot dilute HF/NH_4F (1% HF and 5% NH_4F in water) which dissolves silicon by oxidising it to silicate[39]. This mixture gives an etch rate of approximately 0.3-0.5 μm $minute^{-1}$ in glass[21]. The use of wet etching with a positive photoresist produces an isotrophic etch, whereby the etch rate proceeds at an equal rate in all directions with the end result that the channels produced are usually twice as wide as they are deep.

Silicon may be etched using reagents such as ethylenediamine pyrocatechol or KOH[30,39] at approximately 115°C, with an average etch rate of 2.5 μm $minute^{-1}$. The final size of the etched channels will depend of the width of the lines on the mask, the substrate and the method of etching. It has been observed that the EOF is not reproducible in channels with widths greater than 300μm, as explained in section 1.3.

The photoresist can be removed using photoresist remover, for example from Shipley (Coventry, UK) and the chrome layer can be dissolved by Microposit chrome etch 18 (Shipley, Coventry, UK). The finished manifolds are bonded to pre-drilled top plates, which seal the channels. Liquid access is obtained via the holes in the top plate lined up with the end of the capillaries, which form the reservoirs.

The bonding methods include adhesives, thermal bonding and anodic bonding are described in section 1.2.1.

Other methods of etching include use of a plasma or discharge which uses a high energy electric field to produce energetic species such as ions, radicals or electrons that bombard the substrate surface inducing chemical reactions that remove a layer from the planar surface. This is termed dry etching and can produce profiles in crystalline or amorphous materials[38]. Wet etching procedures are often preferred due to lower cost. Sputtering (ion etching) and deposition techniques or ion-beam etching (milling) may also be used[40].

1.2.2.2. LIGA, injection moulding and hot embossing

LIGA is the German acronym for X-ray lithography (Lithiographie), electrodeposition (Galvanoformung) and moulding (Abformung)[41], which was developed at the Karlsruhe Nuclear Research Centre (KfK) in Germany. The process combines the use of lithiographic techniques with the more traditional manufacturing methods. A very thick X-ray photoresist layer (up to centimetres deep) is exposed to very high intensity radiation, followed by electrodeposition to fill the resulting mould with metal. Once the resist is removed, a metal structure is left which can either be used directly, or used as a mould for injected plastic. The LIGA process allows the design and production of detailed miniaturised structures made from a range of substrates with very high aspect ratios[42] (i.e. large height with respect to lateral surface area). An extension of this technique is hot embossing[43-45], which can be used for polymer microfabrication with substrates such as polymethylmethacrylate (PMMA) or polycarbonate (PC)[44,45]. LIGA or laser-LIGA techniques can be used to fabricate embossing masters made from metal with high aspect ratios using resists such as EPON SU-8[44]. During the embossing step, the planar polymer substrate is heated in a vacuum chamber to above the glass transition

temperature of the polymer[45]. It is then pressed together under force with the master and cooled while the two plates are still in contact with each other to produce an imprint on the polymer surface. After the imprinted polymer surface has been removed from the master, it can be drilled or bonded to other substrates to complete the miniaturised manufacturing process.

1.2.2.3. Soft lithography and imprinting techniques

Soft lithography covers a range of fabrication techniques that does not involve photolithography. This includes the use of microcontact printing and micromoulding to produce microstructures in polymer substrates[38].

Microcontact printing uses a stamp with a design in relief to generate an imprint on a self-assembled monolayer (SAM) contained on a planar or curved substrate. SAMs often consist of alkylsiloxanes on glass surfaces or hydroxamic acids on metal oxide surfaces and are usually of the order of 2-3 nm thick[38].

Imprinting has been used to manufacture microfluidic channels in plastic substrates such as polymethymethacrylate (PMMA)[46]. The channels may also be formed by using wire imprinting methods, whereby a chromel wire (13 or 25 μm diameter) can be clamped into the substrate under tension and the plastic heated to its softening temperature to ensure successful indentation[46]. Alternatively, a three-dimensional silicon template is used in relief[31,32] to form more complex manifolds in both PMMA and PDMS[31-33].

The advantages of using LIGA and moulding or soft lithography techniques for microfabrication is that once the master or mould is produced, multiple designs can be rapidly produced when required, whereas the photolithographical and wet-etch

production procedures can be lengthy and require careful attention. However, these polymer and plastic surfaces are often naturally hydrophobic, hence surface oxidation to ionise the surfaces producing hydrophilic character is required before they will support electroosmotic flow. This may be carried out using an oxygen plasma[47, 48] or a hand held Tesla coil[49].

1.3. Basic working principles

This section will discuss the operation of miniaturised chemical analysis systems including methods of fluid manipulation, the factors affecting flow and how injection and separation can be brought about in a miniaturised system. The types of reactions carried out using these systems and suitable methods of detection will also be described in addition to the use of surfactants in miniaturised capillaries for the purpose of surface modification.

1.3.1. Fluid manipulation in miniaturised chemical analysis systems

Flow may be induced mechanically, by using a miniaturised pump or motor; electrokinetically, whereby a voltage is applied across the capillary inducing current flow in the reagent stream and hence electroosmotic or electrophoretic migration; or finally by use of gravity or hydrostatic pressure.

1.3.1.1. Mechanically or electrically operated pumps with valves

There is a wide range of suitable, valve containing micro-pumps available, which are often based on piezoelectric materials[50-52]. Piezoelectricity is observed in materials with a crystalline ionic structure[50]. An applied voltage will cause a deformation of the crystal surface by causing an ion to be displaced from the crystal lattice. Repeated voltage application causes the surface to show successive deformation and hence typical applications for these types of materials involve oscillation. Piezoelectric pumps used for fluid manipulation commonly incorporate a microchemical silicon membrane forming a one-way pulsating valve[21], operated by the oscillation of the crystal on which it is embedded. Other types of mechanically driven flow systems incorporating valves include those based on thermo-pneumatic principles, in which thermal expansion of a gas deforms a flexible membrane covering the pump chamber[53], or those which are based on an electrostatic driving principle[54]. In these systems, a thin, pump membrane electrode is repelled from a fixed counter electrode by using electrostatic repulsion.

The main disadvantage associated with all these valve-containing systems is the materials used for their manufacture must be chemically inert to the species pumped. Also, the devices sometimes require extensive priming and are very susceptible to the presence of air bubbles and micro-particulates such as dust, which consequently can severely reduce their useful lifetime.

1.3.1.2. Valveless fluid manipulation

This consists of electrokinetically driven systems[55-58], operated by applying a voltage across a capillary with a charged surface containing (preferably) ionic species in solution

that migrate under the influence of this voltage. In addition, diffusion controlled systems and also systems operated by using hydrodynamic pressure differences are available.

1.3.2. The factors affecting flow velocity in valveless micro-fluidic systems

The total flow velocity (υ) in an electrokinetically operated system is defined by the sum of the mobilities of the electroosmotic (EOF) and electrophoretic (EOP) components, multiplied by the applied electric field (E), as shown in equation 1.1.

$$\upsilon = (EOF + EOP)E \qquad (1.1)$$

The electric field is defined as the voltage divided by the distance between the electrodes for channels of uniform resistance per unit length[56]. The size of the electric field strength dictates the relative magnitude of each component in the overall flow rate in addition to the sample plug shape during injection[57]. At low field strengths (~80-150 V cm^{-1}) electroosmotic flow dominates, while the migration of ions and consequent separation becomes apparent at field strengths of >150 Vcm^{-1}.

1.3.2.1. Electroosmotic flow

In order for electroosmotic flow to occur, two prerequisites must be met. Firstly, a substrate with a readily ionisable surface must be used, such as silica or glass, which when placed into contact with a suitable solution, results in a negatively charged layer of $Si\text{-}O^-$ groups being produced. Secondly, the solution must be at least partly dissociated to allow the positively charged ions to line up against the negatively charged surface and form a double diffuse layer, known as the Guoy-Helmholtz layer. The Helmholtz layer

can be defined as the layer of cations (or anions, if the surface charge was positive) that is directly next to the surface wall, as shown in figure 1.2.

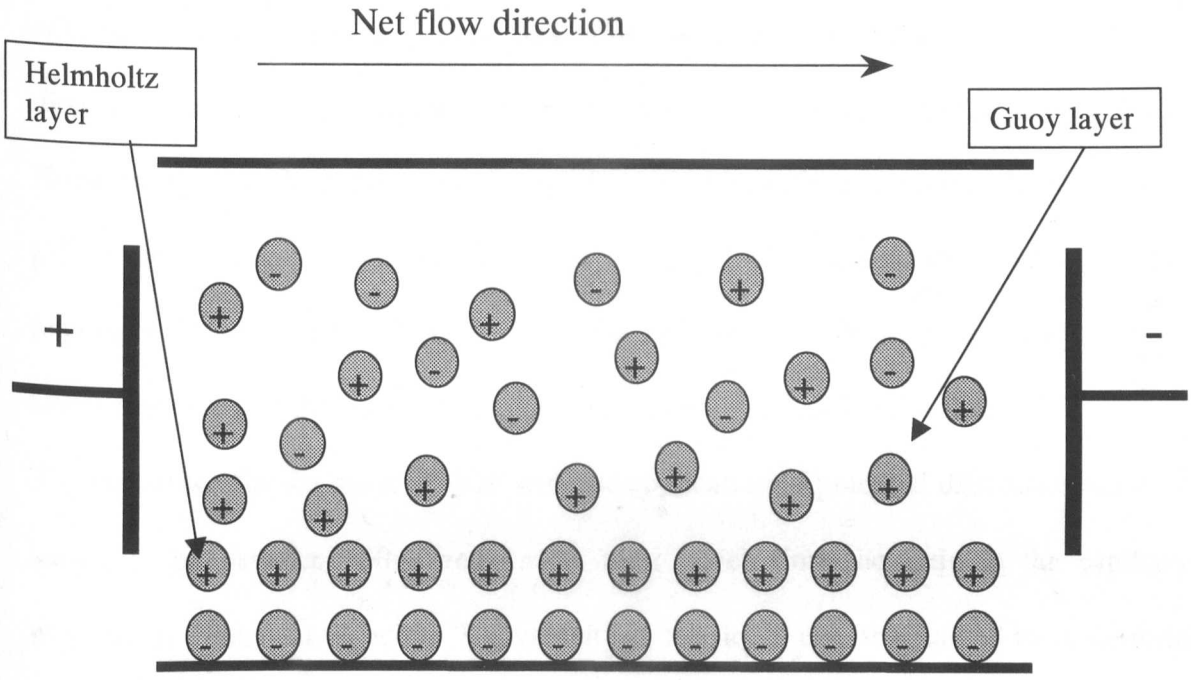

Figure 1.2. Guoy-Helmholtz layer adjacent to a capillary wall.

Figure 1.2 also shows the Guoy or diffuse layer, which neutralizes any excess wall surface charge and extends further out into the bulk solution. The potential difference across the channel liquid interface layer is called the Zeta potential (ξ) and is related to the dielectric constant (D) as shown in equation 1.2, where d is the distance between the charged layers and e is the charge carried on the layer[21].

$$\zeta = \frac{4\pi\, ed}{D} \qquad \textbf{(1.2)}$$

When an electric field is applied across a capillary under these conditions, the ions in the solution will migrate to their respective electrodes. Hence, the positive ions move towards the negative (usually ground) electrode dragging their large hydration spheres with them, which exerts an overall drag on the bulk of the liquid. As a result, the net direction of flow in electroosmosis is usually from the anode (+ve) to the cathode (–ve). However, the double diffuse layer is only formed at surface-solution interfaces when the pH of the solution lies between 4 and 9. At a pH of less than about 4 the cationic population is too high and the EOF is overrun by conductive flow, while at very high pH levels there are insufficient cations to allow the double diffuse layer to form.

The time taken for the onset of EOF with the application of potential difference has been shown to be between 100μs and 1ms[58], after which time the fluid in the capillary migrates at a constant velocity. The velocity of the liquid can be assumed to be uniform in a linear channel, with the exception of a region, of nanometer thickness, directly next to the capillary wall where the double layer is generated[59]. The velocity of the bulk liquid due to electroosmosis (υ_{os}) is related to the electric field strength (E), the relative permittivity of the liquid (ε), the relative permittivity of free space (ε_o), the zeta potential (ξ) and the liquid viscosity (η)[60]. This relationship is shown in equation 1.3.

$$\upsilon_{os} = \frac{-E\,\varepsilon\,\varepsilon_0\zeta}{\eta} \qquad \textbf{(1.3)}$$

The negative sign denotes the direction of electroosmotic flow, i.e. towards the cathode. The flow rate also depends on the cross-sectional area of the channel (A). As can be seen in equation 1.3, the zeta potential (ξ) has a large effect on the electroosmotic flow velocity. The amount of current (I) transported through the solution is related to the

electroosmotic flow velocity by equation 1.4, where λ_o is the electrical conductivity of the liquid.

$$I = \frac{A_{channel} \upsilon_{os} \eta \lambda_0}{\varepsilon \varepsilon_0 \zeta} \qquad (1.4)$$

The zeta potential is affected by both the concentration and the ionic strength of the electrolytic solution[55] and is found to vary with pH and electrolytic concentration[61-63]. The zeta potential also depends on the surface of the glass and may be determined by measuring the streaming potential[62-64] by measuring the steady, laminar flow between two flat, parallel plates in a cell.

The zeta potential may be changed by the presence of species adhering to the surface such as cationic surfactants[64-66], which bind to the glass surface and mask the natural negatively charged state, as explained in section 1.3.4.

Due to the absence of mechanical pumps in electroosmotically driven systems the flow is laminar and the bulk of the solution advances with a flat profile along the capillary. The solution directly nearest the capillary walls experiences a slight increase in resistance to flow as a consequence of electrostatic interaction, which means that in these areas the flow profile is not completely flat. In a pressure driven system, the profile is that of a bullet shape, whereby the flow profile is curved with the solution in the centre of the capillary experiencing far less resistance to flow than the solution near to the capillary walls. The laminar and parabolic flow profiles are shown in figure 1.3.

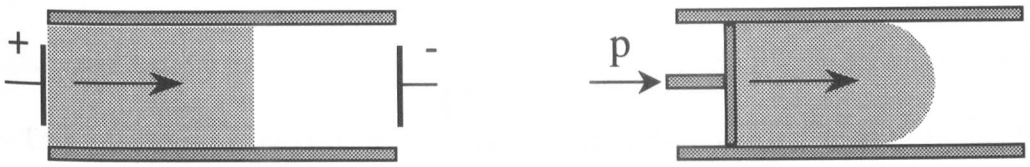

(a) Laminar flow (b) Parabolic flow

Figure 1.3. Laminar and parabolic flow profiles

In order for pure electroosmotic flow to be generated, the capillary used must be free from the influence of hydrodynamic pressure differences. Pressure differences across the capillary will, according to the principles of hydrodynamics, result in a partially parabolic flow profile[56].

Possible causes of pressure differences in a miniaturised analysis system include unequal reservoir liquid height, Laplace pressure differences in the curvature of the liquid menisci in the reservoirs or from blockages in the channels causing back pressure. As very small differences in liquid height can introduce a pressure difference, it is important to monitor the liquid levels very carefully. Increasing the dimensions of the reservoir area with respect to the channel length, i.e. a reservoir diameter of similar size to the distance between the electrodes of the inlet and outlet reservoirs, helps to reduce pressure differences caused by unequal liquid heights[56]. Although the menisci shape in each reservoir is usually the same, the position of the electrode in the reservoir is critical in determining the contact angle of the solution with both the electrode and the wall. Once other sources of error have been eliminated, the position of the electrode in the reservoir often becomes the overriding factor in the reproducibility of measurements made in the system. Providing the system is free from Laplace pressure differences and blockages,

any hydrostatic pressure can be said to be as a result of differences in liquid height only[56]. This relationship is depicted in equation 1.5, where Δh_{res} is the difference in liquid heights in the inlet and outlet reservoirs, $\Delta\rho$ is the density difference between the liquid and the air and g is the acceleration due to gravity.

$$\Delta P = \Delta h_{res} \Delta pg \qquad (1.5)$$

It has been shown[56] that a difference in liquid height between the inlet and outlet reservoirs of approximately 1mm is sufficient to produce pressure driven flow in electroosmotic flow driven systems. Hence in order to obtain accurate and reproducible results, great care must be taken when injecting solutions into the reservoirs.

1.3.3. Injection, mixing and separation in a miniaturised analysis system

1.3.3.1. Injection

Injection in miniaturised analysis system systems commonly takes place by valveless introduction of one solution into another by manipulation of the EOF. The five diagrams of a chip manifold shown in figure 1.4 illustrate the principle of loading and injection in a miniaturised analysis system in its simplest form[21]. Both the floating and pinched injection methods may be carried out in this way[20,25,28, 67,68]. The first three, parts A-C demonstrate the principle of a floating injection, while a pinched injection is shown in parts D and E.

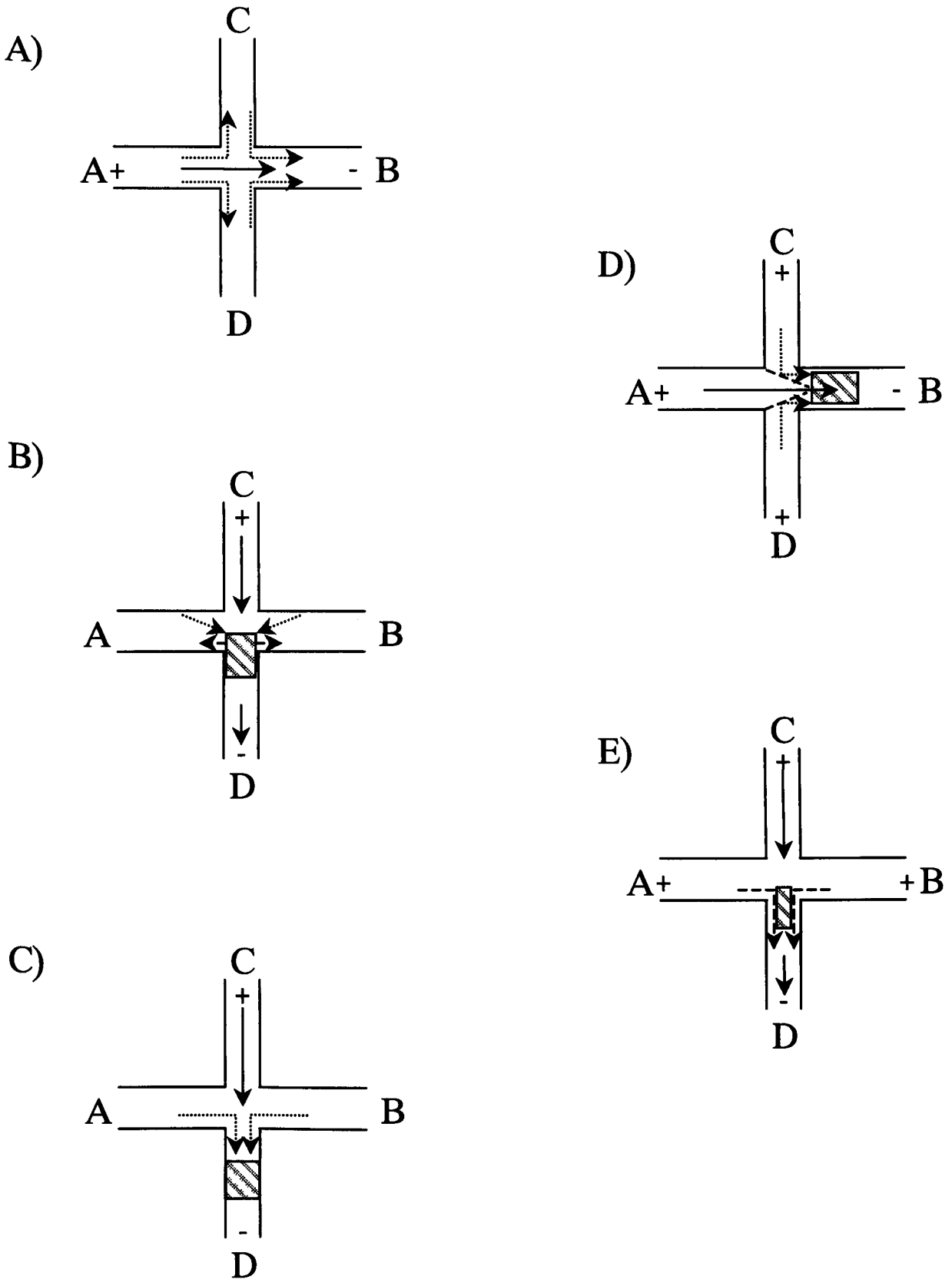

Figure 1.4. Loading and Injection in a miniaturised analysis system.

Using the floating method requires only one pair of electrodes, with which a potential is applied across each channel sequentially. This can be demonstrated using the reaction manifolds shown above, where all the channels have been filled with buffer or solvent, channel A is loaded with reagent 1 by filling reservoir A, a voltage is then applied across AB, so that reagent 1 fills channel AB (part A). As shown, some of the sample also moves into channel CD by diffusion as there are no electrodes in either C or D and hence these reservoirs are floating. Next, reservoir B is loaded with reagent 2. The voltage is then applied across CD so that channel CD is filled with reagent 2 (part B) and the sample runs to ground at reservoir D. The result is that an untidy injection of sample plug is achieved due to sample leakage at the time of sample injection from AB into CD[20] (part C).

The pinched method uses more than one set of electrodes for the simultaneous application of voltage across more than one channel and consequently is usually more accurate. This is shown in figure 1.4, parts D and E. This time, reservoirs C and D, like reservoir A, have a positive potential applied to them with respect to the negative potential in reservoir B. Consequently, less leakage occurs during sample injection (part D) and a much cleaner sample plug is obtained which flows towards reservoir D once the voltages have been switched (part E).

It can be seen that in order to obtain a good tidy sample plug injection, both sets of voltages must be switched simultaneously between the voltages needed for loading and those required for injection. Hence, computer controlled voltage application programmes can be very useful for sample injection in miniaturised analysis systems[69,70].

1.3.3.2. Mixing

In standard laboratory equipment, mixing is often brought about by introducing turbulence. The Reynolds number (R_e) determines the tendency of a liquid system to show turbulence[55]. The factors which determine the size of the Reynolds number are the velocity (v) of the flowing liquid, the diameter of the capillary (l), the density of the liquid (ρ) and the viscosity (μ) of the liquid as shown in equation 1.6.

$$R_e = \frac{vlp}{\mu} \qquad 1.6$$

The lower the velocity and the higher viscosity of the liquid, the lower the Reynolds number. Turbulence occurs at Reynolds numbers greater than the transitional Reynolds number of 2300[51], while laminar flow is found to occur at lower Reynolds numbers. In miniaturised analysis systems the Reynolds numbers are very low with the result that two liquids may flow alongside each other in a capillary without turbulence being generated at their interface[55]. The small amount of interfacial mixing is due to diffusion alone. Controlled mixing in a miniaturised analysis system may be brought about by careful manipulation of the electroosmotic mobility[54] or by introducing turbulence through reactor design[70,71].

Manz and co-workers[54]showed that by selectively enhancing the electroosmotic mobility of one reagent stream relative to that in another, a sample dilution could effectively be carried out. A fluorescein dye solution was progressively diluted using a buffer, by increasing the potential applied across the capillary. The subsequent decrease in fluoresence intensity was recorded.

Turbulence may be introduced in a miniaturised analysis system by introducing a series of branching channel called laminae[70-72] that interweave two laminar reagent streams by sequentially increasing the number of capillaries through which the solutions in the miniaturised system are required flow. An increase in mixing rate is observed due to increased surface interaction between the two solutions being mixed. The increasing number of channels then subsequently merge back into one channel, by which stage the components are usually thoroughly mixed. The number of laminae sub-divisions used depends on the channel dimensions, the diffusion co-efficients of solutions to be mixed and the linear flow rate[71]. Other micromixing devices designed to promote turbulence in miniaturised channels include a matrix injection method[73,74] whereby one liquid is injected through a mesh of very fine holes into another liquid contained in a mixing chamber.

1.3.3.3. Separation

Separation may be carried out in miniaturised analysis systems using electrophoresis where appropriate, which requires field strengths greater than 150 V cm^{-1} [25,75]. Two effects are usually present that dictate how the fluid in the capillary migrates[28]. All the components of the liquid migrate towards the ground electrode as a result of the net drag exerted by the electroosmotic flow. In addition, electrophoretic separation occurs due to variations in the ion mobilities as a result of size and ionic charge[76]. The greater the charge on the analyte, the faster its mobility, although the overall mobility of a species depends on the amount of friction created by the analyte size and shape and the overall viscosity of the medium[76]. In conventional elctrophoresis, i.e. with flow towards the

cathode, positively charged species will migrate faster than the speed dictated by the flow rate alone. This is due to attraction by the negative electrode. Conversely, negatively charged analytes will experience a repulsion effect from the negative cathode and their overall mobility will be slower than that dictated by the mean flow rate. Neutral species will move along the capillary at the mean flow rate. On-chip capillary electrophoresis has proved popular for the analysis of large, biological molecules such as amino acids[13,25,27,77], blood components[78,79] and nucleic acids, particularly DNA[20,26,80]. In addition the use of on-chip electrophoresis for the detection of sugars[81] and environmental monitoring[82] has also been reported.

If electrophoretic mobilities are sufficiently different, separation of two or more analytes may be carried out in a straight channel. Alternatively, incorporation of a series of twists and turns of the capillary to form a Serpentine manifold design[28,68] has proved successful as it allows a much longer column length to be used within a smaller area, though it is noted that at field strengths less than 200 V cm^{-1}, a loss of column efficiency in the form of band broadening can occur[28].

The use of isotachophoresis in miniaturised polymer systems has been described[83,84] to separate metal ions[84]. The sample is placed between a leading and a terminating electrolyte, which are chosen for their respective electrophoretic mobilities; the leading electrolyte should contain an anion that has greater mobility than the anions contained in the sample, while the anion present in the terminating electrolyte should show a reduced mobility with respect to those in the sample zone(s)[83]. Application of the electric field causes the sample components to separate in order of decreasing electrophoretic mobility,

resulting in the production of a series of definite analyte zones in the sample region, shown as defined steps on the isotachopherogram.

1.3.4. Surface modification effects

Due to the intrinsic net negative charge present on the walls of fused silica or glass capillaries, EOF is usually cathodic, i.e. flow proceeds towards the cathode as explained in section 1.3.2.1. However, reversal of the EOF direction can be achieved if the ionisable silanol surface is modified, for example by the adsorption of (cationic) surfactants, to make the walls of the capillary positive. The method by which the surfactants adsorb depends on the ionic strength of the buffer and the natural surface charge of the capillary walls[65]. A smooth reversal in EOF direction was observed at surfactant concentrations >CMC for solutions with a pH>4, however, at pH<4, a gradual change in direction was observed due to the neutralisation of surface charge by the cationic surfactant[64,85].

The combination of cationic and zwitterionic surfactants was effectively used to allow the isotopic separation of [^{14}N]- and [^{15}N]aniline by capillary electrophoresis[85]. This was done by suppressing the amount of EOF with the Rewoteric AM CAS U zwitterionic surfactant, also demonstrated in a previous publication[66] and reversing the direction of the flow by the addition of cetyltrimethylammonium bromide (CTAB). This precise manipulation of the anodic EOF resulted in flow against the analyte mobility, which enabled the ultra high-resolution CE separation of the two cationic, isotopically labelled compounds[64].

1.3.5. Use of silica microstructures

The incorporation of a frit or silica microstructure into a capillary[86] can enhance the mixing of reagents by forcing the movement of fluid through very narrow (between 2 and 10 μm) openings in the porous structure. These numerous, tiny pathways allow for the separation and subsequent recombination of the fluid passing along the capillary. Hence, the use of a frit goes some way towards increasing the Reynolds number of the flowing system. The overall effect of a frit is that it acts like a small pump and enhances the overall flow rate. The increase in flow rate observed with the incorporation of a frit structure into the channel depends on the frit size and porosity with the flow rate increasing with frit area up to 5 mm^2. An image of a frit structure as viewed using an SEM can be seen in figure 3.12.

Hydrodynamic pressure effects are reduced by the presence of a frit in a capillary as the porous microstructure does not enable liquid to migrate easily without the application of potential. Hence, movement of liquid from one reservoir to another as a result of differences in the heights of the liquid does not readily occur, thus different volumes of reagents can be accurately used in each reservoir, if necessary.

1.3.6. Methods of detection in miniaturised analysis system systems

Although miniaturisation of the sample injection, mixing and separation steps of an analytical procedure is reasonably easy to achieve, miniaturising the detection method has proved more difficult. The ideal detector in a miniaturised analytical system needs to be relatively low cost, require low maintenance and be small and light enough to be easily portable. Initial publications in this area cited miniaturised sample manipulation

and treatment systems, but concluded with the coupling of these systems to large-scale conventional detectors[77].

Simple macro scale detectors such as silicon photodiodes[22] or potentiometric[80,87-89] devices could be battery operated and thus easily incorporated into a miniaturised system, however, the range of analytes covered by these methods would limit the analytical utility of miniaturised measurement systems in the long term. Hence, in the last three years work has been carried out into the miniaturisation of conventional analytical detection[90,91].

The choice of detection will depend on the volume of liquid in the detection cell[51], spectrophotometric methods will favour cell volumes greater than 10 pl, which is typical in systems based on FIA[51,92,93], while smaller detection volumes of approx. 1 pl have been reported with potentiometric methods[89]. Conductivity detection has also been shown to very practical for very small volume detection[38]. Special attention must be paid to the detection cell design and size in order to ensure that a reliable and sensitive measurement is made. Due to the simplicity and relative low cost spectrophotometric techniques have proved popular for detection in miniaturised systems[11,12,29,38]. Optical detection may take place via miniaturised PMT, photodiode or diode array. Fibre optics are often employed[11,12,21,38,93] and with some experimentation may be inserted directly into the microchannel[11,12]. This results in a direct contact of the fibre optic with the solution to be analysed, reducing the number of interfaces through which the light must pass and also the path length to the detector[94]. This is especially useful in emission measurements such as fluorescence[95] for example in on-chip immunoassay measurements using electrophoresis[96,97], and the chemiluminesence determination of glucose and lactate

in human serum in a 15 nl cell[92]. Absorption measurements, on the other hand, can benefit from a longer path length by performing detection along the capillary, as described by Liang and co-workers[93].

Non-spectrophotometric detection techniques reported in miniaturised systems include refractive index monitoring using a waveguide sensor to determine EOF flow[98], xylene[99] and carbohydrates[100], the use of anti-resonant reflecting optical waveguides (ARROWS) for the excitation of fluorescein in a cellulose acetate layer[101], and the application of surface plasmon resonance, also for refractive index measurements, to assess the flow rate of ethanol in a PDMS chip[102]. Electrochemical methods have been used for the detection of blood glucose on disposable chips[14,15], phenol[67] and catechol and amines[92]. Recently, the miniaturisation of mass spectrometry has been reported[90]. In spite of a potential loss of resolution as a consequence of the flight path length reduction necessary in a miniaturised mass analyser system, it has been shown that certain types of mass analysers are more suitable for miniaturisation than others[90]. The impression is that miniaturised mass spectrometers will function better if their use is restricted to certain analytes, thus a whole range of miniaturised mass spectrometers for specialist uses is envisaged[90]. So far, quadrupole, magnetic sector time of flight (TOF) and quadrupole ion trap mass spectrometers have all been successfully miniaturised[90, 103-105]. Although such developments are designed to enhance the sensitivity of miniaturised detection for a very small number of analytes, multi sensor detection on a chip system is also possible. The fabrication of a micro analysis system to enable almost simultaneous measurement of pressure, flow rate, temperature, conductivity, UV absorption and fluorescence on a chip has been reported for use with a range of analytes which were separated by LC[38]. The

system consisted of two chips sandwiched together; one part containing the flow cell, made from either silicon coated with silica or silicone rubber, and the other containing the quartz sensor chip for the pressure, flow rate, temperature and conductivity measurements. UV-absorption and fluorescence measurements were carried out using external light sources and detectors that were interfaced to the flow cell by optic fibres[38]. Evaluation with a range of analytes showed comparable performance to conventional stand-alone sensors.

1.4. Chemiluminesence in miniaturised analysis systems

Chemiluminesence (CL), which will be discussed in greater detail in chapter 2, is a sensitive and selective technique, which requires simple instrumentation and is relatively low cost. Some problems associated with CL reactions in macro-scale systems such as large sample and waste volumes and irreversible reactions do not pose problems for use in miniaturised analysis systems. With only micro- and nanolitre sample volumes required for analysis in often one-shot disposable systems, chemiluminesence would seem an ideal detection method. It has been shown that using surface modification, reactions occurring at pH levels outside the range suitable for EOF fluid manipulation are possible. The main disadvantage would be that CL is not universally applicable to all analytes.

Both chemiluminesence[92,106,107] and electrochemiluminescence[108-112] have been successfully used as a means of detection in miniaturised analysis systems as described in section 2.6.

1.5. Future applications of miniaturised analysis systems

The ideal miniaturised analytical device would be a user-friendly, low-cost, disposable unit able to be used by non-analytically trained personnel for rapid screening of the sample at source. Most of the reagents would be present inside the device, possibly in a dehydrated form to prolong shelf-life, so that the user would have very little sample handling to carry out prior to analysis. The disposable device could fit into a larger, but still easily portable base unit, which would carry out detection in addition to data interpretation producing a digital readout in an easily understandable format for the user. These devices could be used to enable rapid environmental monitoring or clinical diagnosis, indeed rapid clinical diagnosis using miniaturised analytical equipment is now becoming a reality[113]. Chemiluminesence detection could be used to achieve this.

2. Chemiluminesence

2.1. General theory

Chemiluminescence (CL) occurs when an electronically excited species is produced in a chemical reaction, which emits light on returning to the ground state (direct CL) or alternatively transfers its energy to another molecule which then emits light (indirect or sensitised CL). The emitted light is usually in the visible or near infra-red regions of the electromagnetic spectrum. Although they are quite rare, chemiluminescent reactions can occur in solid, liquid or gaseous phases.

Chemiluminescence is a form of luminescence[117]. Other related forms of luminescence include fluorescence and phosphoresence. All forms of luminescence are downward electronic transitions whereby an excited molecule looses some of its energy by the emission of a photon of light. Fluorescence and phosphorescence are forms of photoluminescence in which the excitation energy required for the promotion of an electron to a higher orbital comes from the absorption of photons in a light source, whereas in chemiluminescence, this excitation energy comes from the chemical reaction.

2.1.2. Electronic states

Electrons exist in one of two quantised spin states. A magnetic field is generated as the electron spins on its axis. For two electrons to be present in the same orbital, the Pauli Exclusion Principle states that their spins must be opposed. The two electrons are then said to be 'spin paired'. When a molecule is excited, an electron is promoted to a higher energy level. This electron can remain spin paired with the electron in the original orbital to form an electron in an 'excited singlet state' or, more unusually, it

can change its alignment to lie parallel to the electron in the original orbital to form a molecule in an 'excited triplet state'.

Figure 2.1 shows an energy level diagram showing typical transitions within a luminescent molecule.

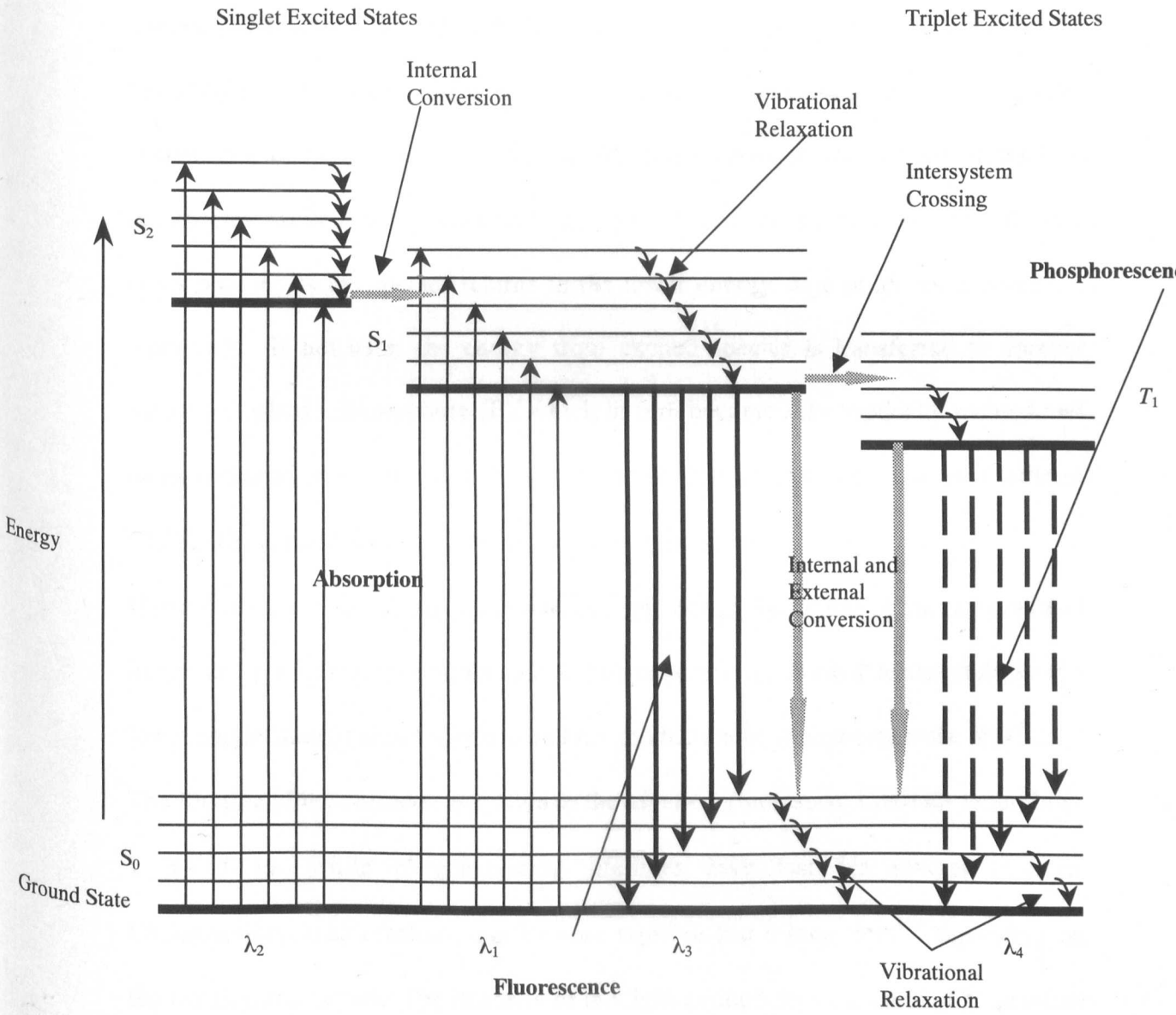

Figure 2.1. Energy level diagram

As can be seen in figure 2.1, excitation of an electron to a higher energy level can in principle, if the required conditions are met, result in two different types of photoluminescent emission.

Chemiluminescence (CL) and fluorescence emissions occur when an electron, chemically excited to a higher singlet state, returns to the ground level with the emission of a photon. In this case, there is no change in spin quantum number and the transition is spin allowed. The wavelength of fluorescence emission depends on the excitation wavelength, whereas chemiluminescence emission wavelengths depend on the species excited in the chemical reaction. A chemically excited molecule that emits photons as the species returns to the lower energy state produces a direct CL emission. If however, the energy from excited species is transferred to another molecule, called a fluorophore (F), which in turn becomes electronically excited and emits radiation as it returns to the ground state, then this process is termed indirect CL[117]. These reactions are discussed further in section 2.2.1.

If the excited electron changes its rotational spin during the course of the reaction, and hence its spin quantum number, the transition from the excited triplet state to the lower singlet state is spin forbidden and the production of phosphorescence results.

The lifetime of the emission is related to the kinetics: fluorescent lifetimes range from 1 ns- 1 μs, while phosphorescent lifetimes may last for several minutes. Chemiluminescence reactions can be very rapid or last a long time[118] depending on the reaction conditions. The intensity of the light emitted depends on the CL quantum yield.

2.2. Requirements for chemiluminescent reactions

2.2.1. Direct and Indirect CL

The prerequisites for a CL reaction include the production of an excited molecule that is capable of either releasing a photon or transferring energy to another species. The reaction must be exothermic to allow sufficient energy to be created in order to produce this excited state and furthermore, a pathway must exist for this excited state to occur.

Most CL reactions occurring in solution produce an electronically excited product that emits direct chemiluminesence as the species returns to its original electronic state. However, in certain cases, the electronically excited product formed in the process of the reaction is unable to release the excess energy itself and thus fails to chemiluminesce. The energy is transferred to another molecule called a fluorophore that then emits this energy as a photon of light. This is known as indirect chemiluminesence or sensitisation[118] and the best example of an indirect solution phase CL system is the peroxyoxalate reaction, which is an exceptionally efficient and hence very sensitive reaction. Quantum yields of up to 0.5 have been reported[119]. Fluorophores are selected for their quantum yield and emission wavelength characteristics. A good fluorophore should be readily excited, stable and fairly resistant to changes in environmental surroundings, such as temperature and pH. The radiation emitted is characteristic of the fluorescence spectrum of the fluorophore.

2.2.2. Instrumentation requirements

Chemiluminesence detection requires very simple, inexpensive instrumentation, for example in a batch system a sample curvette, or in a flowing system, a means of injection coupled with, in both systems, a method of monitoring the subsequent emission[119]. No wavelength selection is necessary.

The advantages of CL detection include high sensitivity and simple, inexpensive instrumentation. There is rarely a background emission and no excitation source is required, as the reaction is chemically initiated. In addition, a wide linear range, often over several orders of magnitude and low limits of detection are usually associated with this technique.

2.2.3. CL detection combined with analytical separation techniques.

Chemiluminesence is useful for monitoring reactions with reasonably high quantum yields that do not require special mixing. Although the technique is very sensitive and selective in the sense that it is only applicable to a few reactions, it is not inherently specific. Specific selectivity can be introduced by means of separation or sample (pre-)treatment with derivatisation sometimes required to incorporate selectivity. Consequently, chemiluminesence is often coupled to either a flowing e.g. FIA system or a chromatographic, especially liquid chromatography (LC), separation. Flow injection is seen as a particularly good choice for combination with CL detection due to it being an inexpensive technique that provides reproducible and rapid mixing. The analyte is injected into a flowing stream and mixes with the reagent very close to the detector. A PMT is commonly used to detect the resulting emission. Due to the ease of use and the relative low cost, the range of analytes that have been detected in this way is vast. These include metal ions[120-126] hydrogen

peroxide[127,128] alcohols[129] amines[130] amino acids[131] carbohydrates[132] enzymes[133,134] vitamins[135] and certain drugs[136] determined by a variety of CL systems. In spite of on-line chemical treatment selectivity is still a problem especially in multi-analyte samples. Liquid chromatography enhances selectivity by isolating compounds of interest and in certain cases by sample pre-concentration prior to subsequent CL detection[137,138]. However, incompatibility of solvent mobile phase with CL can be a problem. Most of the analyses carried out in this way involve organic species, such as amines[139,140], carboxylic acids[141], drugs[142] and polyaromatic hydrocarbons (PAH's)[143-145] and thus the peroxyoxalate CL system is often used as a reaction for post-column derivatisation detection[143-147]. CL detection has also been reported using capillary electrophoresis (CE)[146-151] and supercritical fluids[152].

2.3. The Tris(2,2'-bipyridyl)ruthenium (II) (TBR) reaction.

2.3.1. History

The first instance of chemiluminescence occurring from the $Ru(bipy)_3^{2+}$ species was reported by Hercules and Lytle[153] in 1966, although Paris was reported to have observed chemiluminescence with a ruthenium chelate in 1962[153]. An intense orange emission was seen when the green $Ru(bipy)_3^{3+}$ species (oxidised from $Ru(bipy)_3^{2+}$ by a variety of methods, as explained in section 2.3.4) in acidic solution (0.05M) was reacted with either sodium hydroxide (9M) or hydrazine (0.1M). The orange light (λ_{max} = 610 nm) is emitted at room temperature from the excited state $[Ru(bipy)_3^{2+}]^*$ which is a triplet occurring as a result of a charge transfer process between the metal and the ligand. As a consequence of the triplet state this emission is actually chemically induced phosphorescence which is rare in solution[154].

2.3.2. Structure of the TBR complex

The structure of the tris(2,2'-bipyridyl)ruthenium (II) complex can be seen in figure 2.2 and is a 6 aromatic ring structure of 3 sets of bipyridine groups located around a central ruthenium atom. The complex has an overall +2 charge due to the charge on the metal ion.

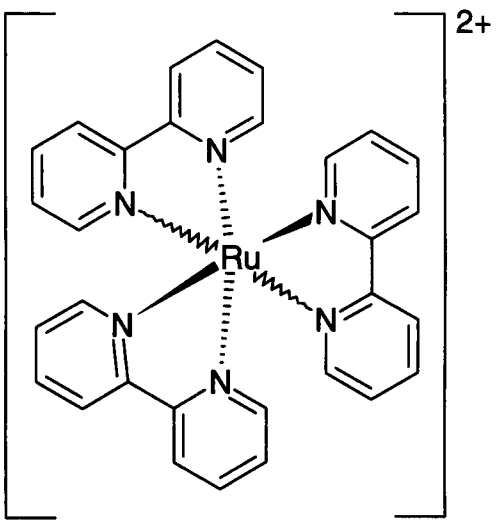

Figure 2.2. Structure of the tris(2,2'-bipyridyl)ruthenium (II) complex

2.3.3. Electrogenerated chemiluminescence (ECL) and non-electrogenerated chemiluminescence (CL) using the TBR reaction

The TBR species maybe utilised in both ECL and chemical CL determinations. Most of the analytes determined by TBR chemiluminesence contain an amine group in the molecule[154] and it appears that straight chained tertiary amines produce a higher emission intensity than branched, secondary and primary amines due to a lower energy non-bonding electrons[154,155].

In the electrochemical reaction the TBR species is oxidised at the electrode prior to interaction with the analyte in solution. In the non-electrogenerated reaction, the orange TBR species is oxidised to form the green reactive oxidant $Ru(bipy)_3^{3+}$, prior to injection, typically into a flowing system. On mixing with the analyte in solution, for example, a tertiary amine, the $Ru(bipy)_3^{3+}$ is reduced to the excited state, $[Ru(bipy)_3^{2+}]^*$ which subsequently reverts to the reduced TBR species, releasing a photon of light. As this reaction occurs with electron transfer and there is no bond breakage, it is reversible and the TBR species may be re-used. The reaction scheme is shown in scheme 2.1.

$$Ru(bipy)_3^{2+} \xrightarrow{\text{oxidation}} Ru(bipy)_3^{3+} \xrightarrow[\text{analyte}]{\text{Reduction}} [Ru(bipy)_3^{2+}]^* \longrightarrow Ru(bipy)_3^{2+} +$$

Scheme 2.1. TBR reaction scheme.

2.3.4. Oxidation of the TBR complex.

Electrochemical oxidation of the TBR species may be carried out *in-situ* at an electrode by remote generation in a flowing system, while the TBR species is mixed in solution with the oxidant to bring about chemical oxidation. *In-situ* electrochemical oxidation of $Ru(bipy)_3^{3+}$ is the most commonly used method, due to the stability of the generated species and the ease of generation. However, with reference to the work described in this thesis, only chemical oxidation will be considered here.

Oxidants which are commonly used in the chemical oxidation include lead dioxide[153,157-159] and cerium IV[160,161], although chlorine[162] and nitric acid[163] have also been used. The solid lead dioxide must generally be removed by filtration prior to

reaction with the analyte. This poses a problem in that the $Ru(bipy)_3^{3+}$ produced off-line is not stable and gradually reverts to the $Ru(bipy)_3^{2+}$ on standing. The concentration of the acid in the TBR solution may affect the stability of $Ru(bipy)_3^{3+}$ species[154,159] as was found in this work (see chapter 4), but re-oxidation is necessary if the $Ru(bipy)_3^{3+}$ species is to remain stable for any length of time. Alternatively, the addition of cerium (IV) to the acidified TBR produces a more stable $Ru(bipy)_3^{3+}$ species, as the cerium (IV) can remain in solution with the oxidised $Ru(bipy)_3^{3+}$ while the reaction with the analyte proceeds.

2.3.5. Applications of the TBR reaction.

The list of analytes that may be quantitatively determined using the TBR reaction is extensive. As stated in the introduction, CL detection is often coupled with separation methods to achieve a quantitative analysis with excellent selectivity and sensitivity; this is especially true in the case of non electrogenerated TBR CL applications. Oxalate and organic acids, amines (aliphatic and cyclic), amino acids and proteins, pharmaceuticals and various other analytes have all been directly determined by the TBR reaction. However, with reference to the work described in chapter 4 of this thesis, only non-electrogenerated TBR CL determinations will be described here.

TBR post-column detection has been successfully used for oxalate determination in Bayer liquor by Barnett *et al.* [161] who achieved on-line oxidation of the TBR species using cerium (IV). A limit of determination of $1x10^{-7}$ mol l^{-1} oxalate was obtained. Cerium was again used as the oxidant in the simultaneous determination of oxalic and tartaric acids in a urine sample, carried out by He and co-workers[164] who achieved limits of detection of $2.7x10^{-8}$ mol l^{-1} and $2.7x10^{-6}$ mol l^{-1} for oxalic acid and tartaric acid respectively. Another publication by He *et al.*[165] describing the determination of

pyruvate in human serum also employed cerium (IV) in the production of $Ru(bipy)_3^{3+}$. The limit of detection for pyruvate was determined as $1.4x10^{-8}$ mol l^{-1}. Although many of the compounds which interact with the TBR species to generate CL include a secondary or tertiary amine group, most of the applications involving amines in the TBR reaction are examples of electrogenerated CL. Codeine[157,159] has however been determined by chemically generated TBR chemiluminescence, as described in section 2.3.5.1. In addition to this, rantidine[158] has also been determined by non-electrogenerated TBR using FIA, with off-line oxidation of the active $Ru(bipy)_3^{3+}$ using PbO_2.

2.3.5.1. Determination of codeine

The analysis of codeine in process streams is most often carried out using ion-pair liquid chromatography[157], however this is often very time consuming. Both morphine and codeine (an O-methyl derivative of morphine) have been successfully determined by FIA-CL using the chemically generated TBR species[157,159,166] and also by permanganate oxidation[167,168]. Codeine has also been determined by capillary electrophoresis coupled with chemically generated TBR chemiluminesence[169], by FIA with electrogenerated TBR chemiluminesence[170] and electrogenerated TBR chemiluminesence in a miniaturised flowing system[115]. The quoted limits of detection in the codeine analyses were $5x10^{-9}$ mol l^{-1}, $3x10^{-7}$ mol l^{-1} and $1.5x10^{-8}$ mol l^{-1} codeine respectively[157,168,169].

2.4. Luminol reaction

2.4.1. History and general background

The luminol reaction, which was first reported in 1928[117], is perhaps the most commonly used solution chemiluminesence reaction suitable for the quantification of a range of analytes. The luminol (3-aminophthalhydrazide) is oxidised in aqueous alkaline conditions, usually by hydrogen peroxide, although permanganate and hypochlorite can also be used, to produce 3-aminophthalate, nitrogen and an intense blue-violet emission (λ_{max} = 425 nm), as shown in scheme 2.2.

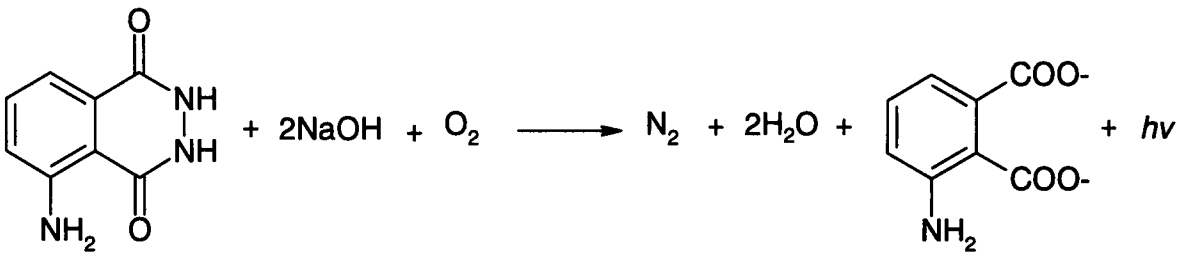

Scheme 2.2. The luminol reaction[117]

A catalyst is used in the oxidation by hydrogen peroxide and this is often a transition metal cation[123,171-174]. The optimum pH for this reaction is pH 10.4. The CL emission is instantaneously observed on mixing the reagents and the wavelength of emitted light depends on the nature of the media, with the oxidation of luminol in DMSO yielding a blue-green emission (λ_{max} = 480-502 nm).

2.4.2. Reaction mechanism

Due to bond breakage in the luminol reaction mechanism, it is an irreversible CL reaction. The mechanism of luminol catalysis has been reported to involve the formation of a metal ion-peroxide, intermediate complex[174], which then reacts with the luminol in alkaline solution to produce a luminol radical. The formation of this

luminol radical is the rate determining step in the whole process. The luminol radical reacts with hydrogen peroxide to produce the excited state from which the emission of light occurs.

According to Burdo and Seitz[174] who made these observations during an investigation into Co(II) catalysis of the luminol reaction and MacDonald *et al.*[175], the observed CL emission intensity was shown to be proportional to the concentrations of metal catalyst and hydrogen peroxide, but not to the amount of luminol present. A decrease in CL emission intensity was observed at high luminol concentrations, which led them to dismiss earlier claims of the presence of a luminol-metal catalyst being involved in the mechanism. An investigation by Chang and Patterson[176] concerning the effects of halide ion enhancement endorsed the presence of a metal ion-peroxide species.

2.4.3. Applications

The traditional applications of the luminol reaction include quantification of transition metal catalysts[122,171-182], peroxides[127,181,182], species which produce peroxides[127,132,183], luminol and compounds labelled with luminol[184]. Recently, chemiluminesence sensors based on immobilised luminol, have been successfully used in the determination of oxalate in plant tissues[185], cholesterol in human serum[186], glucose and lactate in sera and lactate samples[187] and glucose[114].

Another application for the luminol reaction was reported by Cui and co-workers[188], who described the use of inhibition effects by reducing organic compounds on the luminol and lucigenin reactions, with or without cobalt catalysis. Twenty-two reducing organic compounds were tested such as phenol, hydroquinone, benzoic acid and aniline. It was found that some of the reductants were detectable at picomolar levels and it was postulated that the observed inhibition was due to interaction of the

reducing compound with radical intermediates of the luminol reaction such as $OH^{\cdot}$ and O_2^{-}.

2.4.4. Determination of metal ions using the luminol reaction

The luminol reaction is catalysed by a number of metal cations. Co (II)[122,171,172] (see section 2.4.4.1.) is one of the most popular, though Cr(III)[123,173] Cu(II)[177], Ti(IV)[178], Cd(II)[122] Mn(II)[123] and Fe(II)[179] have all proved to be analytically useful. Although many of these metals have been determined at very low (sub-nanomol l^{-1}) levels[123,171,177,179], selectivity in a multi-analyte sample is a problem. For this reason, sample pre-treatment or separation is usually necessary prior to CL detection. Other methods include the use of chelating resins to remove interferences[189,190] or ion-exchange resins[191] to selectively delay elution of certain analytes in order to allow CL determination of trace amounts of metal ions in a wide range of matrices.

2.4.4.1. Determination of Cobalt(II) by luminol CL

Co(II) has been determined using luminol chemiluminescence in the presence of other transition metals, although as stated previously, this does not tend to be very selective. Co(II) is a very efficient catalyst of the luminol reaction with a high quantum efficiency[174] and as a result is a favoured catalyst for the reaction[122,171,172,192].

The limits of detection for Co(II) using the luminol reaction depend of course on the method of separation, where necessary and the presence of any interfering species. Sakai *et al.*[172] obtained a limit of 0.1 pg of Co(II) in a 100 µl aliquot of a synthetic sample matrix using ion chromatography with on-line luminol CL detection, while a limit of 0.1 pg of Co(II) per 100 µl sample was achieved by Jones and co-workers[193] in samples of rice flour also using an ion chromatography separation step. In the

presence of other transition metal ions, sensitivity is compromised, however, a determination of Co(II) and Mn(II) in water by FIA-CL with oxidation of the luminol by potassium permanganate[122] produced detection limits of 0.01 ng ml^{-1} Co(II) and 0.02 ng ml^{-1} Mn(II) respectively.

2.5. Use of surfactant systems in CL reactions

Surfactants are surface active agents, which as the name suggests, are predominantly found at the interface between two systems, be that liquid-liquid, liquid-gas, liquid-solid or solid-gas surfaces[194]. Surfactants are made up of sub-units termed monomers that have a hydrophilic, polar head group, and a hydrophobic, non-polar tail, usually a hydrocarbon chain, which align themselves at the interfacial surface. The number of surface monomers increases with increasing surfactant concentration in solution, which eventually causes the monomer units to aggregate. Above a concentration termed the critical micelle concentration (CMC) the monomers sub-units aggregate in solution to form micelles. In the simplest form, a micelle can be described as a group of monomers orientated in a ring so that in aqueous solution the hydrophilic heads point into the bulk solution and the hydrophobic tails are directed inwards away from the solution. In non-aqueous media the reverse is true, with the head groups drawn together in the micelle and the hydrophobic tails extending into the bulk solvent, hence these micelles are termed reverse micelles. The area inside the micelle is thus free from the external solution. There are four groups of surfactants; cationic, which carry a net positive charge on the polar head group; anionic, which carry a net negative charge, non-ionic, which do not carry a net charge and zwitterionic, which carry both positive and negative charges.

Surfactants can be used in chemiluminescent reactions to overcome any pH imbalance of the system reagents[195,198] by bringing the necessary reagents into close proximity with one another. A wide range of surfactants and surfactant combinations has been successfully used in both CL[195-201] and ECL systems. The most common use of surfactant additions in CL appear to be the luminol[195-201] and the lucigenin reactions presumably due to the high optimum pH requirements, although other CL systems reported include dibromalizarin-violet[202] and the peroxyoxalate[203] reactions. The overall effects of the many surfactant combinations and conditions on the various CL reactions is difficult to easily summarise, as so many different effects have been reported which depend not only on the concentration of surfactants used but also on the nature and concentration of the other reagents present. However the presence of micellar media has been reported to change the microenvironment of the CL system[204], producing a system with a much greater molecular organisation[195]. This can mean differences in microviscosity, pH[196, 200], polarity, solubility[199] and reaction pathways, the latter being a result of a change in the energy transfer process[204] that can occur due to an increase in molecular organisation of the micellar medium with respect to that of the aqueous solution[195]. As a result of these effects, enhanced emission of CL emitting species have been observed in surfactant solutions[204]. These effects are usually observed in the presence of surfactant media at a concentration above the CMC and are believed to be as a result of a high localised reagent concentration around or inside the micelle which cause a range of interactions such as coloumbic or charge attraction[201]. It is thought that it is the close proximity of these high localised concentrations that increase the effectiveness of the energy transfer process, which in turn produces an overall increase in emission intensity[204]. Very

high surfactant concentrations have been found to reduce reaction rates, however, due to a dilution effect of the reagent concentrations[198].

A number of publications report the use of cationic surfactants in aqueous phase luminol CL[192-196], usually either cetyltrimethylammonium bromide (CTAB)[195,196] or cetyltrimethylammonium chloride (CTAC)[198].

CTAB was found to enhance the oxidation of the luminol species and the probability of the electron excitation energy transfer in the presence of fluorescein by up to one hundred fold[195] of that of the pure solutions. The increase in emission intensity was found to occur only once the CMC (~0.2mM) of CTAB had been reached. Abdel-Latif and Guilbault[196] reported the effect of surfactant structure, more specifically carbon chain length, on luminol CL emission enhancement. Increased carbon chain lengths and the presence of bromide as the counter ion were found to show the greatest reaction enhancements, with CTAB producing the maximum intensity. Saitoh and co-workers[197] successfully carried out the simultaneous determination of iron(II) and total iron using tetradecyltrimethylammonium bromide (TTAB) in the presence of citric acid in the luminol reaction. The concentration of the TTAB was fixed at 10 times higher than the CMC, which is much higher than the surfactant concentrations usually reported in CL reactions. The authors suggested the TTAB micelles provided a surface on which a high concentration of citric acid-Fe(II) complexes could accumulate in the close proximity of hydrogen peroxide molecules. The reaction between these two species then took place on the micelle surface, resulting in an enhanced reaction rate. An interesting publication detailing the determination of Co(II) using a xanthone dye-hydrogen peroxide reagent system[205] carried out in the presence of CTAB described the ionic association of dye and surfactant molecules at low surfactant concentrations. This was reported to increase

the non-radiative internal transfer process and hence lower the CL quantum yield. An optimum surfactant concentration above the CMC allowed the determination Co(II) in the presence of other ionic species, with a limit of detection of 6ng ml^{-1}. The authors report enhanced selectivity of this system over similar determinations carried out using the luminol reaction.

2.6. Chemiluminescence (CL) detection in miniaturised analysis systems

2.6.1. Justification for CL detection in miniaturised analysis

Chemiluminesence is a very sensitive detection technique, which requires very simple instrumentation and has a wide linear range. The absence of a radiation source allows high sensitivities as it eliminates scattering and associated noise[117]. However, CL reactions are usually irreversible and thus continual replenishment of reagents is necessary. Miniaturisation can in part overcome this due to the very small volumes required.

2.6.2. Published examples

To date, only a few examples of chemiluminesence detection in miniaturised analysis systems have been reported[96,109,111-115].

A publication by Hashimoto and co-workers[109] described the use of peroxyoxalate chemiluminesence (PO-CL) as the method of detection in miniaturised, on-chip capillary electrophoresis (CE). The device was manufactured from quartz and although the manifold design was fairly simple, it was certainly very effective for the rapid separation and detection of two dansyl amino acids. Manz, de Mello and Arora[206] utilised the electrogenerated TBR reaction to demonstrate a CL model for small volume analysis. The idea behind this work was also to demonstrate detection

of very low reagent concentrations, in this case the tris(2,2'-bipyridyl)ruthenium (III) species, with a limit of detection of $1x10^{-13}$ mol l^{-1} which the authors state equates to 30, 000 molecules of $Ru(bipy)_3^{3+}$ in a cell volume of 100 nl. The use of the electrogenerated TBR reaction has also been reported in several other publications[111,113-115].

Preston and Nieman[114] described the development of a probe that was used in a similar way to a pH electrode. Glucose and oxalate determinations were carried out using electrogenerated luminol coupled with glucose oxidase and electrogenerated TBR systems respectively. The limits of detection for each analyte were found to be 3.0 μM glucose and 0.5 μM oxalate.

A publication by Fiaccabrino *et al.*[113] reported the electrogenerated chemiluminescence of tris(2,2'-bipyridyl)ruthenium in water without added electrolyte or reducing agents by using carbon interdigitated microelectrode array. ECL was observed with the naked eye at concentrations of TBR greater than 1 mM. The limit of detection for $Ru(bipy)_3^{2+}$ in the detection cell using the microelectrode array was over 300 times less than conventional ECL with a 0.25 mm^2 area. The ECL reaction was attributed to the annihilation reaction of the reduced and oxidised forms of the $Ru(bipy)_3^{2+}$ as a result of the very small spaces between the glassy carbon electrode array. ECL of $Ru(bipy)_3^{2+}$ had not previously been shown to occur in water.

A further publication by Fiaccabrino's group[115] utilised the electrogenerated TBR reaction in a miniaturised flow cell. Three ruthenium complexes were synthesised and their electrochemical properties and hence analytical performance in the determination of codeine was evaluated with respect to the conventionally used tris(2,2'-bipyridyl)ruthenium (II) dichloride hexahydrate complex. The chip consisted

of two identical cells, one active and one reference cell; each one contained a gold or platinum interdigitated electrode array placed on top of a silicon photodiode. ECL emission was generated in the active cell, while the reagents that passed through the reference cell did not generate any light. The method of fluid propulsion through the cell in the flowing system is not specified, however the overall dimensions of the chip were 5.0 x 6.0 mm^2, with a flow cell volume of 2.25 μl. Although similar electrochemical behaviour and emission spectra were observed, the ruthenium (II) bis(1,10-phenanthroline) dichloride, $[Ru(bipy)_2(phen)^{2+}]$, complex was found to produce a greater emission intensity than the conventionally used TBR complex. Limits of detection for codeine in the batch and flowing systems using the $[Ru(bipy)_2(phen)^{2+}]$ complex were quoted as 0.1 μM and 50 μM respectively.

2.7. Conclusions

There have been few examples of chemiluminesence detection applied to miniaturised analysis systems. With the exception of the work carried out by Hashimoto's group[109] and for ECL determinations the work by Fiaccabrino's group[111,113,115], the quoted publications relate to the demonstration of the feasibility of combining CL detection into the lab-on-a-chip concept and do not detail particular analyte quantification. The aim of this work was to demonstrate not only the feasibility of CL detection in a miniaturised analysis system but to develop a device that would allow quantification of useful species.

3. Development of the Chemiluminescent Miniaturised Analysis System

This chapter discusses the development of the miniaturised analysis system which is applicable to both the tris(2,2'-bipyridyl)ruthenium (II) and the luminol reactions.

3.1. Preparation of miniaturised analysis system

Prototype miniaturised analysis chip systems had been manufactured and used for preliminary miniaturisation research at Hull[207]. The miniaturised analysis chips can be manufactured from various materials; the choice of substrate depends on the method of fabrication and the eventual use of the completed miniaturised analysis system. Although silicon would normally be a good choice for this purpose, as described in the introduction, silica or more often glass is used. Both these substances have readily ionisable surfaces and thus are suitable for electroosmotic flow (EOF) and therefore in this work glass was used.

3.1.1. Plates

The glass plates from which the miniaturised analysis system manifold bases were made were coated with chromium (~0.7 μm thick). This controlled the degree of etching by preventing the majority of the glass surface from contact with the etch medium. As described in section 1.2.2.1, the photoresist layer was deposited on top of the metal layer and this allowed the manifold designs to be transferred onto the glass surface using photolithography as described in the next section. The exposed photoresist and the metal coating were removed using Photoresist remover 112A and

chrome etch 18 respectively (both from Shipley, Coventry, UK) to leave the bare glass ready for etching. This process is shown schematically in figure 1. 1.

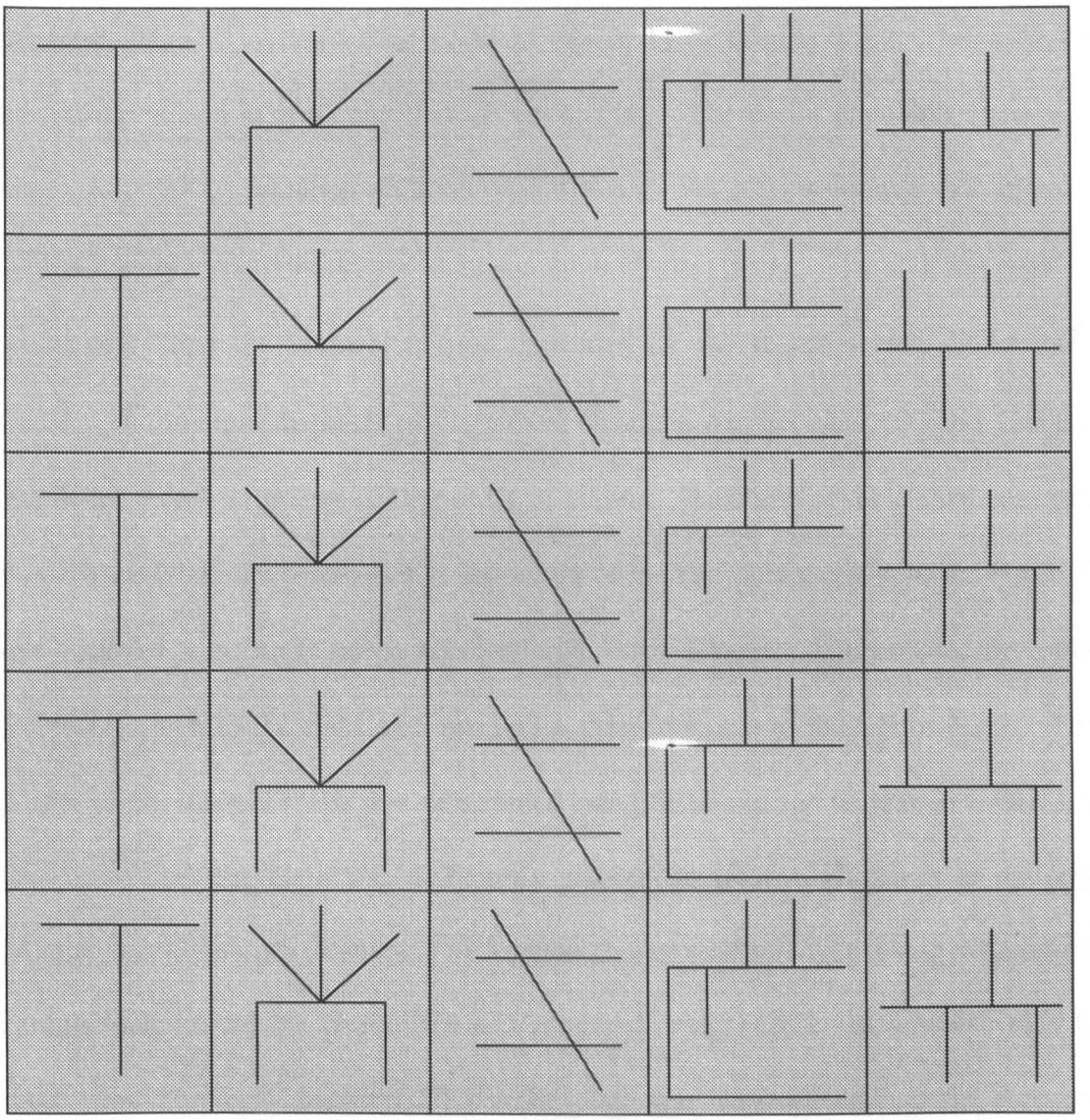

Figure 3.1. Plate of manifold base designs

Twenty-five miniaturised analysis system manifold bases of five different designs were prepared simultaneously on a plate of approximately13 cm by 13 cm by 0.5 cm. A CAD file with the five designs was provided to a company (Align-rite Ltd., Bridgend, Wales) who coated a glass plate with chrome and photoresist and

superimposed the designs onto this surface using photolithography. The five manifold designs can be seen in figure 3.1.

The plate was then returned to us for "in house" etching. The designs may be prepared using a variety of methods as described in section 1.2.2. The in-house method optimised at Hull was that of wet-etching. The entire plate was immersed into a hot (70°C) wet-etch solution (1% HF and 5% NH_4 solution) and agitated approximately every 10 minutes to encourage uniform etching. The etch rate was 3 - 5 μm min^{-1} and the immersion time depended on the required etch dimensions. Usually, the internal diameter of the etched channels was between 100 and 250 μm and hence the etch time was of the order of 1 hour. The width of the etched channels was always twice the depth, due to the nature of the isotropic etching used. The etch rate occurred at the same rate in all directions, hence for every 1 μm depth, there was a sideways etch to the right of 1 μm and a sideways etch to the left of 1 μm. The profile of the channel shape was determined using SEM and can be seen in figure 3.2. On completion, the plate was thoroughly washed, to remove all traces of the etch mixture and then left to dry. The chrome layer was removed using Microposit chrome etch 18 and the photoresist was removed using Photoresist remover 1112A, (both from Shipley, Coventry, UK). The plate was then cut up into the separate manifold bases.

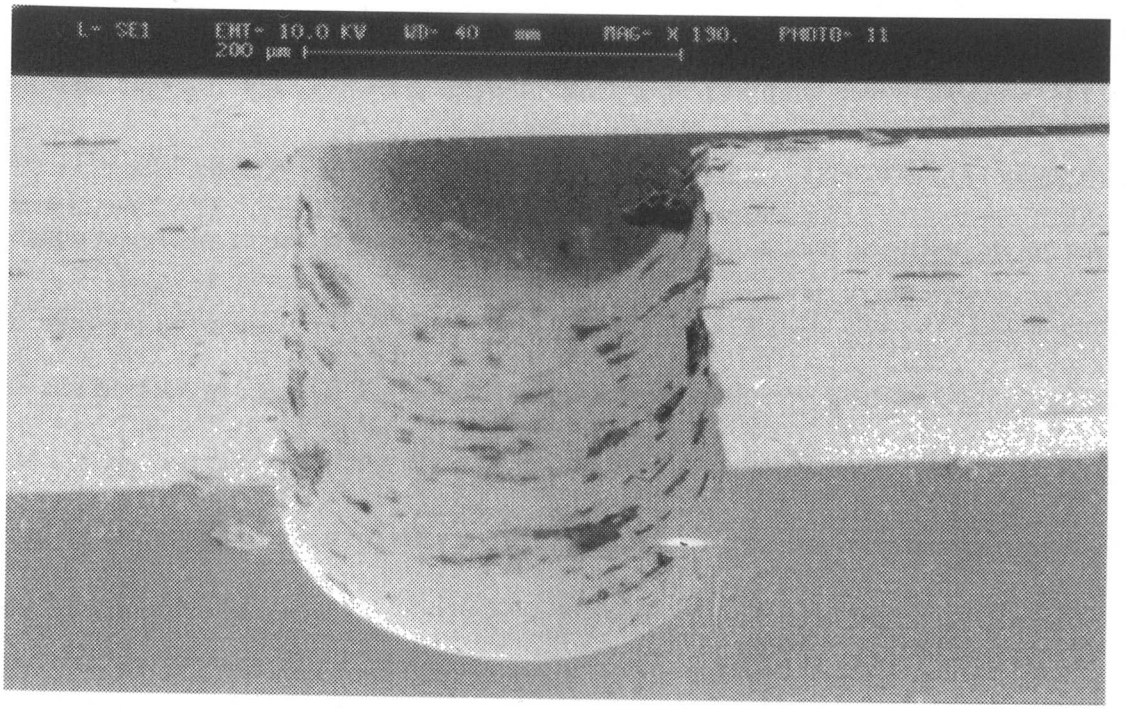

Figure 3.2. SEM profile of channel shape

3.1.2. Thickness of top plates

In order to seal the capillaries and thus form a complete miniaturised analysis system, a top plate had to be affixed. In the initial prototypes, the top plates were of the same dimensions as those of the manifold bases, i.e. 20 mm x 20 mm x 5 mm. Holes were drilled into the top plate prior to the bonding process to form reservoirs that were positioned near the end of the capillaries. These holes had to be drilled prior to bonding to prevent damage being caused to the capillaries. Once the etched channels were sealed to form capillaries, these holes became the base of the reservoirs through which liquid could be injected onto and removed from the miniaturised analysis system. Plastic pipette tips were originally used to form the main part of the reservoir. These were attached over the holes in the top plate and the edges sealed using glass bonding glue (Loctite, Welwyn Garden City, UK). Although this worked reasonably well in principle, certain solvents readily dissolved the glue. In addition to that, the structure of the reservoirs was not robust and frequently had a very short

lifetime, hence it was decided to examine further possibilities. It was decided that it would be advantageous to use a much thicker top plate (ca. 17 mm thick) to allow the plastic reservoirs to be disposed of altogether. Holes would then be drilled all the way through the plate to form the reservoirs to produce one complete and more robust unit, as can be seen in figure 3.3. It was unclear whether this new structure would effect the bonding process, as it was felt that the much deeper holes could well distort with intense heating. Fortunately, after some optimisation of the bonding programme, this was not found to be a problem.

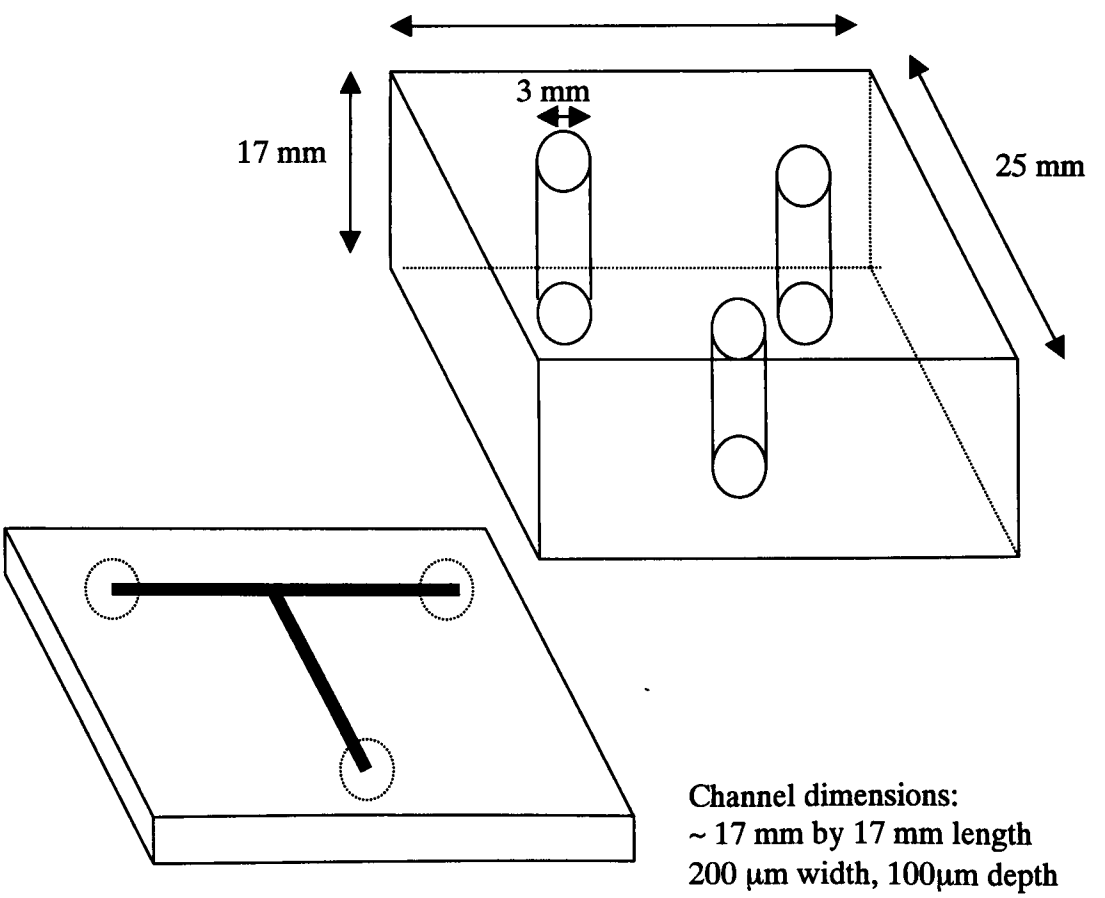

Figure 3.3. Miniaturised analysis system design with thicker top plate

3.1.3. Thermal bonding

There are several possible methods of bonding the top plate to the manifold base. The method used at Hull was thermal bonding, which was carried out in a microwave furnace (CEM Corporation, Matthews, USA), as this was found to be easy to programme and enabled successful bonding in a relatively short period of time.

The temperature programme used had to be optimised for a specific glass type. It was found that thermally bonding two glass plates with slightly different expansion co-efficients gave the best results. The expansion co-efficient relates to the amount of expansion in μm/°C as measured over a linear temperature range. If the difference between the expansion coefficients of two glass types is too large, one glass will expand more due to heating than the other resulting in the introduction of strain or even physical distortion of the glass. This will not produce a uniform bond. It was also discovered that rapid heating or cooling of the glass should also be avoided. Exposing glass to such conditions did not allow uniform fusing along the plates and was more likely to cause stress features, such as cracks or faults appearing in one or both plates which would often result in the glass spontaneously shattering or shearing. The optimum difference in expansion coefficients has been shown by the glassblower at the University of Hull to be within 0.02 μm/°C. Hence for the miniaturised analysis chip systems used in this work, the two glasses used were Crown White (Align-rite Ltd. Bridgend, Wales) (0.93 μm/°C) and Superwhite B270 (Instrument Glasses, Middlesex, UK) (0.92 μm/°C). Both are types of Crown glass that are noted for their good optical properties, allowing better transmission of light than is normally observed in conventional soda-lime glass. Crown White was used as the material for the manifold base plates prepared by Align-rite Ltd. Superwhite was chosen as the material to manufacture the thicker top plate for the reasons described above.

3.1.4. Temperature programme

In order to minimise strain features in the glass, special attention was paid to the heating up and cooling down periods of the bonding programme. After bonding, a strain viewer could be used to examine the optical patterns to determine whether or not strain had been introduced. Strain is usually introduced into glass as a result of work carried out using the glass such as fusing. The strain viewer consists of a light source such as a bulb and two sheets of polaroid film with their planes at right angles to each other on either side of the object to be viewed. The strain shows up under the viewer as a series brightly coloured areas that relate to the type and severity of the strain. Non-strained glass on the other hand is clear. Strain induced into the glass as a result of work carried out on it can often be removed by heating the glass up to its annealing point.

Advice was taken from the glass blowing workshop regarding the correct temperature ranges to bring about uniform bonding. The temperature was allowed to remain at two specific temperatures; the softening and the annealing temperatures, for longer periods of time than the other temperature steps in the bonding programme. The softening temperature is the temperature at which glass becomes molten and in effect begins to move. The annealing temperature is the temperature at which the glass bonds to another (glass) medium. For the glass in question, the softening temperature was found to be ~700°C and the annealing temperature ~505°C. We were advised to ensure that these temperatures were reached slowly, using some pauses at in-between temperatures to prevent rapid heating or cooling occurring. As there were six possible different set temperature slots available in the programmer, it was decided that the profile should be as follows:

The initial temperature was 75°C, then this was increased to 150°C, before an increase to the highest temperature of 680°C, at which the temperature remained constant for at least one hour. From the maximum temperature, the heat was dropped slowly to 630°C and then through 570°C to 505°C, the temperature nearest the annealing temperature. After another longer pause at 505°C, the oven was then switched off and allowed to cool overnight. The furnace was never opened until the temperature fell to at least 100°C or below.

The length of time the temperature remained constant at each setting was determined by trial and error. The eventual programme for the Crown glass miniaturised analysis system chips with thicker top plates looked like this:

Initially the temperature was held at 75°C for 30 minutes and then at 150°C for 30 minutes before a longer period of 60 minutes at 680°C followed by 30 minutes at both 630°C and 570°C. Finally the temperature remained at 505°C for 60 minutes before the furnace was switched off and allowed to cool.

Later, a newer microwave furnace was purchased, also from CEM with eight temperature slots available. Further heating and cooling stages could then be incorporated if necessary.

The miniaturised analysis chip systems were originally placed facing upward, onto an upturned quartz ashing pot (CEM Corporation, Matthews, USA), with the top plate on top of the manifold base. The ashing pot provided a flat level on which to rest the two glass plates and keep them clean by keeping them from the dust on the furnace floor. In addition to this, it also ensured that the glass did not retain too much heat, by effectively insulating it from the furnace floor. However, because the ashing pot had a pattern imprinted onto the base, this pattern was often picked up and retained on the glass after the bonding was complete. This patterned base was not ideal for

increasing clarity during optical measurements and although sanding down the surface of the ashing pot reduced the degree of imprint transferred to the miniaturised analysis system base, it was still not perfect.

After the arrival of the second furnace, clay slabs were also used to determine their potential as a flat surface on which to bond the miniaturised analysis system chips. The clay was rolled out into flat slabs of various sizes with an approximate thickness of 6 mm and fired in the microwave furnace prior to use in the bonding process using a programme consisting of six temperature slots and including a slot at 800°C for 60 minutes. The clay was then left to cool before use.

The clay slabs provided an excellent, flat base for the miniaturised analysis system bonding. However it was discovered that clay retained heat well, thus producing the effect of prolonged exposure to the highest temperature with the result that the miniaturised analysis system chips became disfigured during the bonding process and the capillaries often disappeared. Hence further optimisation of the temperature programme was necessary to reduce the length of time which the temperature remained at 680°C. The final optimised temperature programme for bonding miniaturised analysis system chips, using the clay placed on top of the ashing pot, was as before, but with the temperature remaining at 680°C for five minutes only.

The top plate was secured in position along the edges where the two plates meet using Blu-tack (Bostik, Leicester, UK). This ensured that the heavier top plate did not move slightly over the surface of the manifold of the lower plate while the two glass plates were being placed into the furnace. The Blu-tack dehydrated during the bonding process to form a white powdery like substance, which usually dropped to the floor of the furnace before the end of the cycle. It did not affect the bonding procedure, nor did it enter the channels of the miniaturised analysis system chip.

Small traces were sometimes found along the edge of the finished miniaturised analysis system chip. These were removed using a wet cloth. The furnace door was not opened at all during the bonding process and not before the temperature fell below 100°C. On removal from the furnace the miniaturised analysis system chips were usually tested to ensure that all capillaries and reservoirs were water-tight and that the bonding procedure had been satisfactory. All the reservoirs were filled with water and the level of the water noted at regular time intervals. If, after approximately 20 minutes, there was no change in water level, the bonding was deemed to have been successful. If necessary, the miniaturised analysis system could be put back into the furnace and the procedure repeated. If the bonding procedure had been successful, the miniaturised analysis system chips were robust and usually had a long life span. Impaired performance of a miniaturised analysis system as a result of use could be overcome even though the two parts of the miniaturised analysis system cannot be separated once firmly bonded. A concentrated nitric acid wash was used to remove build up of deposited layers on the channel walls and also to help dissolve and remove precipitated particulates. In cases of major channel blockages, the miniaturised analysis system could be returned to a bath of wet etch mixture for a short time to allow partial re-etching of capillary walls.

3.2. Instrumentation

3.2.1. Flow injection analysis system

A conventional FIA apparatus using a PMT for the detection of chemiluminescence[118] was used to find the initial reagent conditions for the determination of codeine described in chapter 4. This apparatus was also used as part of the experimental design work in the luminol reaction described in chapter 5.

3.2.2. Bioluminometer

A bioluminometer was used in this work for some of the CL characterisation experiments. The model used was LB 9500T (Berthold Instruments Ltd, St Albans, UK). A diagram of the layout of the bioluminometer is shown in figure 3.4.

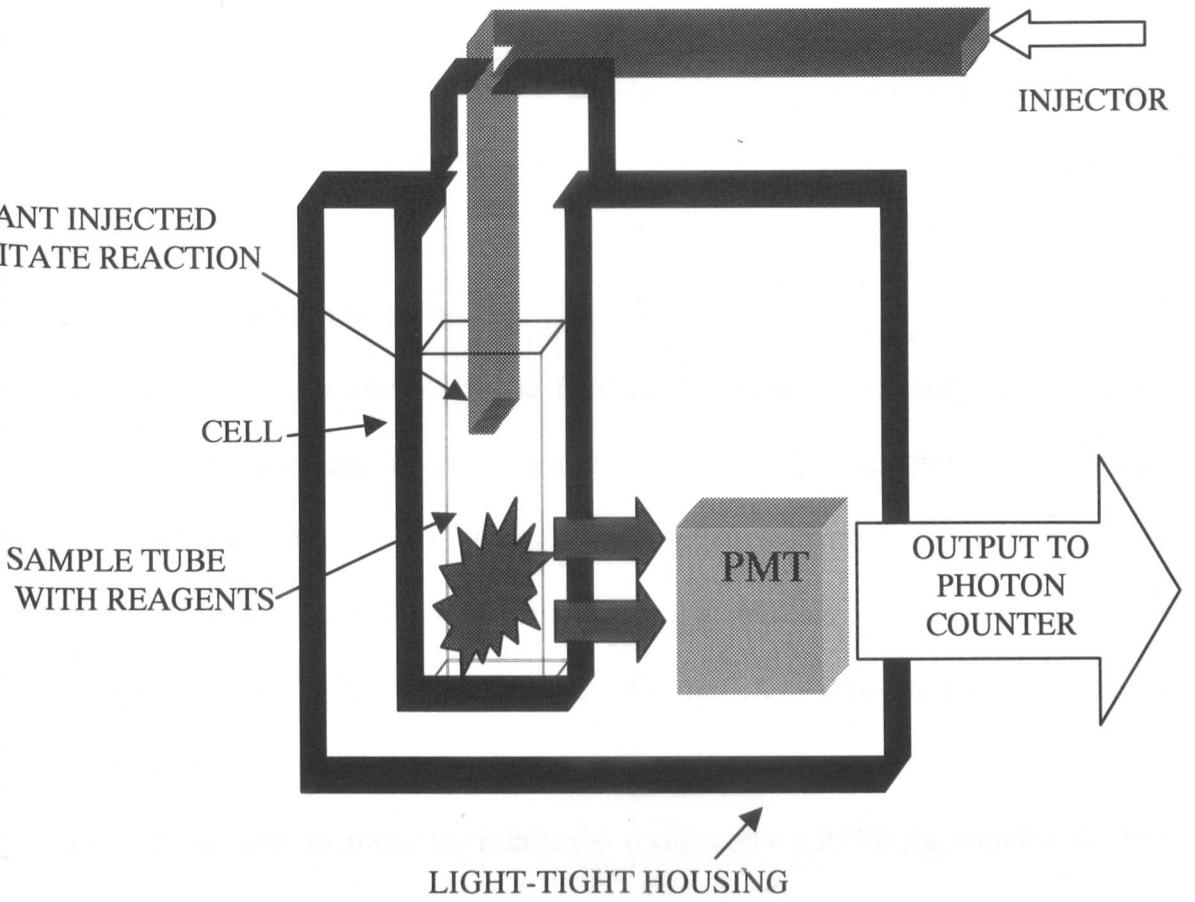

Figure 3.4. Bioluminometer

It consisted of a sample chamber into which a small sample tube containing the analyte solution could be placed. The bottom third of this tube would be directly in front of a detector window behind which a PMT was positioned. The sample chamber was completely light-tight when the housing, which contained the injector fitting, was closed. 100 μl aliquots of the injected (oxidant) solution passed through the tubing on top of the housing and into the sample holder when a small button was pressed and thus, the CL reaction was initiated. A digital readout displayed the CL emission intensity, in photon counts per second, every 2 seconds. This apparatus was used to determine the relative CL intensities of sets of reagents in both the tris(2,2'-bipyridyl)ruthenium (II) and the luminol reactions. It was particularly useful in the

experimental design work described in chapter 5 for determining the effect of various surfactants on the CL emission levels.

3.2.3. Instrumentation set-up

In order to generate electroosmotic flow in the miniaturised analysis system, the application of a voltage across a channel was required. The electrodes used were made in-house using 2.5 cm lengths (10 mm exposed length in the solutions in the reservoirs) of 0.15 mm diameter platinum wire sealed into a plastic pipette tip with silica gel compound (RS Components Ltd, Corby, UK). They were inserted into the solutions contained in the reservoirs.

Blu-tack was used to mount the miniaturised chips onto a PTFE rig, which had a hole in the base and was manufactured in-house. The PTFE rig ensured the miniaturised analysis system remained stable and in the same position when the electrodes were in place. The miniaturised analysis system and PTFE rig were contained within an isolation box, built in-house, which was essential to ensure safe working at high voltages. The power was automatically cut off once the box lid was opened. The isolation box also ensured that the reaction was free from external electrical and light interferences.

A power supply (Advance Hivolt, West Sussex, UK) with a power output of up to 50 W, voltages up to 30 kV and currents of 1.7 mA was used to apply power to the electrodes. A 1906 model computing multimeter (Thurlby Thandar, Huntingdon, UK) monitored current and voltage. For later work, two power supplies, two sets of electrodes and two multimeters were used. This enabled independent application of two sets of voltages within the one manifold or stopped flow injection of one reagent

stream into another by timed application of voltage at a time, t, after the start of the experiment. A schematic view of the set-up is shown in figure 3.5.

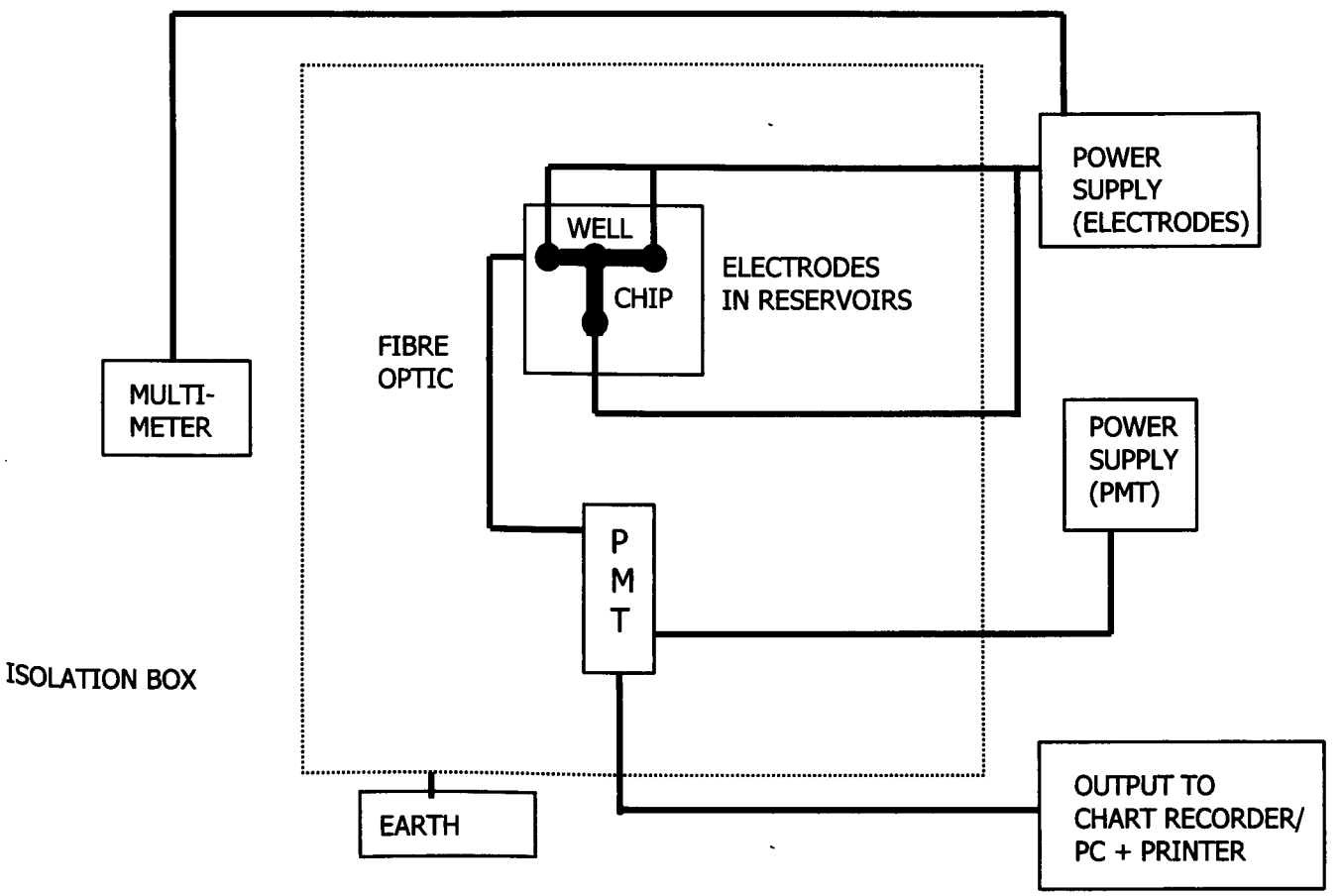

Figure 3.5. Schematic view of overall set-up

3.3. Detection

Four detection systems were evaluated in this work.

3.3.1. Silicon photodiode detector situated below miniaturised analytical system

Initially, a silicon photodiode (S5590, RS Components Ltd., Corby, UK), with a surface area of 2.4 mm^2, was used for detection. A detector box (approx. 15 cm by 10 cm by 5 cm) containing the photodiode was produced in-house which also included its own power supply and amplification system. The amplification of the output could be adjusted from within the isolation box. The detector box had a hole cut into the top through which the photodiode window was visible and the miniaturised analysis system was placed over this window.

The sensitivity of this photodiode was determined by initially carrying out the reaction in a small sample tube with small (~ 1 ml) reagent volumes. The sample tube was placed directly onto a microscope slide placed over the silicon photodiode window. The $Ru(bipy)_3^{3+}$ ($1x10^{-3}$ mol l^{-1}) in sulphuric acid (0.05 mol l^{-1}) and cerium (IV) sulphate ($4x10^{-3}$ mol l^{-1}) solution was placed in the tube. The codeine ($1x10^{-3}$ mol l^{-1}) in acetate (0.01 mol l^{-1}) solution was injected via capillary tubing fed through the side of the isolation box, into the sample tube containing the $Ru(bipy)_3^{3+}$ in sulphuric acid and cerium (IV) sulphate solution. The observed output was shown on a chart recorder. Following successful qualitative detection using this method, the reaction was then transferred to a 'T' manifold chip system shown in Figure 3.4. The concentration of the $Ru(bipy)_3^{3+}$ in the solution was increased to $2x10^{-3}$ mol l^{-1} in order to enhance the CL intensity. The $Ru(bipy)_3^{3+}$ in sulphuric acid and cerium (IV) sulphate solution was placed into one of the reservoirs and the codeine in acetate

solution was again injected using a syringe and capillary tubing, that led to the same reservoir, through the side of the isolation box, in order to bring about the reaction.

The volumes of the $Ru(bipy)_3^{3+}$ ($2x10^{-3}$ mol l^{-1}) in sulphuric acid (0.05 mol l^{-1}) with cerium (IV) sulphate ($4x10^{-3}$ mol l^{-1}) solution and the codeine ($1x10^{-3}$ mol l^{-1}) in acetate (0.05 mol l^{-1}) solution were continuously reduced to determine the sensitivity limits of the detector. The volume of $Ru(bipy)_3^{3+}$ in sulphuric acid proved to be the limiting factor as would be expected. Thus, 3.0 µl codeine in acetate solution and 2.0 µl $Ru(bipy)_3^{3+}$ in sulphuric acid with cerium (IV) sulphate solution produced a smaller peak than 2.0 µl codeine (equating to $2x10^{-9}$ moles codeine) in acetate solution and 3.0 µl $Ru(bipy)_3^{3+}$ in sulphuric acid with cerium (IV) sulphate solution. The peaks were almost instantaneously produced due to the method of injection.

The limit of response for the SPD detector was found during the reaction between 1.0 µl codeine in acetate solution and 2.0 µl $Ru(bipy)_3^{3+}$ in sulphuric acid with cerium (IV) sulphate solution, which was not sufficiently sensitive for analysis on-chip.

The existing silicon photodiode detector was replaced by a larger, more sensitive version (active area 5.8 mm^2) in an attempt to increase the chance of capturing light produced by the reaction. However, the reaction could still not be readily observed even though reagent concentrations were fairly high ($2x10^{-3}$ mol l^{-1} $Ru(bipy)_3^{3+}$ and $1x10^{-3}$ mol l^{-1} codeine).

Unfortunately, using a silicon photodiode as the detector did not prove very successful and while this method of detection would be advantageous to the overall portability of the eventual system, it was felt that a detector with greater sensitivity was required to generate meaningful results.

3.3.2. Miniaturised photomultiplier tube under the miniaturised analysis chip system.

A miniaturised, H5784 Series photomultiplier tube detection system (Hamamatsu, Middlesex, UK) was thus obtained to address this problem. The miniaturised PMT detection system was contained within a smaller, plastic box consisting of two halves sealed using velcro. This plastic box was attached to the base of the inside the isolation box and had a removable front portion to allow access between experiments. A shelving system allowed the miniaturised analysis system to sit on a rack directly above the PMT window. The chip could be slid out of the box to be cleaned or refilled for the next experiment. The rack was securely fastened to ensure that there was no risk of the chip moving during analysis and to improve reproducibility of the measurements by keeping the chip at a known distance from the PMT window. The electrodes could be inserted into the reservoirs through holes in the top of the detection box. The sensitivity of the PMT detection system could be adjusted using an amplification box, manufactured in-house, also located within the isolation box. The set-up can be seen in figure 3.6.

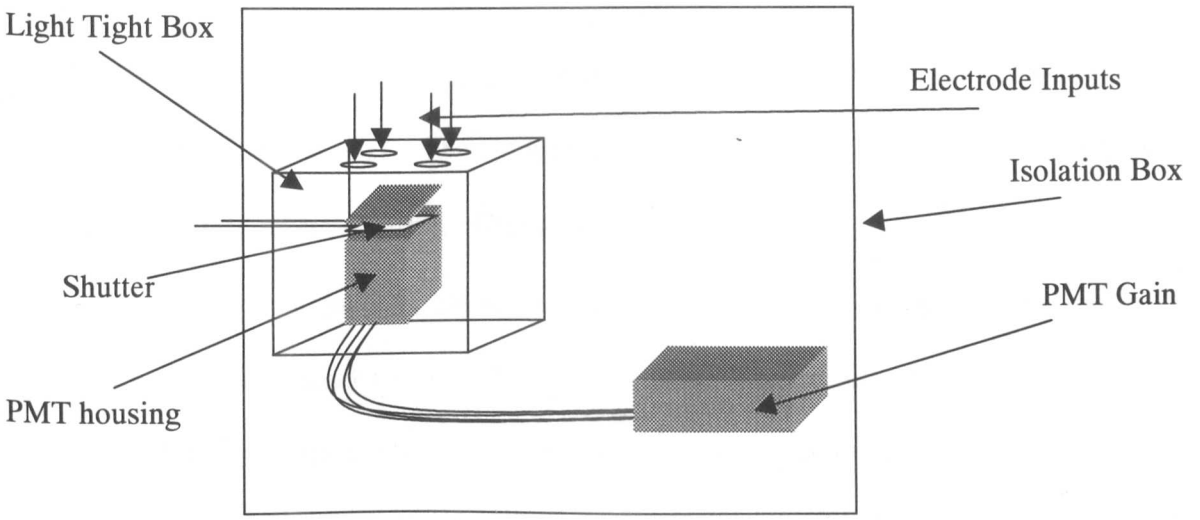

Figure 3.6. Structure of the miniaturised PMT and detector box

The PMT was mounted in casing and while the system was not in use, a foam padded metal shutter covered the PMT window. This shutter could be opened from outside the isolation box, as shown in figure 3.7, without affecting the position of the chip placed on the rack inside the detector box. This meant that the chip could be set up in front of the PMT window. The isolation box was then closed and the shutter was opened from outside the isolation box at the same time as the voltage was applied to begin movement of the reagents and thus initiate the reaction.

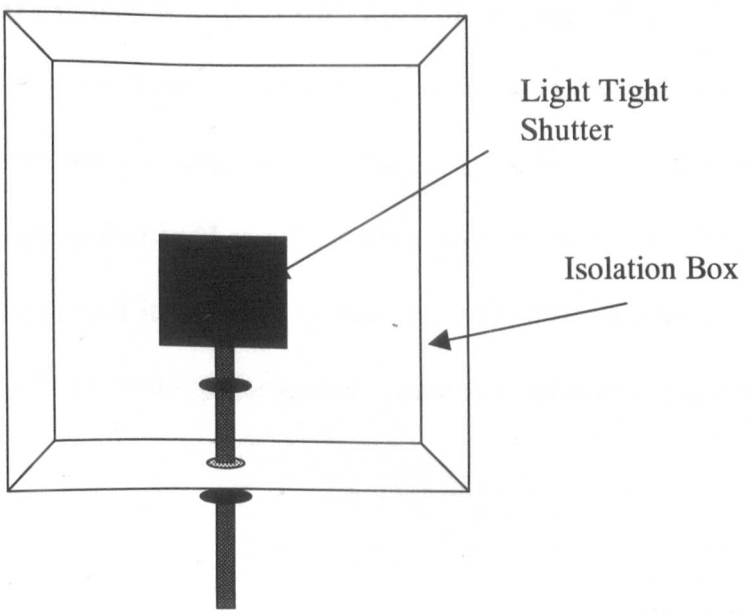

Figure 3.7. Shutter attachment

The wavelength range suitable for detection using the PMT was 300 – 650 nm, with a peak spectral response at a wavelength of 430 nm. The maximum output from the PMT was 10 V with an output offset as anode dark current quoted as ± 3 mV. Output from the PMT detector was fed via a sealed hole in the side of the isolation box to a chart recorder (Chessel BD-40-04, Kipp & Zonen, Netherlands, distributed by EML, Driffield, UK) where the emission intensity of the chemiluminescence produced was monitored by peak height in mV.

Although the sensitivity of the detection was vastly improved using the PMT, chemiluminescence generated from the reaction was not always detected even though the glass chip was positioned directly over the PMT window. It seemed that there were problems with light scattering in the glass chip, which could have been acting as a waveguide and directing some light away from the PMT window. A lot of noise in the form of spikes was also observed on the chart recorder trace. The whole system was earthed to the isolation box and a filter consisting of a capacitor and resistor was later also attached to the PMT output to reduce associated noise.

3.3.3. Miniaturised PMT detection system with fibre optic connection

In order to reduce some of the light scattering away from the detector, a fibre optic was used to gather light from a small area of the chip, where the emission was greatest. Initially, a larger polymer fibre optic with a diameter of 0.5 mm (Optiflex, Doncaster, UK) was positioned in the base of the PTFE rig directly under the chip beneath the area of maximum chemiluminescence intensity, as seen in figure 3.8.

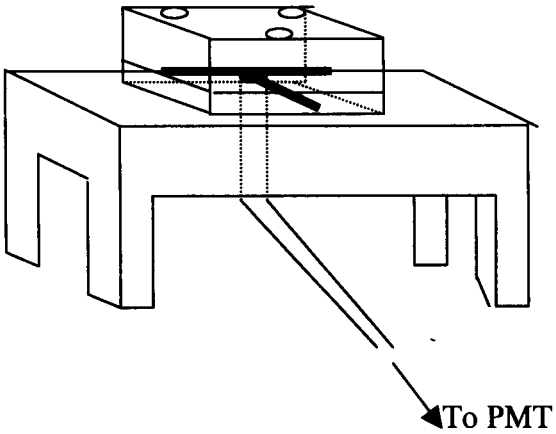

Figure 3.8. Fibre optic positioned under miniaturised analytical system in PTFE rig

The other end of the fibre optic was connected to the PMT detector via a fibre optic adapter (E5776, Hamamatsu, Middlesex, UK). Later, a smaller silica fibre optic with 125 μm i.d. that was housed in a plastic outer covering giving an o.d. of 200 μm (Optiflex, Doncaster, UK) was used. This was attached into the side of the capillary as described in the next section.

3.3.4. Miniaturised PMT detection system with fibre optic inserted directly into the channel

Although the combined use of a fibre optic with PMT detection was very successful, it was felt that the sensitivity could still be improved. The insertion of a fibre optic directly into the channel could potentially improve sensitivity by bringing detection directly into close proximity of the reaction and also by reducing the number of interfaces through which light was required to pass before reaching the PMT.

In order to insert the fibre optic into the channel, a portion of the bonded miniaturised analysis system had to be removed so that the end of the channel led to the outside edge of the finished chip. This was carried out in the glass blowing workshop.

Excess material covering the unexposed end of the channel was then dissolved using a 1:1 mixture of concentrated HNO_3 (5 %) and HF (2 %). The HNO_3 is necessary to remove traces of the white silica fluoride, which forms as a by-product of the etching process. Thorough washing with water was required after treatment with this mixture to ensure that all traces of acid, but particularly HF were removed. Residual HF will continue to etch into the glass if not flushed away, resulting in damage to the capillaries. With repeated treatments using this mixture, the capillary end became sufficiently large enough to allow insertion of a fibre optic (up to 125 μm i.d.) directly into the channel. The outer protective fibre optic coating was removed by dissolving it in paint and varnish remover (Nitromos, Henkel Home Improvement and Adhesive Products, Cheshire, UK) for a few seconds. This did not impair the fibre optic or its optical properties, but allowed sufficient exposure of the inner fibre to allow positioning into the channel. A diamond cutter was used to carefully remove the end of the fibre to provide a flat edge for placing into the channel, which ensured that the maximum amount of light was captured. Great care had to be taken when inserting the fibre optic as the structure was very fragile and liable to easily break off leaving small fragments inside the capillary which were difficult to remove. The fibre optic was secured using glue (Bostik, Leicester, UK). Once this had dried, the whole area was sealed using silicon rubber compound (RS Components Ltd, Corby, UK) which set to form a rigid shell. The chip was then left for 24 hours prior to use.

3.4. Movement of liquid through the channels by EOF

In all cases, the solutions were placed in the reservoirs using a micropippette (Sealpette, Jencons, Leighton Buzzard, UK). Platinum electrodes were carefully introduced into the respective reservoirs and a known voltage was applied to the solutions contained in the reservoirs for a specified time. The mean flow rate per minute was calculated at a specific voltage.

To begin with, the moving analyte in each experiment was injected into reservoir A (+ve) and moved by electroosmotic flow to water or solution held in reservoir B (-ve) (See figure 3.9), however for the determination of codeine all three reservoirs were utilised. The volumes injected varied between 20 and 50 μl, although a volume of 40 μl was discovered to be adequate. A mean value of three measurements was usually calculated unless stated otherwise.

Due to the nature of the reactions involved and the need for light-exclusion, the flow was measured in microlitres $minute^{-1}$ rather than movement along the channel in millimeters $minute^{-1}$. The contents of the reservoir containing the reagent under investigation were measured before and after the experiment and an average value of flow in microlitres per minute with an associated error value was quoted. As differences in miniaturised analysis system dimensions are not taken into account, each quoted value relates to the chip on which the flow rate determination was carried out only.

3.4.1. Joule heating

Joule heating was observed to be a problem at higher voltages. This was due to increased resistance to flow at higher voltages. Hence, the lower the optimum voltage, the more reproducible the flow rates were likely to be.

3.5. Miniaturised analysis system manifold designs

As described in section 1.3.2, flow rates can be regulated by controlling factors such as the voltage, the zeta potential and hydrodynamic flow. In order to minimise hydrodynamic flow the height of liquid in the reservoirs and the position of the electrodes in these reservoirs in particular, should be carefully monitored. 'Floating reservoirs', i.e. surplus reservoirs which are not involved in the reaction should therefore be avoided, if possible, in the interests of experimental reproducibility. With this in mind, a large amount of this work was carried out in 'T' shaped chip manifolds, as shown in figures 3.3 and 3.9. In addition to the three reservoirs shown in figure 3.3, figure 3.9 also depicts the mixing well added to ease detection of the TBR reaction as explained in section 3.6. This well was situated at the point where the reagents met and reacted and was equally as deep as the reservoirs, though 1 mm narrower than the reservoirs, which were 3 mm in diameter.

The voltages and polarities used depended on the reagents and are therefore indicated in the relevant experimental sections in chapters 4 and 5. The 'T' manifold with mixing well design was used for most of the work described in chapter 4.

For the luminol work described in chapter 5, a larger manifold was specially designed, which can be seen in figure 5.1. This was devised partly to enable easier incorporation of a fibre optic into the channel as detailed in section 3.3.4.

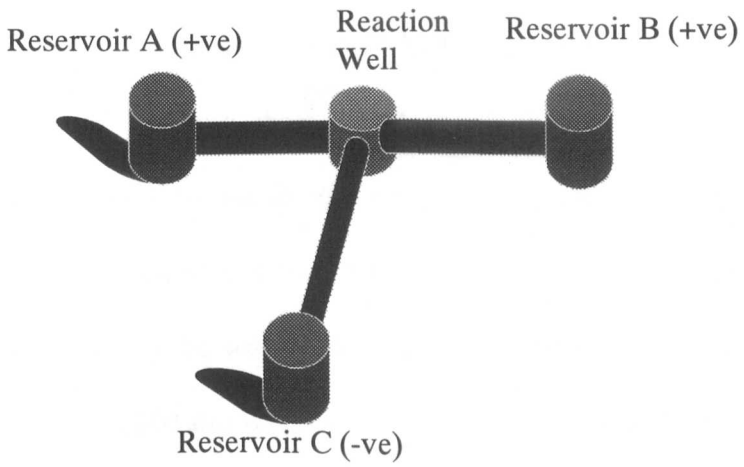

Figure 3.9 'T' manifold miniaturised analysis system with well

Additional work for the luminol reaction was carried out using a 'starburst' design in which five channels met at a central point as shown in figure 3.10.

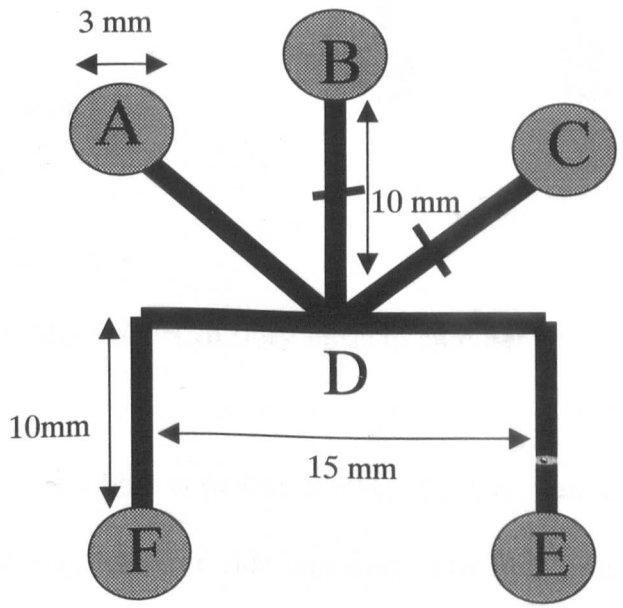

Figure 3.10. 'Starburst' design

The incorporation of the fibre optic into the channel was initially carried out using half of one of the original plate designs as shown in figure 3.11. It was easier to use

this design than the 'starburst' design which was being used for studying the reaction as it consisted of one long channel AD, in which to place the fibre and a sufficient number of reservoirs to use for the reagents. In addition to this, parts of the chip could be easily removed in order to increase access to the channel without having a detrimental effect on the rest of the manifold. The process proved to be successful with a fibre optic (200 μm o.d. and 125 μm i.d.) inserted at point A and extended to the intersection of capillary B with the main channel AD as shown in figure 3.11.

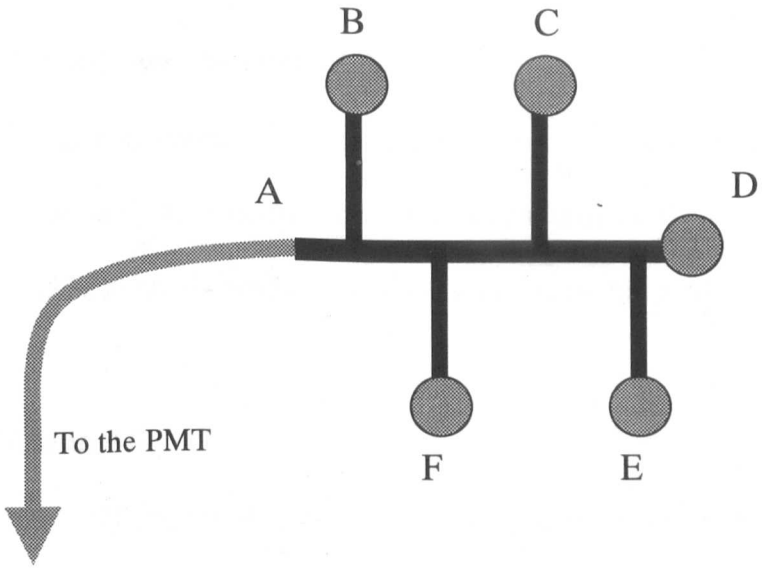

Figure 3.11. Manifold with fibre optic in channel

Incorporation of a fibre optic into another chip was then tried. This was a portion of a 'starburst' design with one side removed. The fibre optic (62 μm i.d.) was inserted into the main horizontal channel.

3.6. Maximising output

As previously stated, reactions at interfaces are far more important in miniaturised systems than reactions in the bulk. Maximising the interface should therefore lead to increased product. In the case of chemiluminescence detection in a miniaturised analysis system, maximising the reaction interface should increase the amount of light emitted and hence the quantum yield of the reaction should also increase. In addition to this, the ability to monitor the production of light exactly where it arises from an interaction at the interface should substantially increase the amount of light captured and as a result, lower the limits of detection.

There are several methods of increasing mixing using manipulation of reagents in a miniaturised analysis system, as described in the introduction.

Some specific methods used to optimise detection in this work are described here.

3.6.1. Mixing well

To improve mixing of reagents, a well (an additional reservoir positioned at the channel interface) was included into a T-manifold as shown in figure 3.9.

The flowing reagents converged on the well from opposite sides of the miniaturised analysis system, with the reagents interacting and reacting directly in front of the fibre optic detector. The well was useful in that the reagents had to flow to it and thus by regulating the flow rates, it was possible to ensure optimum mixing. In addition to this, it was known where the reaction would take place, thus ensuring that the fibre optic was receiving the maximum amount of light emitted. This design was used with success in the determination of codeine as described in chapter 4.

Although, the use of the mixing well was good for the initial experiments that enabled the feasibility of CL detection in a miniaturised analysis system to be

determined, it was felt that the design was primitive and the sensitivity required improvement.

3.6.2. Fibre optic in channel

As described in section 3.3.4, it was decided that incorporation of the fibre optic directly into the capillary would increase the sensitivity of the analysis, by allowing the light to be monitored as it was produced at the reacting interface between the two solutions in a channel. The light produced would then pass directly into the fibre optic, rather than passing through a number of glass or air interfaces before reaching the detector. Although, light would be required to pass through a short (up to 1.0 mm) slug of solution in the channel before reaching the end of the fibre optic, it was felt that this method would still prove to be more sensitive than the well design. This approach was used for some of the work described in chapter 5.

3.6.3. Use of silica microstructures

The theory relating to hydrodynamic flow is described in detail in section 1.3. As discussed in sections 1.3.1.2 and 3.5, the effects of hydrodynamic can be minimised practically by avoiding the presence of 'floating reservoirs', and by paying careful attention to electrode positioning and reservoir liquid heights. However, these measures, while certainly helpful do not completely remove all hydrodynamic flow effects. One practical method, developed at Hull, is the introduction of a device called a frit[208] into the capillary which allows better control of the reagent movement by the electric field and effectively prevents back pressure and hydrodynamic flow.

A frit is a tiny, porous silica microstructure[208]. It has a highly porous structure that resembles the structure of a sponge as can be seen in the scanning electron microscopy picture shown in figure 3.12.

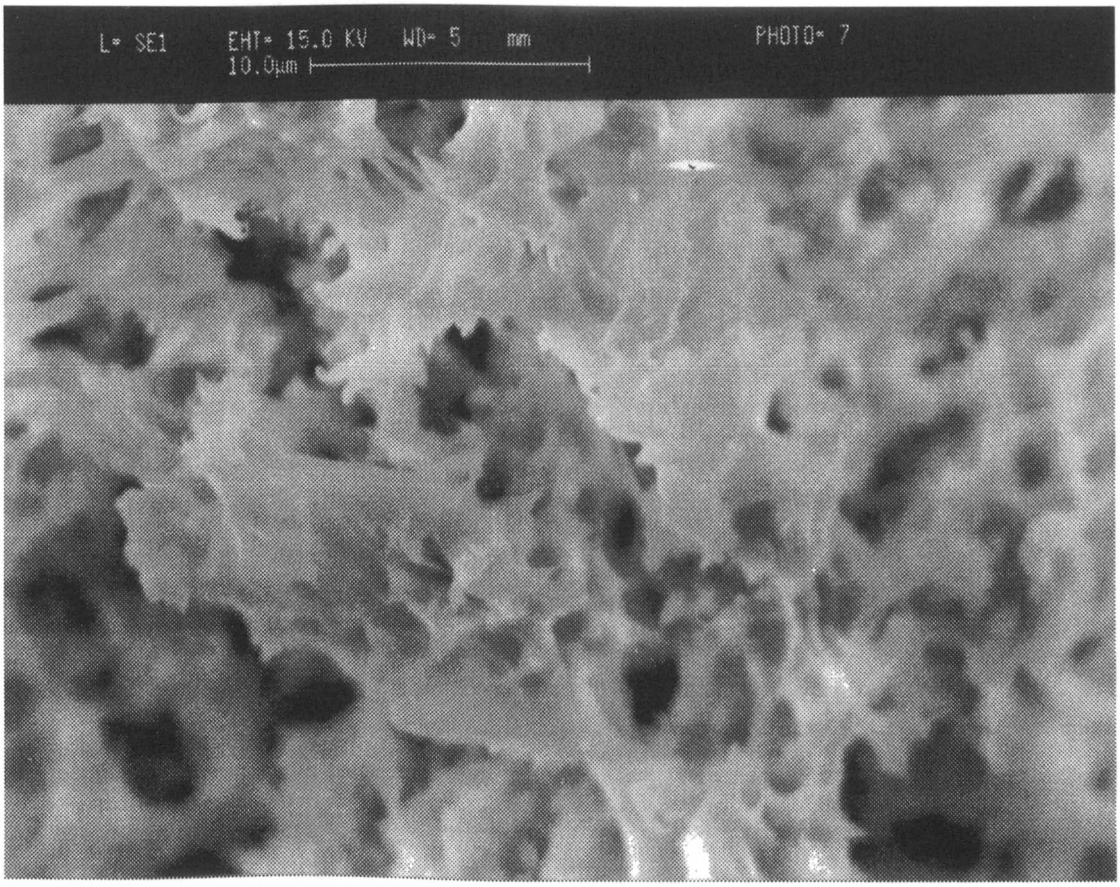

Figure 3.12. SEM of frit structure

The frits were prepared using potassium silicate (21% SiO_2, 9% K_2O, Prolab, Hampshire, UK) and 98% formamide (Avocado Research Chemicals Ltd., Heysham, Lancashire, UK) at room temperature. The two reagents (140 µl silicate and 18 µl formamide or any multiple of these amounts) were mixed vigorously for approx. 30 seconds. Small amounts of the mixture were applied to specific sites in the channels using a pipette. The rest of the manifold area was covered in blu-tack to prevent excess coverage. The plate was then baked at 100°C to harden the frit mixture that

formed as white, solid, porous deposits in the channels. Excess frit mixture was removed using a combination of scalpel, fine mesh sandpaper and KOH solution. Care had to be taken to ensure that the surface of the glass did not become marked or scratched in any way, as this would have detrimental effects in the bonding process. The finished frits were also washed well with de-ionised water before they were thermally bonded. This ensured no excess unreacted frit mixture remained to block the frit when it was re-hyrated. Further deposition of silica in the channels as a result of a new reaction between unreacted reagents would block the frit after the miniaturised analysis chip system had been bonded and render it useless.

Frits were employed as part of the cobalt determination using the luminol reaction as described in chapter 5.

3.7. Removal of waste

The waste was removed at the end of each reaction using syringes. The microlitre syringes used for this purpose did remove the vast majority of waste solutions and any remaining solution were removed when the miniaturised analysis system was washed out well with water between each experiment. Positive pressure was applied to one or more reservoirs to force the wash solution through the channels at least twice to ensure the minimum amount of 'carry over' from one run to the next was observed. Excess surfactant build-up was removed in the same way using a dilute nitric acid mixture.

3.8. Conclusions

The development work described in this chapter resulted in robust, practical, miniaturised analysis chip systems and a sensitive detection system for chemiluminescence measurements. Several novel developments were described in this chapter. These included the use of thicker top plates that enabled the reservoirs to be contained within the single unit structure. This design was intended to prolong the lifetime of the chip system and increase the available reagent volumes. The use of a microwave furnace for thermal bonding of the two glass plates was also employed for the first time and additionally the detection of the chemiluminesence produced in the chip system was monitored from underneath the chip base.

The instrumentation described in this chapter was then used to study the chemiluminescent systems based on the tris(2,2'-bipyridyl)ruthenium (II) reaction (chapter 4) and the luminol reaction (chapter 5).

4. Tris(2,2'-bipyridyl)ruthenium(II) (TBR) reaction

This chapter describes the initial application of a CL reaction into a miniaturised analysis system. The aims of this work were to investigate whether it would be possible to observe chemiluminescence in a miniaturised analysis system, to examine the relative sensitivity of such a device and to determine how the best optimisation of on-chip light production and detection could be achieved.

4.1. Introduction

The tris(2,2'-bipyridyl)ruthenium (II) reaction was selected as the test reaction to optimise the miniaturised analysis system due to its high chemiluminescence emission intensity[209]. In addition, the analyte solution had a pH of approximately 6, which lies in the correct pH range for mobility by electroosmotic flow (EOF)[21].

4.2. Background

4.2.1. Tris(2,2'-bipyridyl)ruthenium (II) chemiluminescence reaction

A detailed discussion concerning the structure, chemiluminescence reaction mechanism and applications is covered in section 2.3.

4.3. Experimental

4.3.1. Instrumentation

The apparatus was set up as described in chapter 3. Most of the work was carried out using a 'T'- manifold, which had three reservoirs and a fourth narrower well, at the intersection of the 'T', as described in chapter 3. A schematic of this design can be seen in figure 3.9.

4.3.2. Reagents

All the chemical standards and reagents used were analytical grade unless stated otherwise and the water used was high purity de-ionised (18 M Ω cm resitivity) (Elgastat UHQ PS, Elga, High Wycombe, UK).

Tris(2,2'-bipyridyl) ruthenium (II) chloride hexahydrate (TBR) ($1x10^{-3}$ mol l^{-1}) was obtained from Fluka (Gillingham, Dorset, UK) and made up in sulphuric acid solution (0.05 mol l^{-1}) (Fisher Scientific Ltd., Loughborough, UK). The overall pH of this solution was pH 2-3.

The oxidising agents used were cerium (IV) sulphate 4-hydrate ($4x10^{-3}$ mol l^{-1}) (BDH, Merck, Lutterworth, Leics. UK) made up in de-ionised water and lead (IV) oxide (Merck, Poole, UK). The codeine ($1x10^{-3}$ mol l^{-1} stock solution) was purchased from Sigma Aldrich (Gillingham, Dorset, UK) and was made up in sodium acetate (0.01 mol l^{-1}) solution, pH 5.8, with the sodium acetate obtained from Merck (Poole, UK). Tri-n-propylamine (TPA), 98%, ($1x10^{-4}$ mol l^{-1}) was obtained from Avocado Research Chemicals Ltd., (Heysham, Lancashire, UK). The surfactants used were Triton X-45, Triton CF-10, (both from Fluka, Gillingham, Dorset, UK), sodium n-dodecyl sulphate (SDS) (Lancaster, Morecambe, UK), Tween 80, Tween 20 (both from Fluka, Gillingham, Dorset, UK) and cetyltrimethylammonium bromide (CTAB) (BDH, Merck, Lutterworth, Leics., UK).

4.3.2.1. Codeine as the analyte

The analyte chosen for this reaction was codeine. Codeine is an amine, closely related in structure to both morphine and heroin, as shown in figure 4.1, and is commonly used as a painkiller[210].

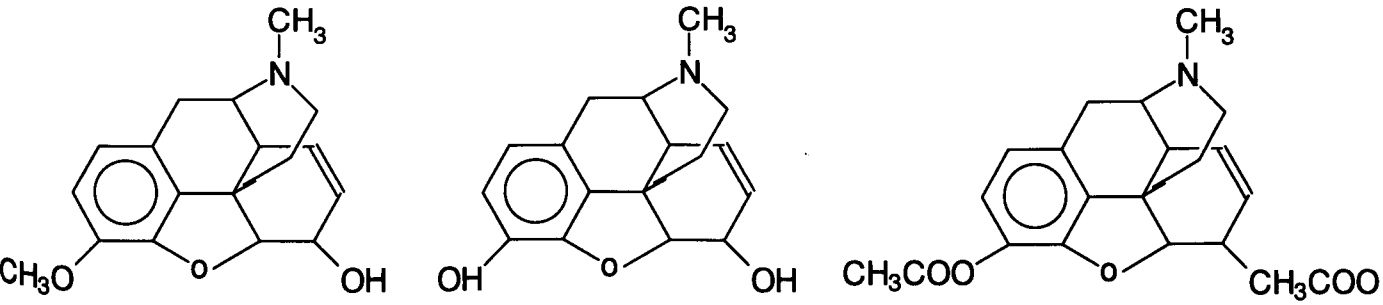

Figure 4.1. Chemical structures of codeine, morphine and heroin

Neil Barnett *et al.* reported a very intense CL emission for a codeine concentration of $1x10^{-5}$ mol l^{-1} using the TBR reaction that was observed by the human eye[157]. The codeine was made up in sodium acetate solution, which had a pH of 5.8.

4.3.3. Procedure

Each manifold had to be characterised to determine flow rates for specific reagents at known concentrations and pH. A mean flow rate in microlitres $minute^{-1}$ was determined for a specified reagent over a range of voltages, as described in section 3.4.

4.3.3.1. Oxidation of tris(2,2'-bipyridyl)ruthenium (II), ($Ru(bipy)_3^{2+}$)

Oxidation of the orange $Ru(bipy)_3^{2+}$ to the active green $Ru(bipy)_3^{3+}$ is required to allow the reaction with the analyte to occur. There are several oxidants that can be used to carry out this step. Lead (IV) oxide (PbO_2) and cerium (IV) sulphate 4-hydrate were investigated in this work. Initially solid lead (IV) oxide was chosen[157] and this was shaken with the ruthenium in acid mixture. On standing, the lead compound fell to the bottom of the container allowing most of the upper liquid layer

to be siphoned off. Filtration of this mixture to remove small lead (IV) oxide particulates was sometimes necessary, otherwise the $Ru(bipy)_3^{3+}$ in sulphuric acid solution was injected directly onto the chip. However, in the absence of the lead (IV) oxide, partial reduction of the green $Ru(bipy)_3^{3+}$ to the orange $Ru(bipy)_3^{2+}$ form began to occur.

The cerium (IV) sulphate was originally mixed with the $Ru(bipy)_3^{2+}$ in acid solution in a ratio of five parts $Ru(bipy)_3^{2+}$ in sulphuric acid mixture to two parts cerium (IV) sulphate solution, though later the concentrations used were altered to three parts $Ru(bipy)_3^{2+}$ in sulphuric acid mixture to one part cerium (IV) sulphate solution, as it was felt that less cerium (IV) was needed to achieve stable $Ru(bipy)_3^{3+}$. The cerium (IV) sulphate mixture remained in solution with the $Ru(bipy)_3^{3+}$ in acid mixture during the reaction with the analyte so negating the need to filter the solution prior to use.

There were several apparent advantages of using cerium (IV) sulphate 4-hydrate rather than lead dioxide as the oxidant. The $Ru(bipy)_3^{3+}$ remained stable in solution for up to two hours and there were no particulates to remove prior to injection onto the chip.

4.3.3.2. Codeine calibration

A series of standards were prepared by dilution of the codeine stock ($1x10^{-3}$ mol l^{-1}) solution using sodium acetate (0.05 mol l^{-1}) solution from $1x10^{-4}$ to $1x10^{-9}$ mol l^{-1}. These were analysed using the manifold design shown in figure 3.9 and using the set-up shown in figure 3.8. The codeine in acetate solution was injected into reservoirs A and B (both +ve), with the $Ru(bipy)_3^{3+}$ mixture in reservoir C (-ve). Initial quantification of the CL response was carried out using the $Ru(bipy)_3^{3+}$ in sulphuric

acid with cerium (IV) sulphate solution. The reaction occurred in the reaction well, positioned at the intersection of the three channels. Each run lasted approximately 2 minutes. These results are discussed fully in section 4.5.

4.4. Results and Discussion

4.4.1. Miniaturised analysis system design

Several designs were investigated during this work, but as described in chapter 3, the 'T'-piece manifold proved to be the most suitable design for the analysis. Using the 'T' manifold with the well, shown in figure 3.9 it was easy to ensure that the reaction was occurring above the point where a fibre optic was placed to transmit the light to the PMT. This set-up proved to be ideal for studying the conditions required for CL reactions in a miniaturised analysis system. Compromise conditions were required for the reaction between those conditions needed for good electroosmotic flow of the bulk solution and those conditions needed for a high CL emission intensity.

4.4.2. Effect of oxidising agent on initial intensity of CL emission intensity

A series of experiments were carried out concurrently with the flow rate work to determine the effect of varying the concentrations of the both $Ru(bipy)_3^{3+}$ in sulphuric acid and the oxidising agents, lead dioxide cerium (IV) sulphate, on the initial chemiluminesence intensity. Eight experiments were performed using the bioluminometer.

Two sets of four codeine solutions containing concentrations of codeine at $1x10^{-3}$ mol l^{-1}, $5x10^{-4}$ mol l^{-1}, $1x10^{-4}$ mol l^{-1} and $5x10^{-5}$ mol l^{-1} in 0.05 mol l^{-1}acetate solution and two sets of four solutions of $Ru(bipy)_3^{2+}$ in sulphuric acid solution with $Ru(bipy)_3^{2+}$ concentrations of $2x10^{-3}$ mol l^{-1} , $1x10^{-3}$ mol l^{-1}, $2x10^{-4}$ mol l^{-1} and $1x10^{-4}$

mol l^{-1} in 0.05 mol l^{-1} sulphuric acid were used. One set of $Ru(bipy)_3^{2+}$ in sulphuric acid solutions was mixed with cerium (IV) sulphate solution in order oxidise the $Ru(bipy)_3^{2+}$ to $Ru(bipy)_3^{3+}$ immediately prior to measurement and the other set of solutions was shaken with PbO_2 immediately prior to measurement. Commencing with the lowest concentrations, each set of $Ru(bipy)_3^{2+}$ in sulphuric acid solutions was then placed sequentially into the sample chamber of the batch luminometer and the corresponding codeine solution was sequentially injected. The emission was recorded in photon counts per second every five seconds, commencing five seconds after the codeine solution was injected, for a period of five minutes. The results of the addition of the four codeine solutions to the four concentrations of $Ru(bipy)_3^{3+}$ solutions are shown in figures 4.2 and 4.3.

The results show that at higher concentrations of codeine in acetate solution and $Ru(bipy)_3^{3+}$ in sulphuric acid solution, using PbO_2 rather than cerium (IV) sulphate generally produced a greater initial intensity of light, while at lower reagent concentrations the opposite was generally true. However, the overall lifetime of the emission produced using the cerium (IV) sulphate was longer than that produced using PbO_2. The lifetime effect was observed to be greater with the higher $Ru(bipy)_3^{3+}$ concentrations. At lower concentrations of $Ru(bipy)_3^{3+}$, the effect that the cerium (IV) sulphate had on the lifetime of the emission was virtually negligible.

Since, it was more important to generate the maximum intensity of the initial CL emission, it was decided that PbO_2 should be used as the oxidising agent from then on.

The reduced intensity of CL emission observed from the solutions, at higher concentrations, containing cerium (IV) sulphate could possibly be due to a quenching effect by high concentrations of the cerium (IV) sulphate solution.

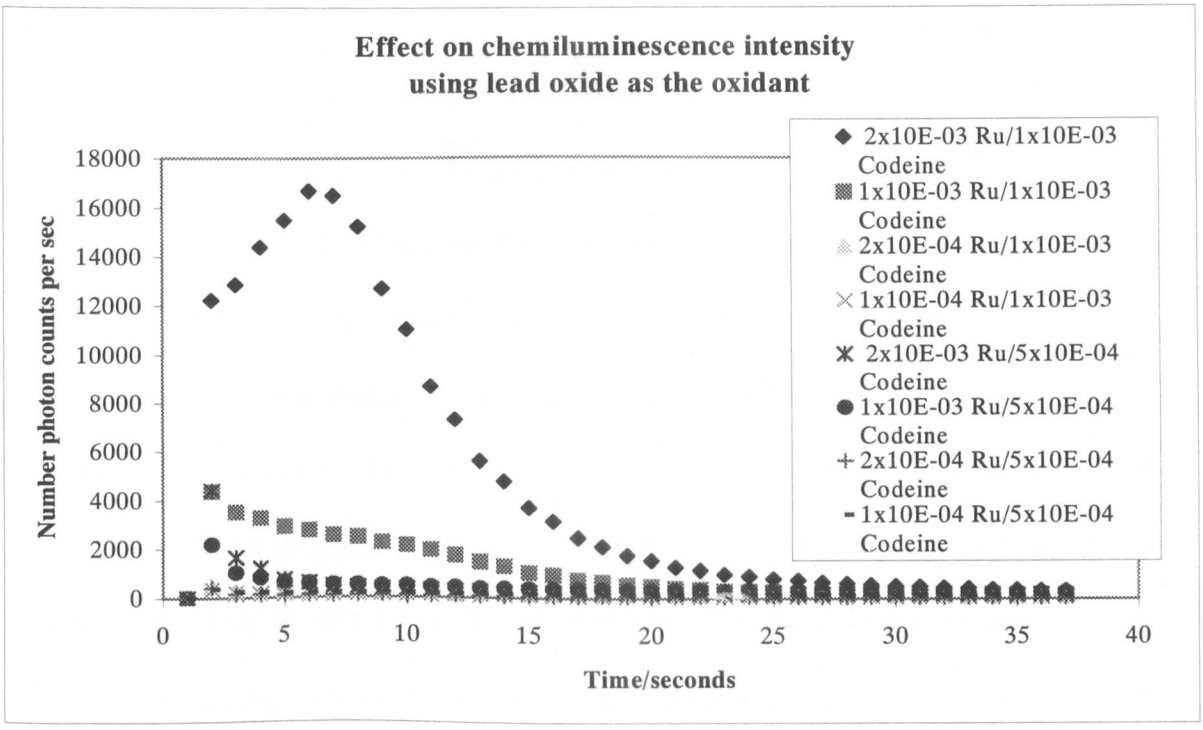

Figure 4.2. Comparison of CL emission intensity using lead oxide as the oxidant

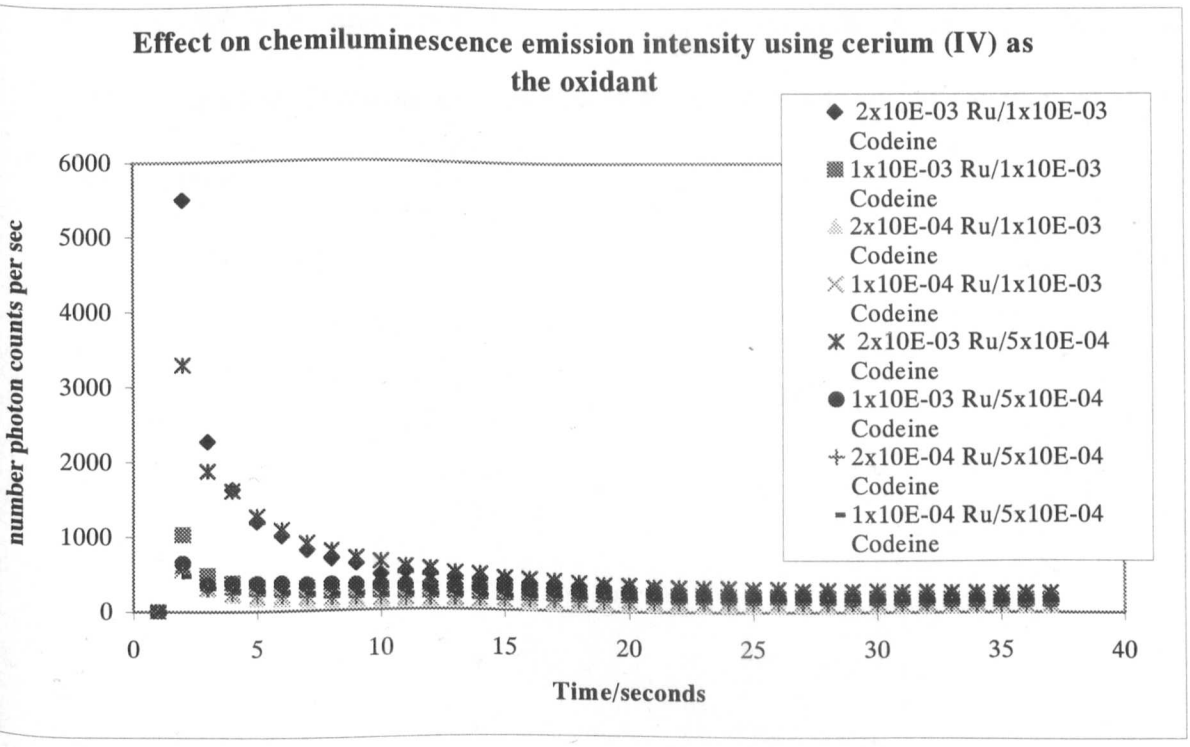

Figure 4.3. Comparison of CL emission intensity using $1x10^{-4}$ mol l^{-1} cerium (IV) sulphate solution

4.4.3. Characterisation of reagent flow rates

4.4.3.1. Movement of codeine in acetate solution

The effect of applied voltage on the flow rate of codeine in acetate solution was studied as it flowed from reservoir A towards the $Ru(bipy)_3^{3+}$ in sulphuric acid with cerium (IV) sulphate solution in reservoir B (see figure 3.9).

High voltages tend to cause bubble formation and heating effects, as was found to be the case in this experiment, hence a voltage range of 100-500 V was chosen for the flow rate study, as can be seen in figure 4.4. The flow rate increased over the experimental range, reaching an optimum of 1.8 $\mu l\ min^{-1}$ at 400 V before tailing off due to a heating effect. A mean volume change for three runs at each voltage was plotted for the movement of codeine ($1x10^{-4}$ mol l^{-1}) in acetate solution (0.01 mol l^{-1}). The flow rates showed good reproducibility with an associated error of approximately 6% up to 300 V, however above this the error increased as the voltage increased up to 20%. A mean (n=3) maximum flow rate of 1.8 ± 0.2 $\mu l\ minute^{-1}$ at a voltage of 400V was obtained.

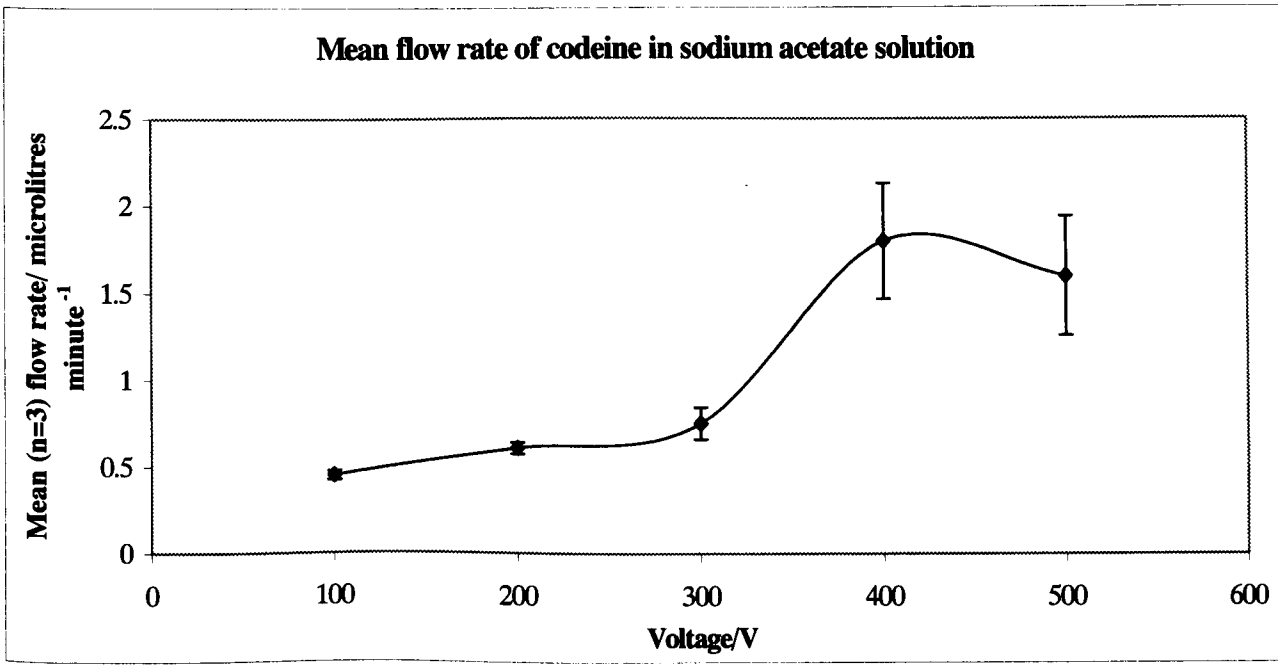

Figure 4.4. Flow rate of codeine in acetate solution

4.4.3.2. Movement of the $Ru(bipy)_3^{3+}$ in sulphuric acid mixture

The ruthenium complex was more difficult to move using the conditions described by Barnett *et al.*[157] because it was made up in sulphuric acid and had a pH of less than 3. As a result of the negligible flow rate observed, conversion to the reduced form, $Ru(bipy)_3^{2+}$, appeared to take place in the capillaries as the experiment was carried out. An initial approach to solve this problem was to premix the $Ru(bipy)_3^{2+}$ in acid with cerium (IV) sulphate 4-hydrate as used by Neil Barnett *et al.* in the determination of oxalate[161], which oxidised the $Ru(bipy)_3^{2+}$ to $Ru(bipy)_3^{3+}$, in an attempt to increase the EOF by increasing the pH.

However, although mixing the $Ru(bipy)_3^{2+}$in sulphuric acid mixture with the cerium (IV) sulphate solution appeared to prolong the lifetime of $Ru(bipy)_3^{3+}$ species, it failed to substantially increase the pH and thus improve the EOF rate, in fact it was uncertain whether there was any movement at all. An optimum mean (n=3) flow rate of 0.25 ± 0.25 μl min^{-1} at a voltage of 600V was obtained for a 3:1 v/v mixture of

$1x10^{-3}$ mol l^{-1} $Ru(bipy)_3^{3+}$ in 0.05 mol l^{-1} sulphuric acid and $4x10^{-3}$ mol l^{-1} cerium (IV) sulphate in water as can be seen in figure 4.5.

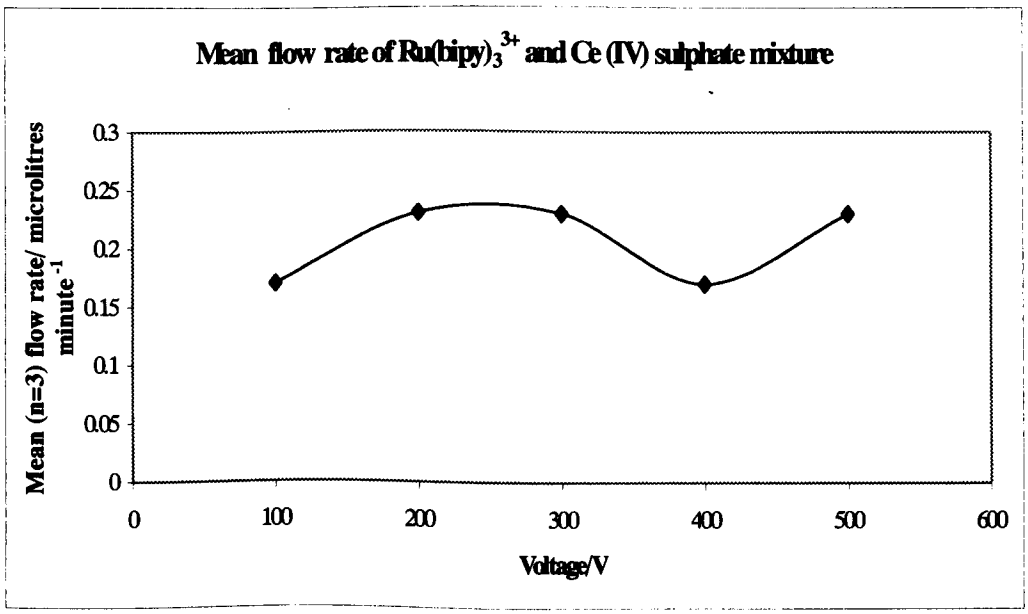

Figure 4.5. Trendline of flow rate of ruthenium and cerium mixture

As a consequence of these findings and the low CL emission observed with cerium (IV) sulphate as the oxidising agent, this method was discarded.

Hence in order to try and encourage faster EOF, it was decided to determine whether the pH of the $Ru(bipy)_3^{3+}$ in sulphuric acid solution, could be increased, without excessively decreasing the stability or the lifetime of the $Ru(bipy)_3^{3+}$ species.

Although $Ru(bipy)_3^{3+}$ species was found to show reasonably good stability in concentrations of sulphuric acid solution down to $5x10^{-4}$ mol l^{-1}, the pH was still too low to enable greater EOF mobility. Addition of aliquots of acetate solution to increase the pH as part of the dilution of the mixture was then tried but this reduced the overall stability and the lifetime of the $Ru(bipy)_3^{3+}$ species quite substantially.

Hence, another method had to be found to improve the flow rate of the $Ru(bipy)_3^{3+}$ species which is described in section 4.4.4.

4.4.4. Use of surfactants

It was envisaged that the two sets of reagents could eventually be made to meet in a capillary resulting in a reaction producing light that could be monitored from under the chip. However, due to the negligible flow rate of the $Ru(bipy)_3^{3+}$ in sulphuric acid with cerium (IV) sulphate solution, it was discovered that this would be difficult to achieve. Although, the codeine in acetate solution had been successfully moved in the miniaturised analysis system by EOF, it was felt that ideally both sets of reagents should be mobilised.

As previously stated in sections 1.3.4 and 2.5, surfactants have been found to effect both the EOF and the luminol CL reaction, therefore it was decided to investigate their effect in the miniaturised analysis system. A surfactant or combination of surfactants was required that would, at the correct concentrations, enhance the EOF, without greatly diminishing the intensity of the CL emission. It was decided to investigate the effect of surfactants on the CL emission intensity first.

4.4.4.1. Effect of surfactant on CL

A preliminary investigation using simple experimental design was carried out to determine the effect on CL emission of a range of surfactants, cetylammonium bromide (CTAB), a cationic surfactant; sodium dodecylsulphate (SDS), an anionic surfactant; Tween 80 and Triton X-100, both non-ionic surfactants), at high (1.0g l^{-1}) and low (0.1g l^{-1}) concentrations using the bioluminometer. (Experimental details of the bioluminometer can be found in section 3.2.2). A volume of 500 µl $Ru(bipy)_3^{3+}$

($1x10^{-3}$ mol l^{-1}) in sulphuric acid ($5x10^{-2}$ mol l^{-1}) was pre-mixed with 500 µl of the relevant surfactant in water mixture and placed in the sample chamber. The codeine ($1x10^{-3}$ mol l^{-1}) in acetate mixture (0.05 mol l^{-1}) was injected dropwise, in 100 µl aliquots. The emission in photon counts per second was recorded at 5 second intervals for 10 minutes, commencing 5 seconds after the injection of the codeine in acetate solution. Each set of solutions was measured three times and the mean emission levels in photon counts per second recorded for each solution as the emission proceeded with time in seconds.

The results of the effect of surfactant on initial emission intensity can be seen in table 4.1.

HIGH CONCENTRATIONS					
Solution:	TBR in acid	Addition of	Addition of	Addition of	Addition of
	only	SDS	CTAB	Tween 80	Triton X-100
mean no. counts per second	475	389.5	548	620.5	895

LOW CONCENTRATIONS					
Solution:	TBR in acid	Addition of	Addition of	Addition of	Addition of
	only	SDS	CTAB	Tween 80	Triton X-100
mean no. counts per second	475	401	424.5	518	734

Table 4.1. Effect of different types of surfactants on initial chemiluminescence emission intensity measured in mean photon counts per second with time in seconds.

As can be seen in table 4.1, these experiments showed that the SDS strongly suppressed the CL emission, while the CTAB showed a slight overall enhancement. The two non-ionic surfactants were found to give a strong enhancement effect and thus non-ionic surfactants were selected for further study. An expanded range of

non-ionics, which included Triton X-45, Triton CF10, Tween 20 and Tween 80, at both high (1.0g l^{-1}) and low (0.1g l^{-1}) concentrations was then examined, using simple experimental design, to determine which showed the best enhancement. Three measurements were carried out for each set of solutions. The mean CL emission intensities in photon counts per second with time in seconds for the first minute of each reaction, can be seen for the higher surfactant concentrations (1.0g l^{-1}) in table 4.2 and for the lower (0.1g l^{-1}) surfactant concentrations in table 4.3.

HIGH CONCENTRATIONS					
Solution:	Addition of Tween 20	Addition of Tween 80	Addition of Triton X-100	Addition of Triton X-45	Addition of Triton CF-10
mean no. photon counts per second	712.5	620.5	895	967	1060

Table 4.2. Mean enhancement of CL emission intensities using Triton X-45, Triton CF-10, Tween 20 and Tween 80 and the blank, at a concentration of 1.0g l^{-1}.

LOW CONCENTRATIONS					
Solution:	Addition of Tween 20	Addition of Tween 80	Addition of Triton X-100	Addition of Triton X-45	Addition of Triton CF-10
mean no. photon counts per second	658	518	734	1260	1245

Table 4.3. Mean enhancement of CL emission intensities of Triton X-45, Triton CF-10, Tween 20 and Tween 80, at a concentration of 0.1g l^{-1}.

As can be seen in tables 4.2 and 4.3, the lower (0.1g l^{-1}) surfactant concentrations generally produced a greater enhancement effect. The Triton X-45 and the Triton CF10 were found to produce the greatest enhancement effect during the first few seconds of the CL reaction as shown in figure 4.6. Hence it was therefore decided to

investigate what effect these two surfactants would have on the flow rate of the $Ru(bipy)_3^{3+}$ in sulphuric acid mixture.

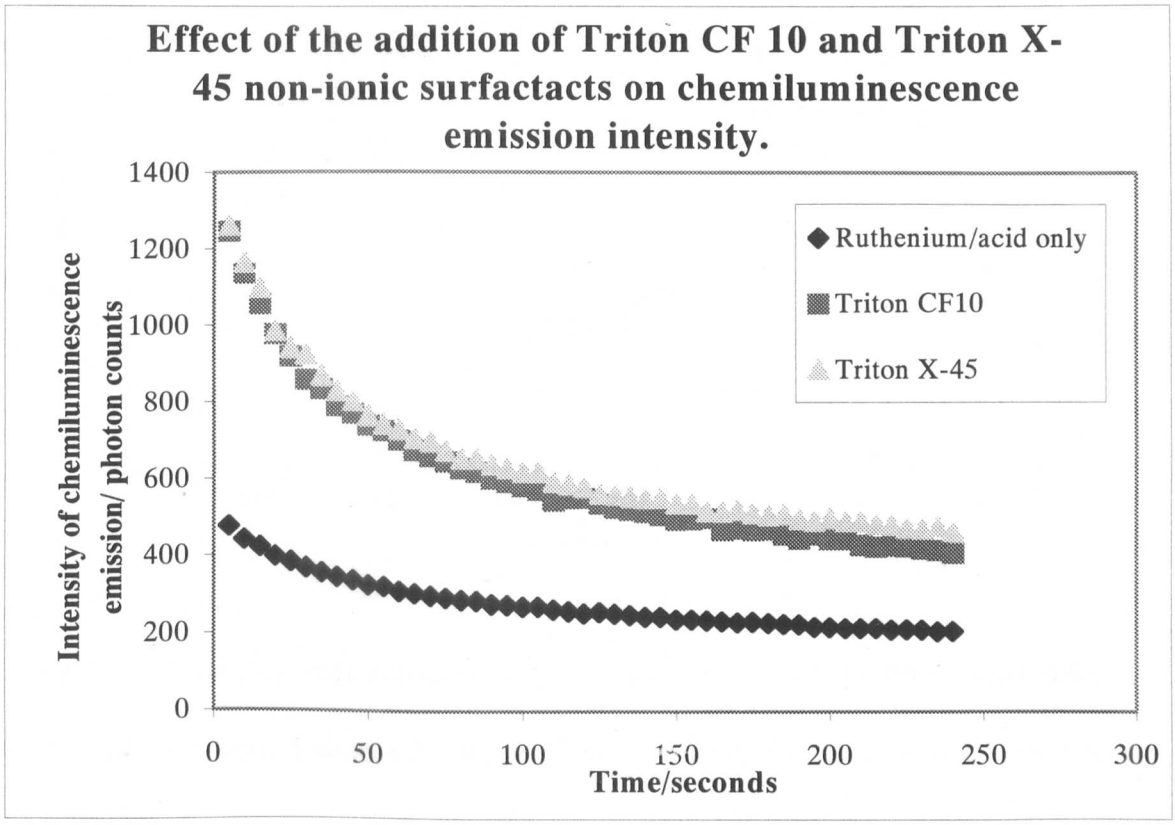

Figure 4.6. Effect of addition of Triton CF 10 and Triton X-45 on initial chemiluminescence emission intensity

4.4.4.2. Effect of surfactant on EOF rate

The two surfactants, Triton X-45 and Triton CF10 at a concentration of 0.1g l^{-1} were made up in solution with the $Ru(bipy)_3^{3+}$ ($1x10^{-3}$ mol l^{-1}) in sulphuric acid ($5x10^{-2}$ mol l^{-1}) mixture. Three flow rate experiments were carried out for each solution over a range of voltages for a time of 10 minutes. The mean flow rates, calculated in µl min^{-1} for each solution at each voltage were obtained. A plot for each solution over the voltage range can be seen in figure 4.7.

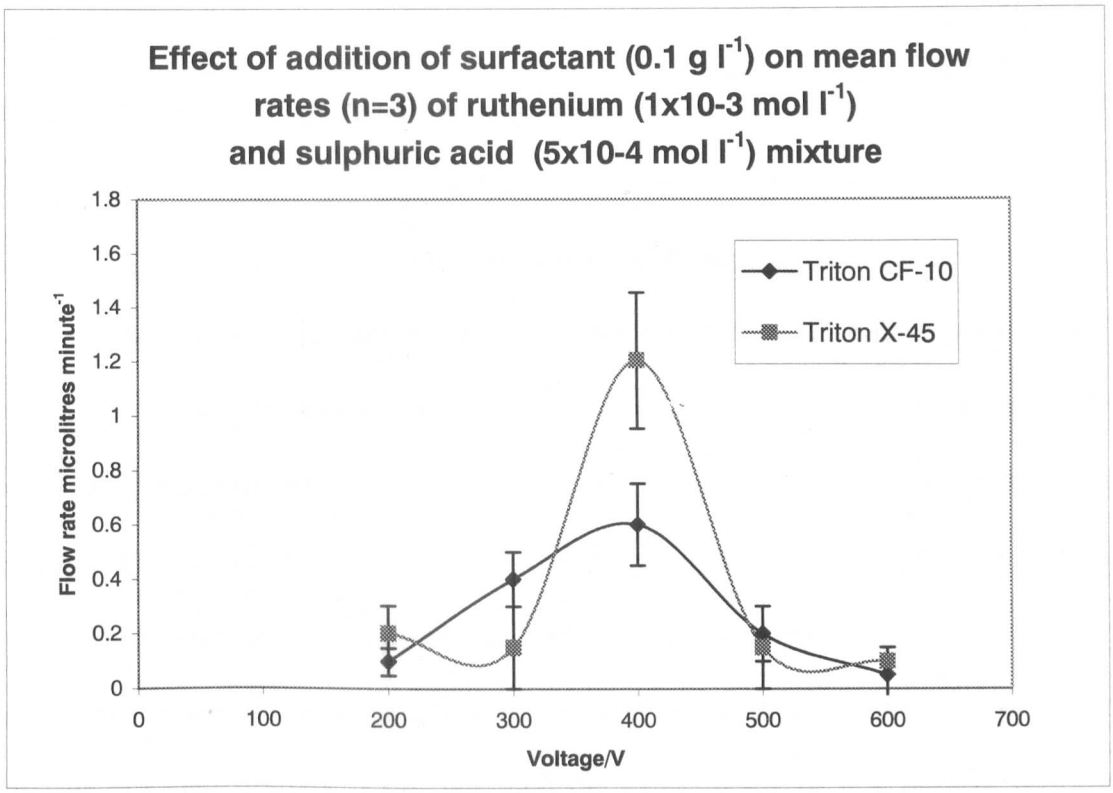

Figure 4.7. Mean flow rate for $Ru(bipy)_3^{3+}$ ($1x10^{-3}$ mol l^{-1}) in sulphuric acid (0.05 mol l^{-1}) mixture with Triton CF-10 and Triton X-45 (0.1g l^{-1}) in μl min^{-1} over a range of voltages.

In both cases, a marked increase in the flow rates was observed, the solution containing Triton X-45 however showed considerably faster movement than the solution containing Triton CF-10. As can be seen in figure 4.7, the optimum flow rate for the $Ru(bipy)_3^{3+}$ ($1x10^{-3}$ mol l^{-1}) in sulphuric acid ($5x10^{-2}$ mol l^{-1}) mixture with Triton X-45 proved to be 1.2 ± 0.25 μl min^{-1} at a voltage of 400 V, the same as the optimum voltage for the codeine in acetate mixture. Although the flow rate of the mixture with surfactant was observed to be substantially faster than in the absence of Triton X-45, the direction of flow was away from the ground electrode rather than towards it, as would usually be the case.

As outlined in section 1.3.4, it is known that cationic surfactants are able to reverse the direction of EOF in systems with negatively charged glass surfaces by altering the zeta potential[69] . In this system, a non-ionic surfactant was used, however the solution used has a pH of around the isoelectric point of glass, which has been shown to be at pH 2-2.5, which could account for the anomolous behaviour[211]. The important point in this study is that $Ru(bipy)_3^{3+}$ is a large highly charged species. This species could be forming a monolayer of positively charged $Ru(bipy)_3^{3+}$ complex on the capillary walls. A similar effect has been shown in a study where $LaCl_3$ solutions were shown to reverse the sign of the zeta potential of various samples of glass[63].

When the chip was viewed under a microscope a brownish coloured coating was observed on the capillary walls, although the exact nature of this coating was not identified. This build up did not pose any problems during the reaction and could be removed using dilute nitric acid.

4.5. Detection of codeine using the TBR reaction in a miniaturised analysis system

As described in section 3.3, four detection systems were evaluated in this work.

4.5.1. Detection using a miniaturised photomultiplier tube (PMT)

The PMT with fibre optic attachment proved to be far more sensitive than the silicon photodiode detectors and suitable for evaluating the tris(2,2'-bipyridyl)ruthenium (II) reaction on the miniaturised analysis system.

4.5.2. System noise and electrode positioning

Using the procedure described in the experimental section, 4.3.3.2, an initial calibration for codeine in acetate solution was obtained using the tris(2,2'-bipyridyl)ruthenium (II) reaction, but the reproducibility was still poor. In addition, noise was observed which was shown on the chart recorder.

A filter consisting of capacitor and transistor was fitted to the PMT output to reduce the noise problem. In addition to this, the whole miniaturised analysis system was earthed to the inside of the isolation box. As a result of these measures, the unwanted noise problem was vastly improved.

With the noise substantially reduced, it was then found that the correct positioning of the electrodes inside the reservoirs became the main variable regarding reaction response. Smaller amounts of noise output were again observed if the electrodes were placed too close to the walls or base of the reservoir. The exact positioning of the electrodes in the reservoir was critical to ensure good reproducibility of emission intensity due to the surface tension and hydrodynamic flow effects as explained in section 1.3.2.1. The reproducibility of emission intensity was vastly improved by the use of an electrode stand, which kept the electrodes rigid. This ensured the placement of the electrode in the reservoir was approximately at a constant depth and position for each experiment.

4.5.3. Codeine calibration

Following the modifications to the miniaturised analysis system as described above in section 4.5.2, a reproducible calibration was achieved over the codeine concentration range of $5x10^{-7}$ to $1x10^{-3}$ mol l^{-1}, the log-log calibration plot is shown in figure 4.8.

Correct codeine calibration

Linear portion of plot

Concentration/ mol l-1 (x10-4)	Response/mV	S.D/mV
0.005	0.0914	8.18E-07
0.01	0.1523	3.24E-09
0.02	0.2052	2.92E-08
0.1	0.7426	2.57E-06
0.5	3.114	2.25E-07
1	6.1045	2.03E-07
10	37.92	

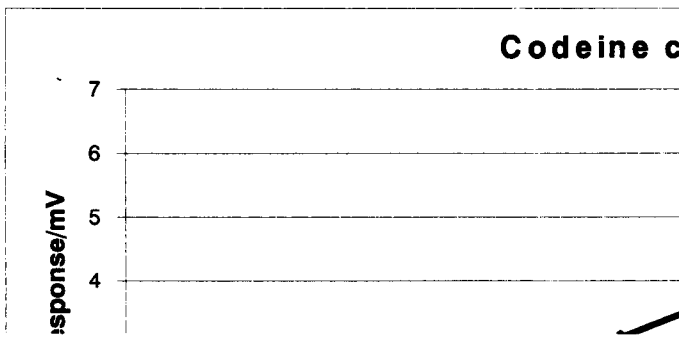

Figure 4.8. Log-log calibration plot for codeine

The graph has a central linear section that tapers off at higher and lower concentrations. The points for the codeine concentrations of $5x10^{-7}$ to $1x10^{-4}$ mol l^{-1} were plotted to give a linear calibration plot. The equation of the line was $y = 6.0136x + 0.0949$, $R^2 = 0.9999$, where x was the codeine concentration in mol l^{-1} and y was the average CL emission intensity (n=5) in mV, as seen in figure 4.9.

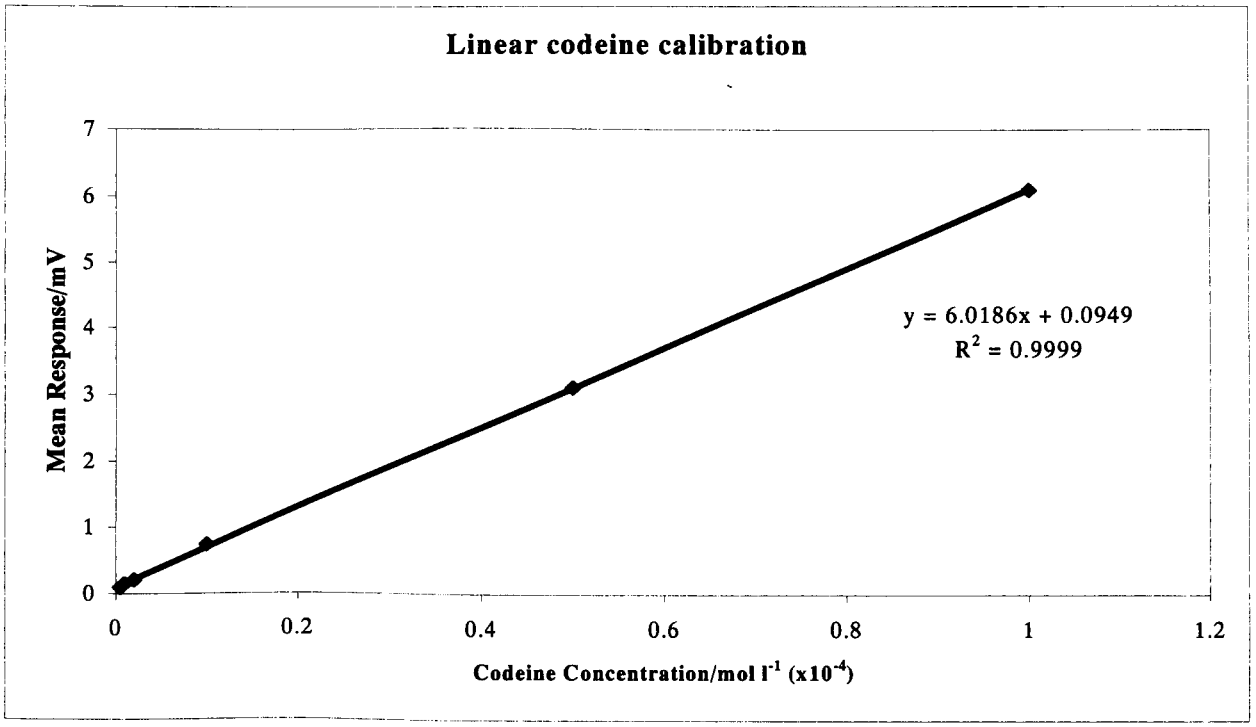

Figure 4.9. Linear portion of calibration graph for codeine

The limit of detection was found by plotting on the linear scale the last three points of the calibration ($5x10^{-7}$ to $2x10^{-6}$ mol l^{-1}), as shown in figure 4.10 and using the equation of the line.

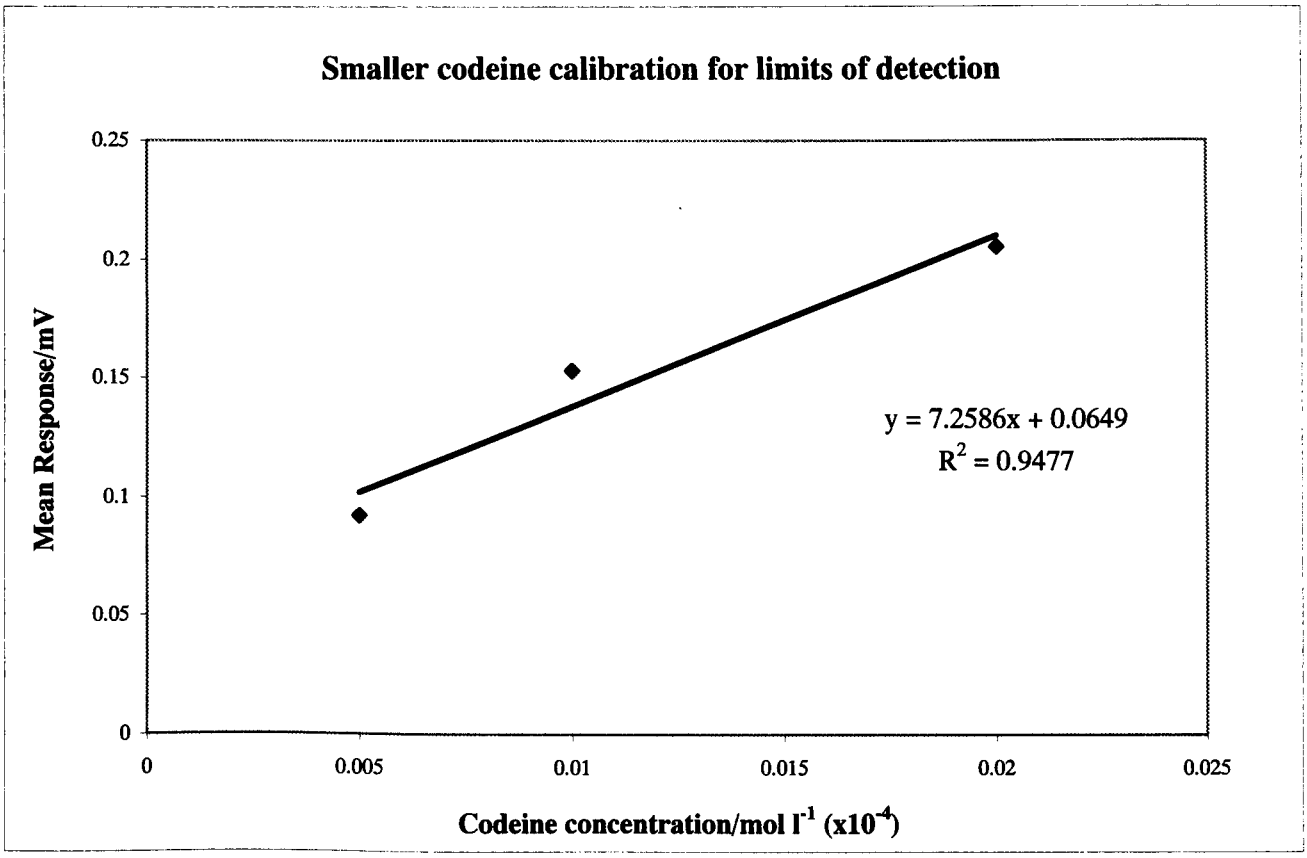

Figure 4.10. Plot used to calculate limits of detection.

It was determined at 95% confidence limits to be $8.3x10^{-7}$ mol l^{-1} codeine. This result compared well with the detection limit for codeine determined by gas chromatography coupled with mass spectrometry detection (GC-MS), which has been found to be $3.3x10^{-5}$ mol l^{-1} [212], however, Barnett *et al.*[157] obtained a limit of detection for codeine determined in process streams using FIA coupled with chemiluminesence detection of $5x10^{-9}$ mol l l^{-1}. An RSD of 8% (n=5) was obtained for the $5x10^{-5}$ mol l^{-1} standard.

After each experiment, the products of the reaction were removed by syringe and the miniaturised analysis system was flushed with water. The sample throughput time including removal of products and water wash was found to be an average of 3 minutes.

4.6. Conclusions

The work described in this chapter has shown that detection of CL emission from a reaction in a miniaturised analysis system is possible. Furthermore, the sensitivity of this manifold design has been evaluated and a successful calibration of codeine carried out. The use of surfactants in developing the system was particularly valuable in both the enhancement of CL emission intensity and modification of the channel surface to allow movement of a solution by EOF that had a pH outside the pH range normally suitable for EOF mobility. The direction of flow was shown to reverse using non-ionic surfactants. This was thought to be due to a build up of positively charged species which adhered to the surface of the capillary walls in the presence of the surfactant resulting in a change of the sign of the zeta potential, which thus allowed reverse EOF to be observed.

Methods for improving the precision of the system could include the use of silica microporous structures[208] to control mixing and improve the hydrodynamic flow. Detection of the reaction in the channel instead of the well could improve the sensitivity. The incorporation of the fibre optic directly into the channel to monitor the moving reactants rather than positioning under the reaction well could also reduce limits of detection.

5. Luminol reaction

The aim of work in this chapter was to design a miniaturised analysis system that would enable the determination of one or more metal. The possible analytes of interest included Pb (II), Zn (II), Hg (II) and Cr(III). The information gained from the codeine determination described in chapter 4 was used to formulate ideas regarding manifold designs and experimental procedures. In order to maximize light production it was decided to carry out some multivariate experimental design to fully optimize the reagent concentrations and conditions.

5.1. Introduction

The luminol reaction was selected as the most suitable reaction to determine metal ions by chemiluminescence[172,173,174,193,213,214]. Although the optimum conditions for this reaction include high reagent pH, which would normally prevent movement by EOF, it was felt that there were compromise conditions that could be employed to allow application of this reaction to a miniaturised analysis system.

5.2. Study into the effect of surfactants on the luminol reaction

It was realised that if the reaction worked best at high pH values the only way to successfully mobilise the luminol would be to use surfactants.

Cationic surfactants have been reported to enhance the CL emission from the luminol reaction[195,196,198,199] and it was therefore decided to confine the study of suitable surfactants to cationics only. Most of the published literature relates to observed CL

enhancement from the luminol reaction using the two surfactants cetyltrimethylammonium bromide (CTAB)[195,196,200] and cetyltrimethylammonium chloride (CTAC)[195,198]. As these two surfactants were readily available in the laboratory, they were selected for the investigation. Optimisation of the luminol reaction involved several inter-related variables and therefore it was decided to investigate how multivariate experimental design could be used to maximise the chemiluminescence signal.

A series of multivariate experimental design measurements using non-symmetrical-D-optimal experimental design was carried out using a traditional flow injection analysis system, with PMT detection and the bioluminometer.

The aim of these experiments was to determine the optimum levels of all the factors involved, using the minimum number of measurements. In addition to this, a stability study was performed to determine the effect of reagent incubation time on the CL emission intensity. This would be important if the reagents were to be stored in miniaturised analysis system, prior to remote use.

The type of experimental design used did not require all possible levels within a given range to be measured. A sufficient number of levels were measured for each factor, in order to generate enough data to set up a model that would accurately predict the optimum levels of all factors. Once the model had been computer generated, the predicted levels were tested experimentally to assess the accuracy of the model.

The parameters chosen for optimisation were the identity of the buffer, the pH, and the surfactant concentrations that would give the greatest overall CL emission intensity.

5.2.1. Experimental

The apparatus was as described in sections 3.2.1 and 3.2.2.

All the chemical standards and reagents used were analytical grade unless stated otherwise and the water used was high purity de-ionised (18 M Ω cm resitivity) (Elgastat UHQ PS, Elga, High Wycombe, UK).

The pH of a sodium carbonate solution (0.1 mol l^{-1}) from Fluka (Gillingham, Dorset, UK) was adjusted to pH 10.4 using sodium hydrogen carbonate (Fisher Scientific Ltd. Loughborough, UK). A sodium dihydrogen phosphate (0.1 mol l^{-1}) solution was adjusted to approx. pH 6.0 using sodium phosphate (both Fisher Scientific Ltd. Loughborough, UK). Twenty volumes hydrogen peroxide (0.1 mol l^{-1}), from Fisher Scientific Ltd. (Loughborough, UK) was used as the oxidising agent.

The surfactants used in this work were cetyltrimethylammonium bromide (CTAB) (BDH, Merck, Lutterworth, Leics., UK) and cetyltrimethylammonium chloride (Fluka, Gillingham, Dorset, UK).

5.2.2. Experiment SET 1

5.2.2.1. Procedure

Five factors were chosen for the first set of designed experiments, this equated to 30 experiments. These were the carbonate and phosphate concentrations, the pH and the nature and concentration of the CTAB and CTAC respectively. The pH levels were assigned as pH 7.5, pH 9.0 and pH 10.5. The outcome would determine the levels set for the next set of experiments.

Three separate solutions were prepared from each buffer stock solution, so that the concentration of each remained 0.1 mol l^{-1} with pH's of 7.5, 9.0 and 10.5. These pH levels were achieved by the addition of concentrated sodium hydroxide and hydrochloric acid respectively so equal amounts of the two buffers could be mixed while keeping the pH constant.

After studying the literature, the surfactant solutions were each assigned five concentrations of 0, $1x10^{-6}$, $1x10^{-5}$, $1x10^{-4}$ and $1x10^{-3}$ mol l^{-1} respectively. Hence, the overall initial factor table was devised which can be seen in table 5.1.

Experiment number	Factor 1 Percentage Carbonate (%)	Factor 2 Percentage Phosphate (%)	Factor 3 Solution pH	Factor 4 CTAB g/100ml	Factor 5 CTAC g/100ml
1	0	100	9	0	0
2	50	50	10.5	0.0036	0.32
3	100	0	7.5	0.36	0.0003
4	100	0	10.5	0	0
5	100	0	7.5	0.0036	0.0003
6	0	100	9	0.0036	0.0003
7	0	100	10.5	0.0036	0.0003
8	50	50	7.5	0.0036	0
9	0	100	7.5	0	0.0032
10	100	0	10.5	0	0.0032
11	100	0	7.5	0	0
12	0	100	7.5	0.36	0.32
13	0	100	10.5	0	0.032
14	100	0	10.5	0.36	0.0032
15	50	50	7.5	0.36	0.032
16	100	0	7.5	0.036	0.32
17	100	0	9	0	0.0003
18	0	100	7.5	0.0003	0.32
19	0	100	10.5	0.36	0
20	100	0	7.5	0	0.32
21	100	0	9	0.36	0
22	0	100	9	0.036	0.032
23	0	100	9	0	0.32
24	100	0	9	0.36	0.32
25	0	100	7.5	0.36	0
26	50	50	10.5	0	0.0003
27	100	0	9	0.0003	0.032
28	0	100	10.5	0.36	0.32
29	100	0	10.5	0.036	0.0003
30	0	100	10.5	0.0003	0.0003

Table 5.1. Initial factor table

All of the solutions additionally contained luminol ($1x10^{-4}$ mol l^{-1}) which was added as the solutions were prepared. This first set of experiments was carried out using a conventional FIA system coupled with a standard PMT detector. The output from the PMT was recorded using a chart recorder as peak height in mV. A mean (n=3) peak height was calculated for each solution.

5.2.2.2. Results for Experiment SET 1

Experiment Number	Mean peak height/mm (n=5 for all experiments)	Rel. S.D (%)
1	44.5	5.5
2	200.0	0.0
3	55.0	1.0
4	200.0	0.0
5	33.0	9.0
6	93.0	6.0
7	200.0	0.0
8	0.0	0.0
9	0.0	0.0
10	200.0	0.0
11	3.0	8.0
12	1.0	0.0
13	42.5	6.0
14	200.0	0.0
15	1.0	19.0
16	8.0	6.0
17	32.0	15.5
18	0.5	0.0
19	22.0	2.5
20	4.5	6.5
21	74.0	16.0
22	3.0	16.5
23	4.5	6.5
24	46.5	16.0
25	0.0	0.0
26	166.0	5.0
27	24.0	18.0
28	16.0	7.0
29	109.0	1.0
30	41.0	1.0

Table 5.2. Mean peak heights of solutions 1-30

The results for the first optimisation experiment can be seen in table 5.2. It was noted from the outcome of the initial experimental design that the length of time the luminol, carbonate or phosphate and surfactant remained in contact in the solution prior to analysis could affect the CL emission intensity. Solutions 2, 4, 7, 10 and 14 were found to show the greatest mean peak heights as can be seen in Figure 5.6. This indicated that the optimum pH level appeared to be 10.5 and that the preferred solution was the carbonate. Detailed information regarding the exact concentrations of the two surfactants was still unclear at this stage, though it appeared that a mixture of the two surfactants was most likely to produce the greatest overall CL emission intensity and enhancement.

Solutions 2, 4, 7, 10, 14, 6, 23, 29 and 30 were re-analysed the next day using the FIA system to assess the effect of extended contact time on emission intensity. Each solution showed a reduction in mean emission intensity in the re-analysis, though it depended on the concentration of the various reagents and in particular on the concentration of the surfactants in the solutions just how much of a reduction was observed, as can be seen in table 5.3.

Experiment Number	Mean peak height/mm (n=3 for all experiments)	Rel. S.D (%)
2	57.5	14.0
4	159.0	1.5
7	43.5	10.5
10	41.0	5.0
14	29.5	7.0
6	1.5	16.5
16	1.0	0.0
23	1.5	9.0
29	54.5	4.0
30	25.5	13.5

Table 5.3. Mean peak heights of re-analysis

Experiment 4, which contained no surfactant showed the least mean reduction in CL emission intensity. Generally, the lower the overall surfactant concentration in the solution, the less the reduction of the overall mean CL emission intensity after overnight refrigeration. Those solutions that contained a large CTAB concentration appeared to be more adversely affected than those solutions that contained a large CTAC concentration. Solutions 16 and 6 appeared to show the greatest reduction in mean CL emission intensity over the two sets of measurements. In the case of 16, this could have been due to the presence of the combined high concentrations of CTAB and CTAC in solution, whereas in the case of solution 6, the presence of the phosphate might have reduced the emission intensity of this solution.

The reproducibility of the injection procedure into the FIA apparatus was checked using three solutions, each containing 50 ml of carbonate solution and 50 ml phosphate

solution, with $1x10^{-4}$ mol l^{-1} luminol, all at pH 9.0. Each of these three solutions was analysed 4 times to give 12 peak heights and the results are shown in table 5.4.

	Mean peak height	S.D /mm	Rel. S.D (%)
Solution 1	6.0	0.5	4.0
Solution 2	6.0	0.5	4.0
Solution 3	6.0	0.5	5.0

Table 5.4. Reproducibility data

Table 5.4 shows that the results for the first two solutions were identical, with a mean peak height of 6.0 ± 0.5 mm and a percentage error for each set of measurements of 4.0%. The results for the third solution also showed a mean peak height of 6.0 ± 0.5 mm with a percentage error of 5.0%.

5.2.3. Experiment SET 2

5.2.3.1. Procedure

	Factor 1	Factor 2	Factor 3	Factor 4	Factor 5
Experiment number	Percentage Carbonate (%)	Percentage Phosphate (%)	Solution pH	CTAB g/100ml	CTAC g/100ml
1A	90	10	10.5	0	0.0003
2A	90	10	10.5	0.0003	0.0003
3A	90	10	10.5	0	0.32
4A	90	10	10.5	0.0003	0.32

Table 5.5 Second factor table with predicted solution concentrations from model

From the results of the first two analyses, a model was produced. Predicted potential optimum ranges of the concentration of carbonate and phosphate solutions and surfactant were identified and from this four new experiments were devised which can be seen in table 5.5.

5.2.3.2. Results for Experiment SET 2

From the results of the analysis of solutions 1A – 4A shown in table 5.6, it appeared that a lower CTAC concentration resulted in a higher overall CL emission intensity. The use of the carbonate buffer only at pH 10.5 was confirmed as the best option for optimum CL emission.

Solution	Mean peak height/mm (n=3 for all experiments)	Rel. S.D (%)
1A	32.0	3.5
2A	32.0	5.0
3A	22.0	10.0
4A	17.5	0.0

Table 5.6 Results of solutions 1A-4A

Due to a possible build-up of surfactant on the PMT window, the bioluminometer was used for all future work to measure emission intensity at various time intervals after initial mixing.

Fresh solutions of 2, 4, 10 and 14 were analysed to determine what effect the contact time of the luminol and surfactant in solution had on the overall CL emission intensity. Each

solution was measured at time intervals of 5, 40, 80 and 120 minutes after mixing and the results are shown in figures 5.1 – 5.4.

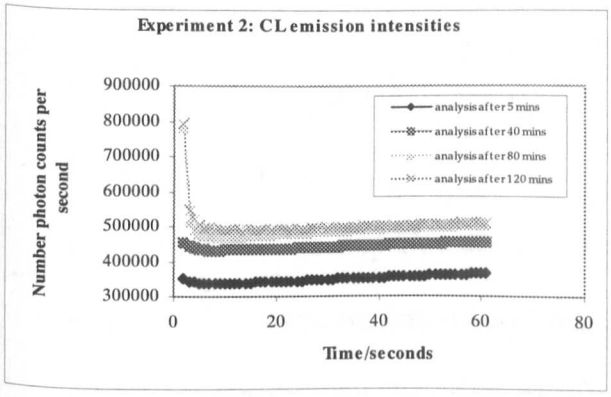

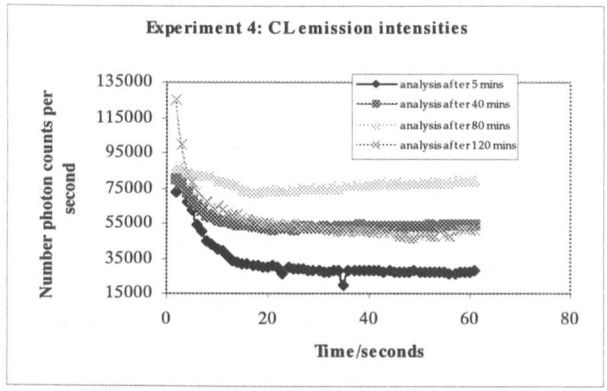

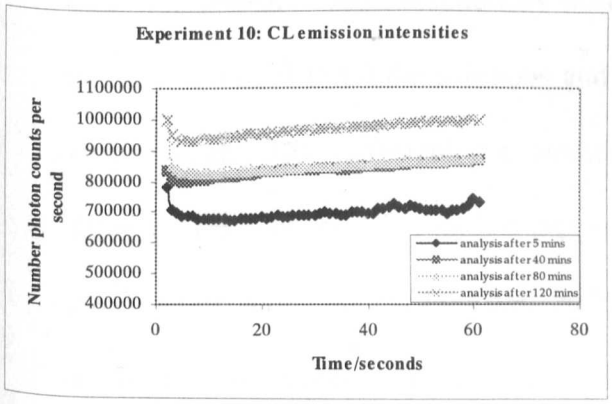

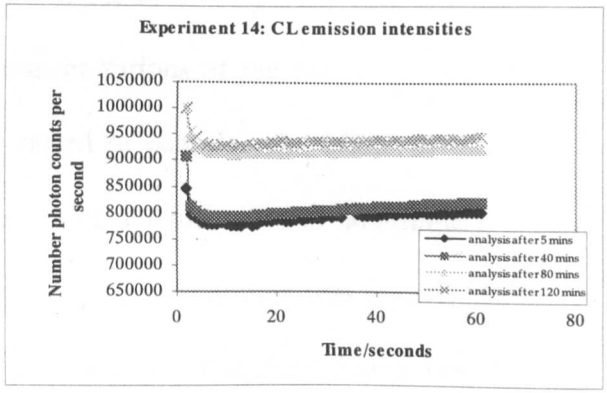

Figures 5.1-5.4 Effect of time on CL emission intensity

Possible reasons for the enhanced emission intensity with increased standing time include a partial formation of a luminol-surfactant complex which leads to the stabilisation of the 3-aminophthalate anion (see section 2.4 for details of mechanism).

Several conclusions can be drawn from the data in Figure 5.5 – 5.8. The observed lifetime of CL emission appeared to be increased in the presence of surfactant and also generally increased with longer contact time of the luminol and surfactants in solution.

This was especially apparent over the first 10-15 seconds of each experiment, during which time a great increase in emission intensity was observed for those solutions that had been analysed after 80 and 120 minutes.

5.2.4. Experiment SET 3

5.2.4.1. Procedure

A third set of nine experiments was carried out to obtain more accurate information regarding the exact concentration of the surfactants required to produce the optimum CL emission intensity. All the reactions were carried out at pH 10.5, with carbonate buffer (0.1 mol l^{-1}) used in all the solutions and only the concentrations of the two surfactants were altered. The surfactant concentrations were varied to examine the effect of the absence of one or the other surfactants on the CL emission intensity and to determine a possible interaction effect of the two surfactants in solution. Each solution was measured at 40 and 120 minutes intervals, after the initial preparation. The third factor table showing the concentration of the nine solutions is shown in table 5.7.

	Factor 4	Factor 5
Experiment number	CTAB Concentratio g/100ml	CTAC Concentration g/100ml
1B	0.0036	0.0032
2B	0.36	0.0032
3B	0.18	0.16
4B	0.36	0.16
5B	0.0036	0.32
6B	0.18	0.32
7B	0.36	0.32
8B	0	0.32
9B	0.36	0

Table 5.7. Third factor table

5.2.4.2. Results of Experimental SET 3

The results of the third set of experiments can be seen in figures 5.5 and 5.6.

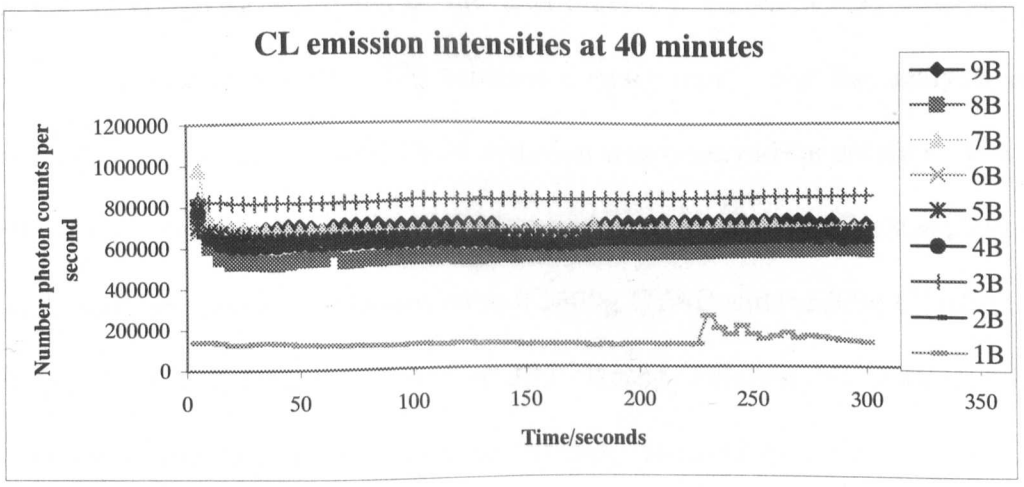

Figure 5.5. Analysis at 40 minutes after preparation for solutions 1B – 9B. CL emission measured in photon counts per second as a function of time in seconds.

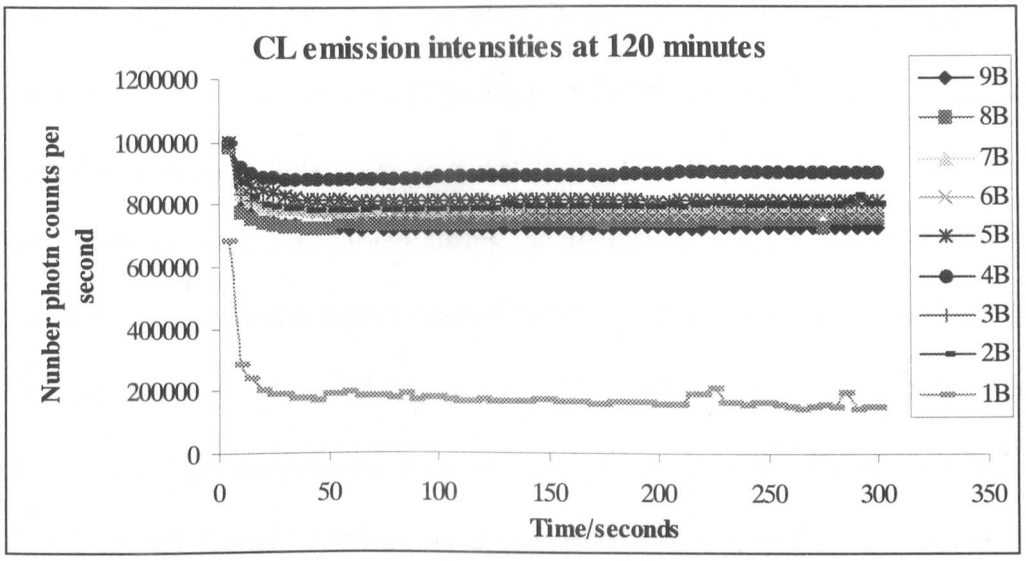

Figure 5.6. Analysis at 120 minutes after preparation for solutions 1B – 9B. CL emission measured in photon counts per second as a function of time in seconds

From this information, the following conclusions were drawn:

With the exception of solution 3B, the maximum CL emission was observed during analysis of the solutions after 120 minutes contact time. For the analysis after 40 minutes, the overall highest intensity of emission was observed for solution 3B while the initial highest intensity of emission was observed for solution 7B. The concentrations of the surfactants in these two solutions were 0.3600g CTAB and 0.3200g CTAC in 7B and 0.1800g CTAB and 0.1600g CTAC in 3B. Hence, solution 3B contained half the concentration of surfactants that solution 7B did. It could be postulated that after an intense initial CL emission observed with solution 7B, the combined high concentration of both surfactants present in this solution then quenched the emitted CL to a certain extent. As a result a gradual overall decrease in emission intensity was observed, as shown in figure 5.5. For the analysis carried out after 120 minutes, the overall highest

emission was observed for solution 4B, followed by 3B. The concentration of CTAC in the two solutions was the same (0.1600g), while the concentration of CTAB was twice as much (0.3600g) in solution 4B, as it was in solution 3B. It is possible that the lifetime of the chemiluminesence observed during the analysis of solution 4B after 120 minutes was due to the presence of a higher concentration of CTAB. The highest initial CL emission intensity was also observed for solution 4B followed by solution 5B, both of which contained a high concentration of one surfactant, (0.3600g CTAB in 4B and 0.3200g CTAC in 5B) though solution 4B also contained 0.1600g CTAC. Again, it could be postulated that a combined higher overall concentration of surfactant does enhance the initial CL emission intensity, though in this case the emission from solution 4B was not quenched. However, the overall concentration of surfactant in solution 4B was less than that in solution 7B. The overall optimum CL emission intensity was observed for solution 4B during the analysis after 120 minutes. The results of this set of experiments were fed back into the computer and the model updated.

The model then produced plots which predicted the optimum surfactant concentrations for analysis after 40 minutes, 120 minutes and also a compromise of conditions suitable for analysis at both times.

The area in the very centre of the plot represented the concentrations of surfactants most likely to produce the greatest CL emission intensity. The area was quite large in all the plots with respect to the overall size of the plot; this represented the margin of error attached to the predictions. The fact that this error was quite large was actually useful, because it meant that the concentrations of the two surfactants could vary slightly and an optimum CL emission could still be produced. The range of optimum CTAB

concentration for analysis after 40 minutes was 0.2600 – 0.3000g in 100ml solution, while the CTAC was 0.1600 – 0.2000g surfactant in 100ml solution. The prediction for the analysis after 120 minutes was for an optimum CTAB concentration in the range of 0.3400 – 0 .3600g surfactant in 100ml solution and an optimum CTAC concentration of 0.1600 – 0.1900g surfactant in 100ml solution. The predicted optimum CTAC concentrations were basically the same, while the predicted optimum CTAB concentrations increased with contact time.

5.2.5. Experiment SET 4

5.2.5.1. Procedure for experiment set 4

	Factor 4	Factor 5	
Experiment number	CTAB g/100ml	CTAC g/100ml	Measurement time/ minutes
1	0.28	0.18	40
2	0.27	0.19	40
3	0.29	0.17	40
4	0.26	0.18	40
5	0.27	0.17	40
6	0.36	0.16	40 and 120
7	0.36	0.18	120
8	0.36	0.14	120
9	0.35	0.17	40 and 120
10	0.36	0.2	120
11	0.34	0.16	40 and 120
12	0.35	0.15	40 and 120
13	0.33	0.17	40 and 120

Table 5.8. Final factor table

The last set of experiments was then carried out. The factor table for this set of experiments can be seen in table 5.8. Experiments 1-5, 6, 9, and 11-13 were analysed after 40 minutes and experiments 6-10 and 11-13 were analysed after 120 minutes.

5.2.5.2. Results for Experiment SET 4

For analysis after 40 minutes, the predicted optimum levels of CL emission should have resulted from analysis of solution 1, then solution 2 and so on up to solution 5. Solution 1 did produce the optimum CL emission, but after that the order was solution 5, solution 2 and then solution 3. For analysis after 120 minutes, the order of maximum emission intensity was observed to be from solution 6, followed by solution 10, solution 9 and then solution 8. The solutions 11-13 were compromise surfactant concentrations, which when analysed were designed to produce fairly high CL emission when analysed after 40 or 120 minutes. It was found that the emission intensity for solutions 11-13 tended to be lower than solutions 1-10.

In the interests of reducing sample throughput time, an emission maximum after 40 minutes standing time was better than after 120 minutes, although this was not actually adhered to once the reaction was applied to the miniaturised analysis system.

5.2.6. Conclusions

The addition of surfactants was found to enhance the both the initial CL emission intensity and the lifetime of the luminescence. Overall, a mixture of the cationic surfactants CTAB (0.2800g/100 ml) and CTAC (0.1800g/100ml) was found to show the greatest enhancement effect. It was discovered that the length of time the luminol in

carbonate buffer remained in contact with the surfactant mixture prior to analysis had a large effect on the emission intensity. A contact time of 120 minutes was observed to produce the greatest enhancement effect.

The principle of the application of experimental design to this work had been demonstrated and the optimum level of multiple factors determined. With more time available further optimisation could have been achieved, however it was decided at this point that it could not be justified to spend more time in further optimising the surfactant concentration to a shortened standing time.

Hence, for the work carried out on the miniaturised analysis system, the surfactant concentrations of 0.2800g CTAB and 0.1800g CTAC in 100ml solution, i.e. the concentrations of experiment 1, were adopted with a standing time of a maximum of 5 minutes.

5.3. The luminol reaction in a miniaturised analysis system

5.3.1. Experimental

The apparatus was set up as described in chapter 3. Several different manifold designs were investigated including one 'T' – manifold, shown in Figure 3.3, and one 'starburst' – manifold, which had five channels meeting at a single point in the centre of the chip, shown in figure 3.10.

A new Y- design manifold was also produced during the work on the luminol reaction. This new design was larger than any of the other manifolds used in this work and was optimised specifically to enable easy incorporation of a fibre optic directly into the

channel. The design and channel dimensions of this Y-manifold design can be seen in figure 5.7.

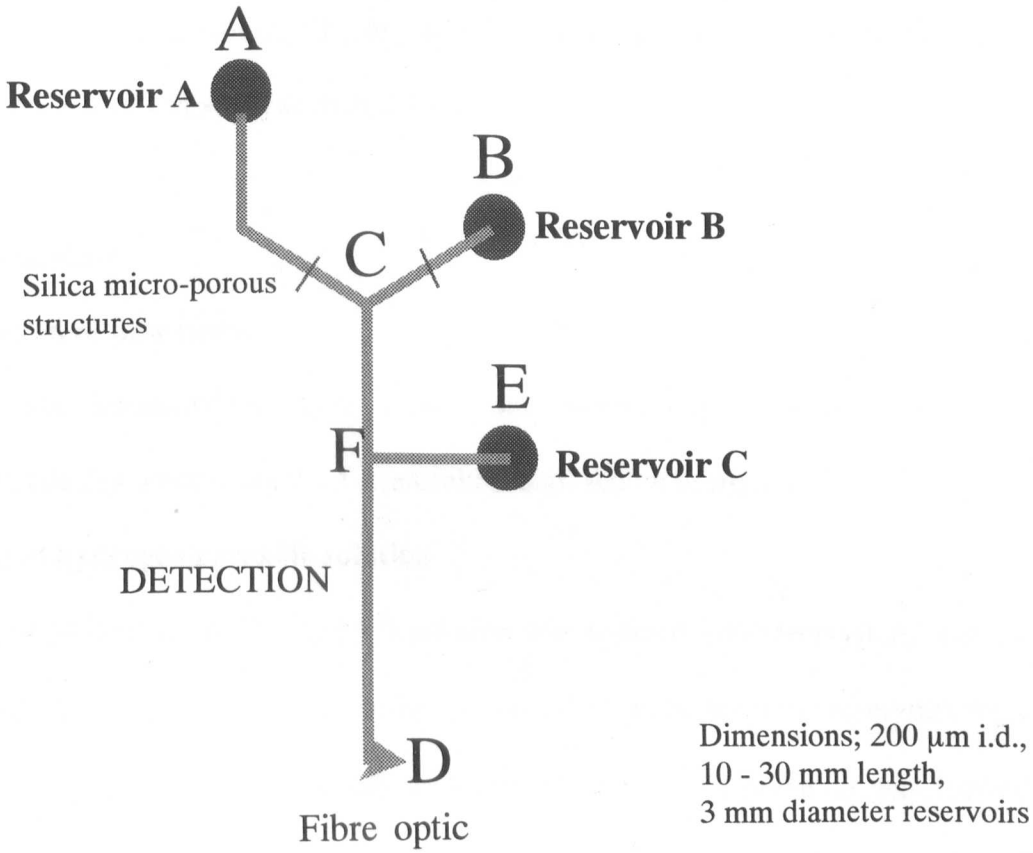

Figure 5.7. Luminol miniaturised analysis system

5.3.1.2. Reagents

Luminol ($1x10^{-3}$ mol l^{-1}) was made up with CTAB (0.28g) and CTAC (0.18g) in every 100 ml carbonate buffer (0.1 mol l^{-1}). Hydrogen peroxide (0.1 mol l^{-1} was used as the oxidising agent.

The cobalt standard solutions were prepared from cobalt nitrate, $Co(NO_3)_2$, obtained from Fisons (Loughborough, UK), which had a pH of approximately 3.4.

Cobalt (II) as the analyte

Cobalt (II) was chosen for the analyte as it is a very efficient metal catalyst in the luminol reaction[172] that produces intense CL emission. The catalytic effect of cobalt (II) on the luminol reaction is described in section 2.4.2.

5.3.1.3. Procedure

Determination of flow rates

The flow rate determinations were carried out concurrently with the multivariate experimental design work using the T-manifold design shown in figure 3.3.

Movement of hydrogen peroxide solution

A volume of 50.0 μl H_2O_2 (0.1 mol l^{-1}) solution was injected into reservoir A, using a micropipette (Sealpette, Jencons, Leighton Buzzard, UK) while the other reservoirs were loaded with 50.0 μl pH 10.4 carbonate (0.1 mol l^{-1}) buffer. A potential was applied across BA and the mean flow rate in microlitres $minute^{-1}$ was determined over a range of voltages. The number of measurements carried out at each voltage was between 3 and 5 and each experiment lasted for 10 minutes.

Movement of $Co(NO_3)_2$ solution

A volume of 50.0 μl $Co(NO_3)_2$ solution was injected into reservoir A, while reservoirs B and C were loaded with 50.0 μl pH 10.4 carbonate buffer. A potential was applied across AB and the flow rate in microlitres $minute^{-1}$ was determined over a voltage range of 100V - 600V. The number of experiments carried out at each voltage was between 3 and 5.

Movement of luminol in sodium carbonate buffer

Prior to the addition of surfactant to the solution, attempts to move the luminol in carbonate buffer were carried out in the same way. It was necessary to determine whether any movement of this solution was possible in the absence of surfactants. However, as suspected, the high pH of this solution prevented successful, reproducible movement by EOF.

5.4. Results and Discussion

5.4.1. Miniaturised analysis system design

A suitable manifold design had to be found to allow inclusion of all the reagents. It was decided that a new 'Y' design, as shown in Figure 5.7, would be advantageous. The design shown in Figure 5.1 contained two capillaries at 45° to the vertical plane, AC and BC that converged to form the single vertical channel, CD. An additional side channel EF joined the main channel, CD, at approximately two fifths of the distance along CD. Frits located in the channels AC and BC would prevent unwanted hydrodynamic flow and thus improve reproducibility.

It was decided that a fibre optic connected to the PMT could be inserted into the bottom end of the channel CD. Here, the two species that would react to initiate the production of CL (i.e. hydrogen peroxide and luminol) would meet at the point, C, and would progress along CD as the reaction proceeded. The emission intensity could then be monitored via the fibre optic, before the reacting species flowed to waste along EF. This arrangement meant that the metal analyte would have to be present in either the luminol or hydrogen peroxide solutions. Another alternative was to detect the reaction in the

channel CD, by placing the PMT directly under the position where it was suspected the maximum intensity of emitted light would occur. This would allow a variety of reagent arrangements, with the hydrogen peroxide possibly flowing along capillary EF to meet and react with the luminol in surfactant solution and the metal analyte flowing along CD, which in turn would have intercepted at position C.

Hence, while the 'Y' design was being prepared, initial work on the luminol reaction in the miniaturised analysis system was using the 'starburst' manifold design, shown in figure 3.10. It was decided that a minimum of three reservoirs (including a waste reservoir) were needed in order to successfully accommodate all the reagents required for the luminol reaction in a miniaturised analysis system and hence the 'starburst' design was the best option, among the designs available. For the initial detection in the miniaturised analysis system, a mixing well was also located at the central point where the five channels met, however detection in the channel was later achieved.

5.4.2. Determination of reagent flow rates

The flow rate measurements were calculated in microlitres minute^{-1}. The standard deviation of the mean flow rate was always less than ± 0.5 µl. This value is quoted as the combined error associated with measurement using the microlitre syringe and the standard deviation of the mean flow rate.

5.4.2.1. Hydrogen peroxide flow rate

Movement of hydrogen peroxide solution

The rate of EOF of 0.1 mol l^{-1} hydrogen peroxide solution was determined over a range of voltages using the procedure outlined in section 5.3.1.3. The relationship between flow rate measured in microlitres $minute^{-1}$ and voltage in volts is shown in figure 5.8.

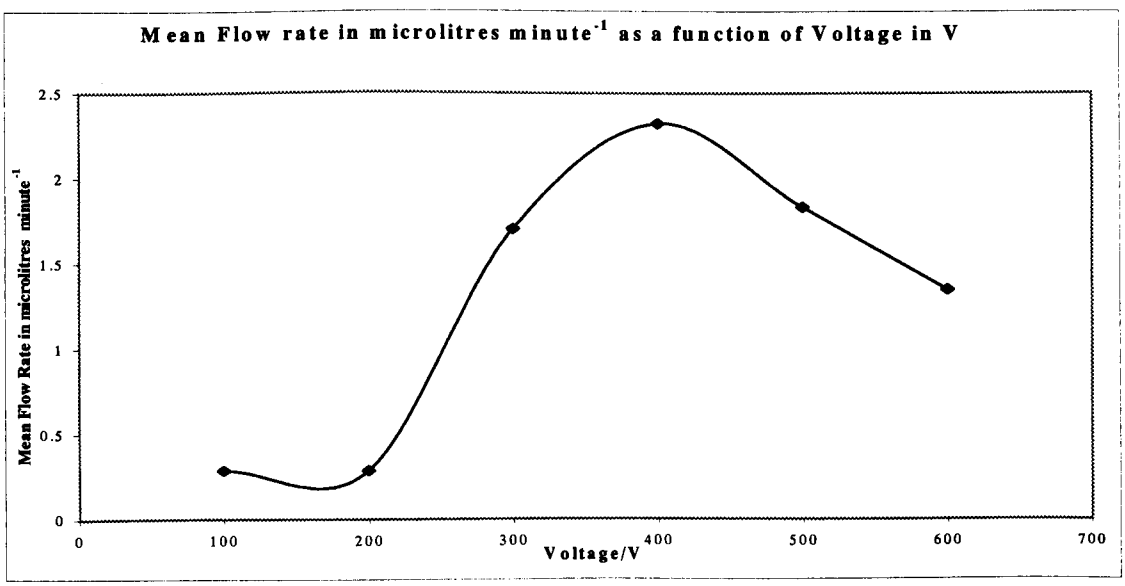

Figure 5.8. Trendline of the flow rate of hydrogen peroxide solution

As can be seen in figure 5.8, the flow rate increased quite dramatically above 200 V to reach a maximum at 400 V of 2.32. ± 0.4 µl $minute^{-1}$ before tailing off due to a heating effect. This was proved during a later examination of the movement of H_2O_2 solution by EOF using a microscope, when substantial bubble production accompanied by localised heating of the miniaturised analysis system was observed at voltages above 400 V.

5.4.2.2. Cobalt nitrate flow rate

The rate of EOF of cobalt nitrate (0.01 mol l^{-1}) solution was determined the voltage range, 200 – 600V using the method described in section 5.2.1.3. The relationship between flow rate in μl $minute^{-1}$ and voltage in volts, V was plotted and is shown in figure 5.9.

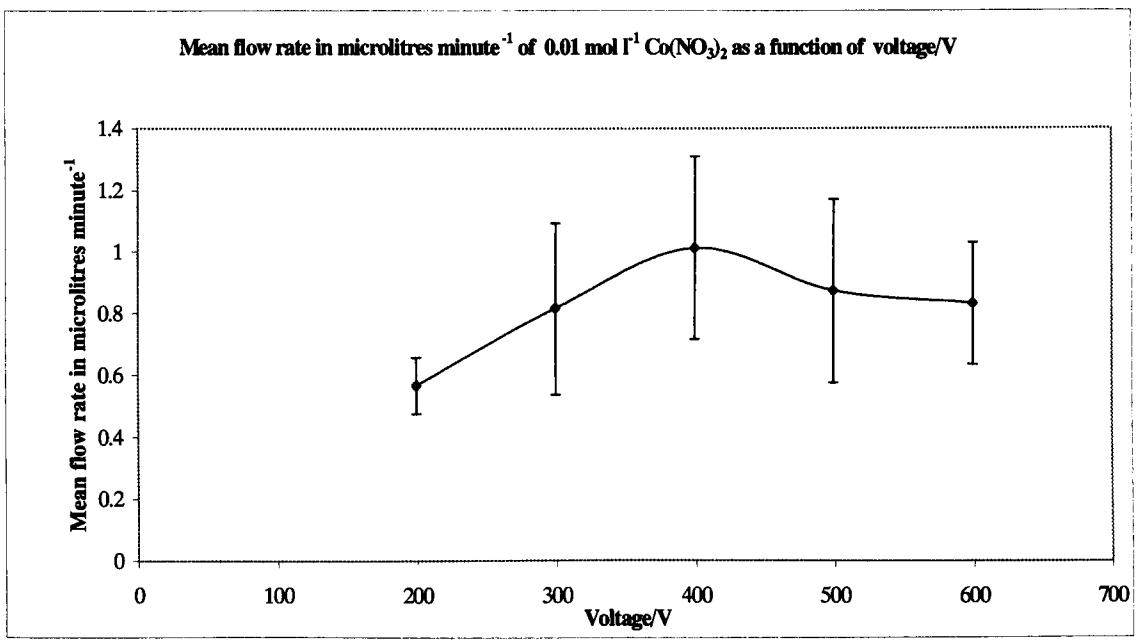

Figure 5.9. Flow rate of the cobalt nitrate solution

As can be seen in the plot, the rate of EOF increased with increasing voltage between 200 V and 400V to a flow rate of 1.01 ± 0.22 μl min^{-1} (n=4) at 400V before dipping to a flow rate of 0.83 ± 0.05 μl min^{-1} (n=5) at a voltage of 600V. It was decided to use a voltage of 400V for further movement of the cobalt nitrate solution in the miniaturised analysis system, as voltages higher than this caused substantial joule heating in the hydrogen peroxide solution.

5.4.2.3. Movement of luminol in sodium carbonate buffer

Due to the negligible movement of luminol in sodium carbonate buffer by EOF alternative methods for the mobilisation of luminol were then considered.

It was decided to investigate the effect of reducing the pH of the luminol in sodium carbonate buffer on the overall emission intensity. This was carried out using the bioluminometer. Solutions of luminol ($1x10^{-3}$ mol l^{-1}) in sodium carbonate buffer (0.1 mol l^{-1}) (100 µl) at pH 10.4 – 7.0 were placed into the sample chamber. A 100 µl aliquot of hydrogen peroxide (0.1mol l^{-1}) solution was injected into the luminol solution and the emission in photon counts per second was monitored every 5 seconds for 10 minutes.

This data has been plotted in figure 5.10 to show the relative CL emission intensity over a time of 5 minutes.

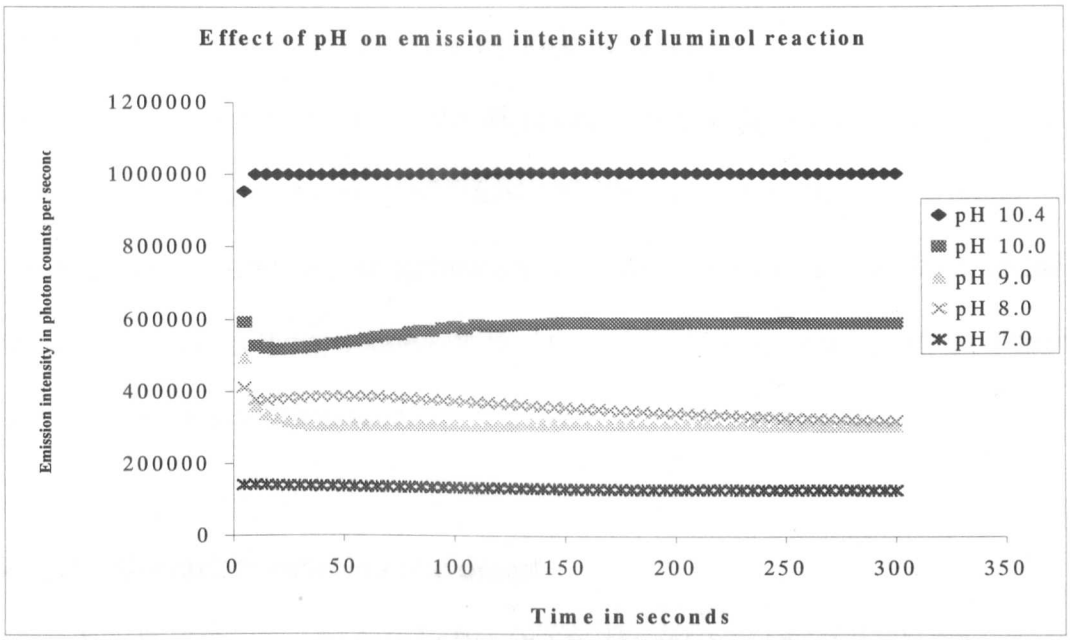

Figure 5.10. Effect of pH on emission intensity with time

Figure 5.10 shows that the intensity of the CL emission drops quite substantially with a decrease in pH. As the amount of light emitted in a glass chip is very small due to the inherently small volumes of reagents used, the aim of the work was to increase the levels of detection by maximising the CL emission. Hence, it was felt that although movement of the luminol in sodium carbonate buffer would be possible using EOF at pH's of 9.0 and below, it would prove advantageous to investigate other methods of mobilisation first. Thus, an investigation of the effect surfactants could have on the luminol reaction in the miniaturised analysis system was carried out as part of the multivariate experimental design work as described in section 5.2.

5.4.3. Experimental design

5.4.3.1. Multivariate optimisation of reagent conditions

As discussed in section 5.2.6, multivariate experimental design was successfully used to optimise the concentrations of most of the reagents in the luminol reaction simultaneously. Although the optimum level of most factors was identified, including the surfactant concentrations, conditions in the miniaturised system would be different and further optimisation was needed.

5.4.3.2. Univariate experimental design

After the pH, sodium carbonate buffer and surfactant concentrations had been optimised using multivariate experimental design, the hydrogen peroxide was optimised using univariate design. This was carried out on the miniaturised analysis system design shown in figure 3.10. The hydrogen peroxide solution was injected into reservoir B, while reservoir A was filled with pH 10.4 sodium carbonate buffer and reservoir C contained the luminol ($1x10^{-3}$mol l^{-1}) in sodium carbonate buffer with the optimised surfactant mixture. A voltage of 400V was applied across BA and CA to mobilise the luminol and hydrogen peroxide solutions. The two sets of reagents met in the reaction well at the intersection of channels A, B, C, D and E and the emission produced was monitored by the PMT via the fibre optic positioned under the reaction well. The solutions then flowed to waste in reservoir A. The output from the PMT was shown on the chart recorder as peak height in mV. Each experiment lasted for approximately 12 minutes.

The effect of adding surfactant to the hydrogen peroxide solution was also investigated to determine whether its presence would produce an increase in the EOF rate that could

increase the CL emission intensity. In effect two calibrations were carried out for hydrogen peroxide solution, with and without the surfactant mixture present.

The calibration data obtained with and without surfactants present is shown in figure 5.11 and figure 5.12 respectively.

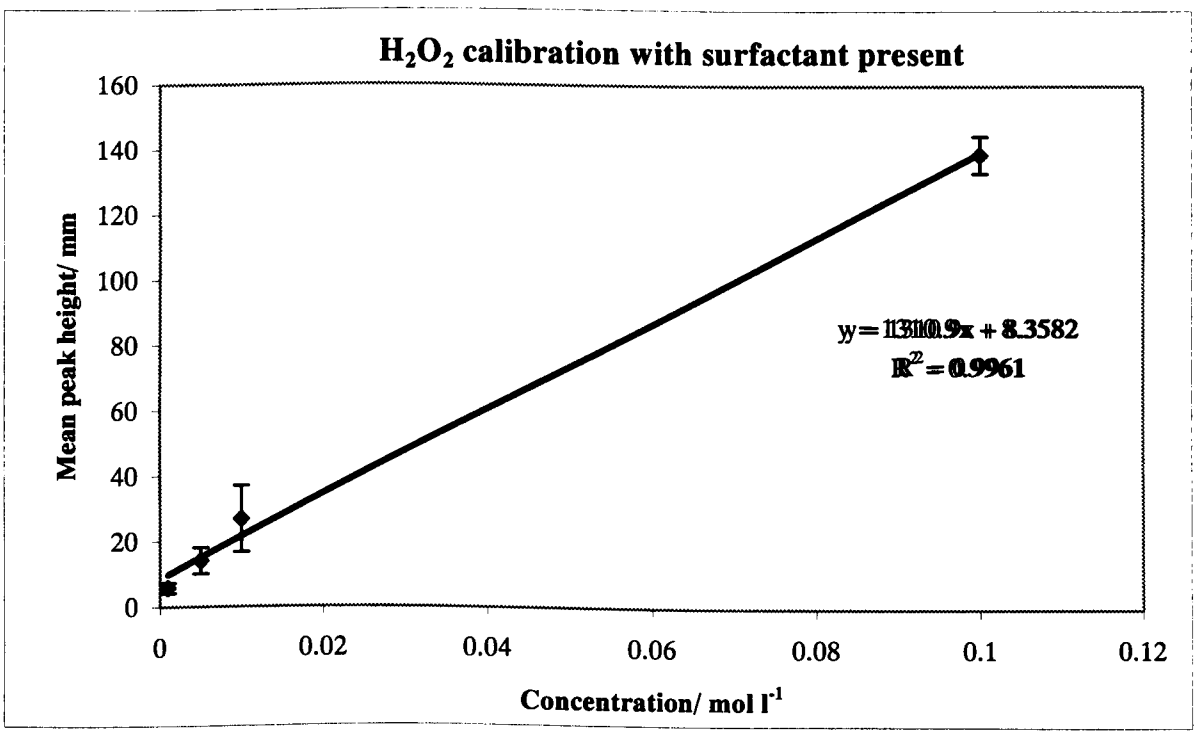

Figure 5.11. Calibration data for hydrogen peroxide solution with surfactant present

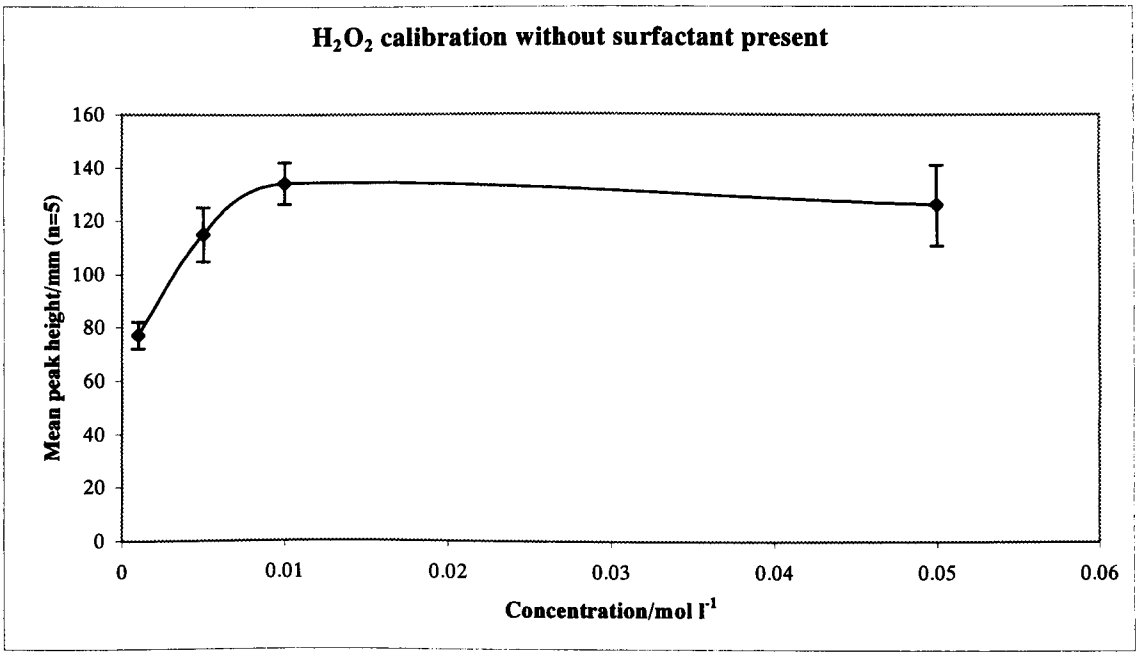

Figure 5.12. Calibration data for hydrogen peroxide solution without surfactant present

Figure 5.11 shows that the CL emission intensity increased linearly with increasing hydrogen peroxide concentration, although there was a deviation from linearity at a higher concentration of 0.1 mol l^{-1}. The mean CL emission intensity observed was far less than that shown at equivalent concentrations in the absence of surfactants, as shown in figure 5.12. As shown in figure 5.12, the CL emission intensity reached a maximum at a hydrogen peroxide concentration of 0.01 mol l^{-1} before tailing off after this point. Increased noise was observed on the chart during experiments containing surfactant. In addition the flow rate did not increase substantially when surfactant was added to the solution and it was therefore decided not to include surfactant in the hydrogen peroxide mixture.

The fact that the same CL emission intensity is observed at lower concentrations of hydrogen peroxide solution in the absence of surfactant can probably be attributed to a dilution of the reagents by excess surfactant. The use of surfactant, with a concentration above the CMC, has been shown to enhance the overall CL emission intensity[210]. However a high surfactant concentration will reduce the overall localised reagent concentrations in or near any given micelle by dilution of the available reagent resulting in an overall decrease in CL emission intensity.

5.4.4. The reaction in the miniaturised analysis system

5.4.4.1. The 'Y' manifold

Due to damage during delivery and bonding, the 'Y' miniaturised analysis system did not prove to be water-tight and therefore could not be used for any kind of accurate analysis. As a result, the reaction was then carried out using the 'starburst' design shown in figure 3.10, with frits placed in channels BD and CD to help control hydrodynamic flow.

5.4.4.2. Initial incorporation of cobalt nitrate solution into the luminol reaction on the miniaturised analysis system

The cobalt nitrate solution was initially kept separate from the other reagents and fed into the mixture of luminol and surfactant as it interacted with the hydrogen peroxide in solution. However this was found to have a negative effect on the CL emission intensity. This was possibly due to the level of the initial concentrations used which were too concentrated and thus had a quenching effect of the CL emission rather than the method of mixing.

Combination of cobalt nitrate with luminol in sodium carbonate buffer and hydrogen peroxide solution

The effect of order of mixing the reagents for the reaction was investigated. It was found that concentrations of cobalt nitrate solution of 0.01 mol l^{-1} and above caused precipitation to occur when the cobalt nitrate solution came into contact with the sodium carbonate or surfactant solutions. A similar situation was observed for most of the metals.

Lower concentrations of cobalt nitrate were then used with greater success. Burdo and Seitz[172] reported the presence of a cobalt-hydrogen peroxide complex in the mechanism for the luminol reaction with Co(II) catalysis. An improvement in both the peak height and associated noise was observed once this method was adopted. The location of the reagents was thus as indicated in figure 5.13.

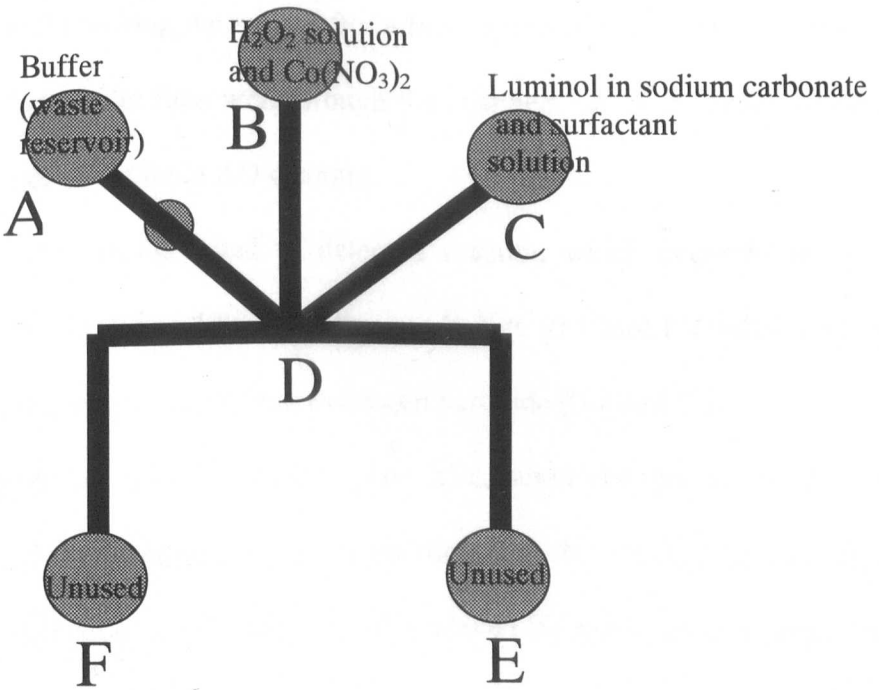

Figure 5.13. Final location of reagents for the luminol reaction

Monitoring the reaction from the fibre optic inserted into the channel

This was carried out in order to try and increase the sensitivity of detection according to the procedure described in section 3.5.

Some small peaks were recorded for the reaction between luminol ($1x10^{-2}$ mol l^{-1}) in sodium carbonate (0.1 mol l^{-1}) buffer and optimised surfactant mixture in reservoir C and hydrogen peroxide (0.1 mol l^{-1}) in reservoir B, however the fibre optic did pick up a large amount of noise as well. Two power supplies and two sets of electrodes were used. The hydrogen peroxide solution was moved from B to E and the luminol in solution from C to F.

As the output was not as great as had been expected, possibly due to the small surface area of the end of the fibre, it was decided that the positioning of the fibre optic in the channel was not right. However, once the fibre optic was positioned it was impossible to remove it without breaking the end. After a few experiments it became apparent that the current did not appear to flow well through the channels. A closer examination revealed a partial blockage of the main AD channel.

Unfortunately, this set-up failed to detect a reaction which occurred in the channel between luminol ($1x10^{-2}$ mol l^{-1}) in sodium carbonate (0.1 mol l^{-1}) buffer and optimised surfactant mixture in reservoir C and hydrogen peroxide (0.1 mol l^{-1}).

Although in principle this was a very good idea, some changes to the procedure and positioning need to be addressed and are mentioned in the conclusions and further work section. The detection of CL was instead achieved by positioning a larger fibre optic directly underneath the channel.

Monitoring the reaction from under the channel

As shown in Figure 5.13, the hydrogen peroxide and cobalt solution flowed from reservoir B along the channel BD towards reservoir A. The luminol, sodium carbonate and surfactant mixture flowed from reservoir C along channel CD and mixed with the hydrogen peroxide and cobalt solution at position D where the two channels intersected. This initiated the reaction that was subsequently monitored from underneath the channel AD as the chemiluminescing species travelled towards the waste reservoir A. The fibre optic was positioned at point E under channel AD. The output from the moving chemiluminesence showed up on the chart recorder as untidy peaks and troughs, which was in direct contrast to the output recorded from reactions taking place in the mixing well which were picked up as smooth peaks. These untidy peaks were generated by the pulsing motion of the luminescing species, caused by bubbles of nitrogen gas produced in the channels during the course of the reaction, as it moved along channel DA.

The movement of the luminescing species in the channel of the miniaturised analysis system was tracked by placing photographic paper (Ilford, Cheshire, UK) under the miniaturised analysis system while the reaction was in progress, and then later photographed using a camera. The camera was set up on a stand above the opened isolation box which had the safety interlock device overridden in order to allow voltage to be supplied to the system with the box lid open. The shutter was held open until sufficient light was visible. Increased concentrations of reagents had to be employed in order to allow sufficient light to be generated in order to take a picture. The concentration of the luminol in the solution with the sodium carbonate buffer and the surfactant was increased to $5x10^{-2}$ mol l^{-1} and the concentration of hydrogen peroxide

was 0.5 mol l^{-1}. The concentrations of the sodium carbonate buffer and the surfactant mixture remained unchanged.

Some of the images obtained from the photographs can be seen in figure 5.14. The bright areas in the channels show the luminescent material.

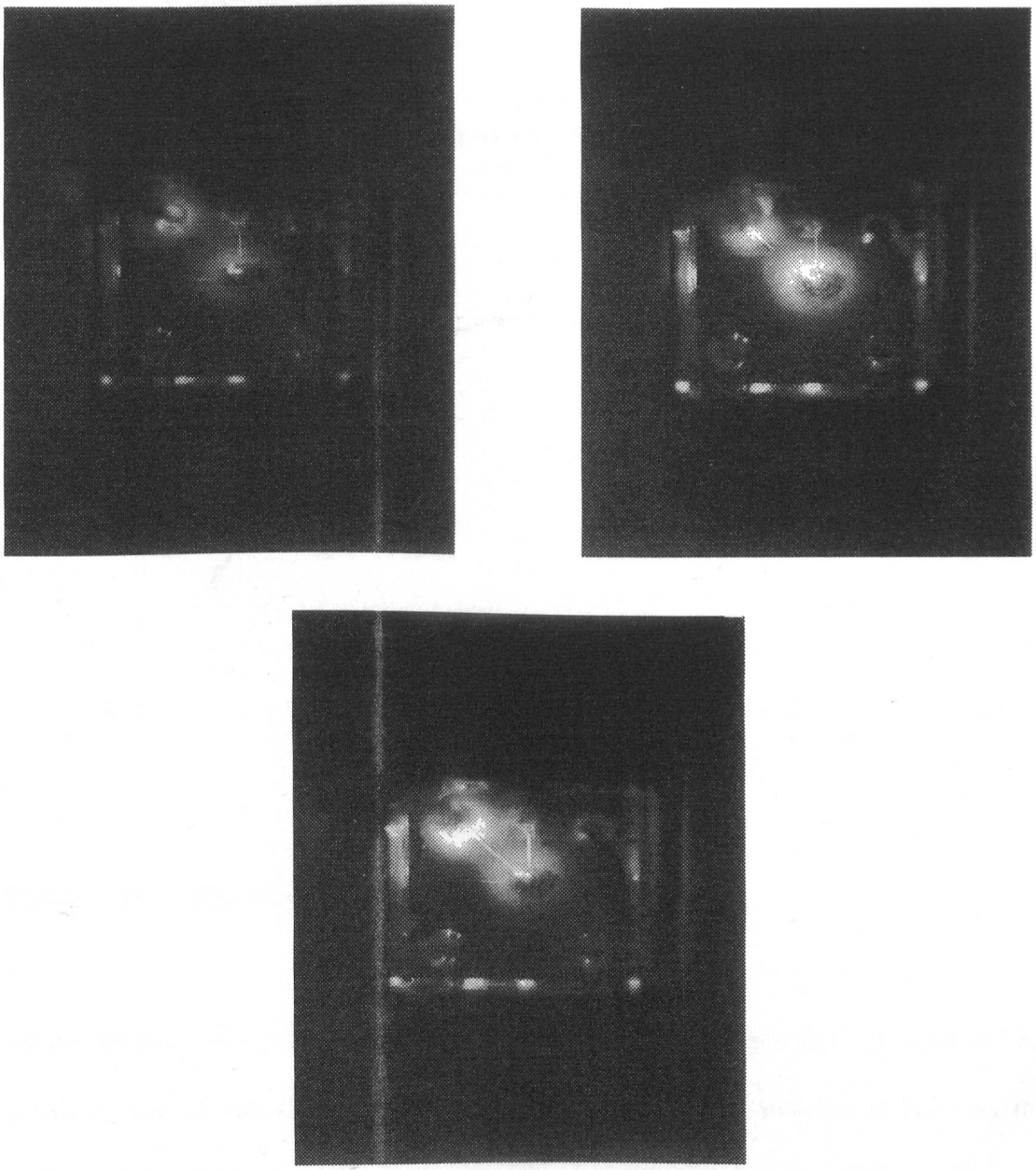

Figure 5.14. Photographic images of the reaction in progress

5.4.4.3. Calibration results for cobalt nitrate solution

A full calibration for cobalt nitrate was then carried out using detection under the channel AD at position E. The concentration range of the cobalt nitrate in hydrogen peroxide solution was 10^{-10}- 10^{-4} mol l^{-1}. The CL output was recorded in mean peak height in mV and is shown in figure 5.15.

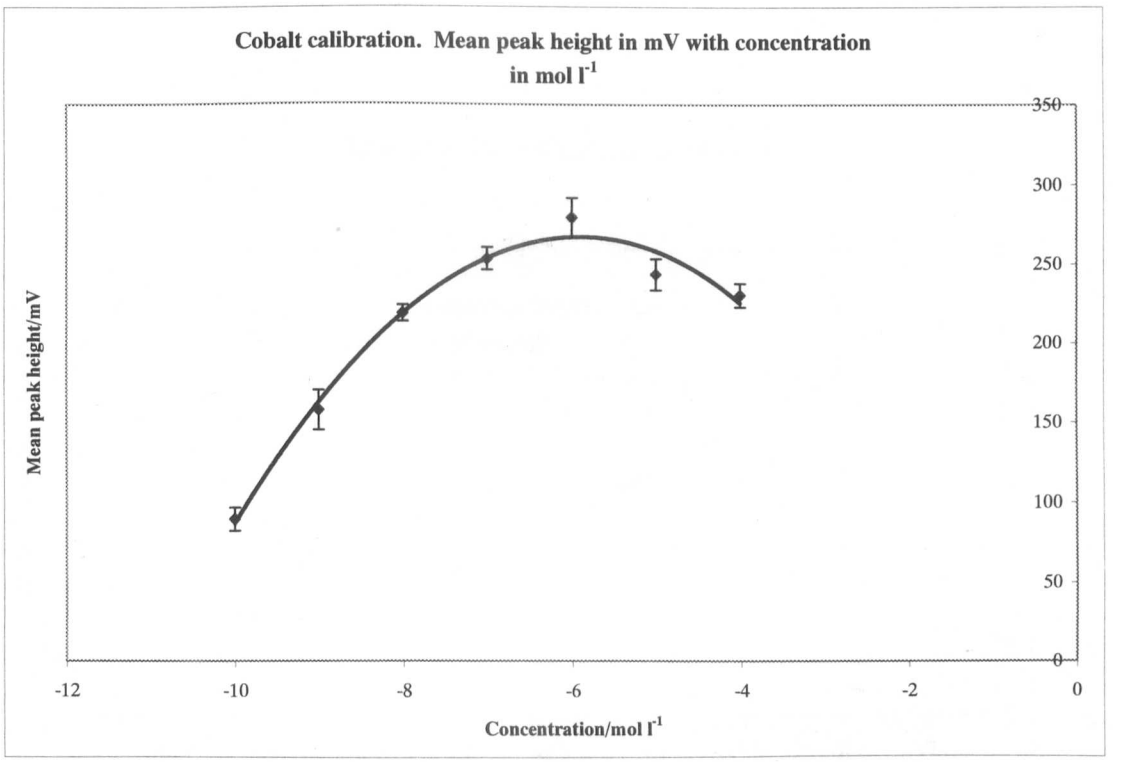

Figure 5.15 Calibration plot for cobalt nitrate solution

As can be seen in figure 5.15, the emission intensity increases linearly with increasing cobalt nitrate concentration up to 10^{-8} mol l^{-1}. A further non-linear increase in CL emission intensity is observed, with a maximum mean peak height of 278.8 mV observed for a cobalt nitrate concentration of 10^{-6} mol l^{-1}. Beyond this, the CL emission intensity is observed to decrease slightly with a further increase in cobalt nitrate concentration. A

similar shape of plot was reported by Chang and Patterson[176] who observed a linear relationship between peak height and concentrations of 10^{-9} - 10^{-6} before the points on the graph became a curve.

The linear portion of the graph (10^{-10} – 10^{-8} mol l^{-1}) was re-plotted as shown in figure 5.16. The equation of the line was found to be y = 64.625x + 735.71 with R^2 = 0.999, where x (n=3) was the concentration in mol l^{-1} and y was the average CL emission in mV.

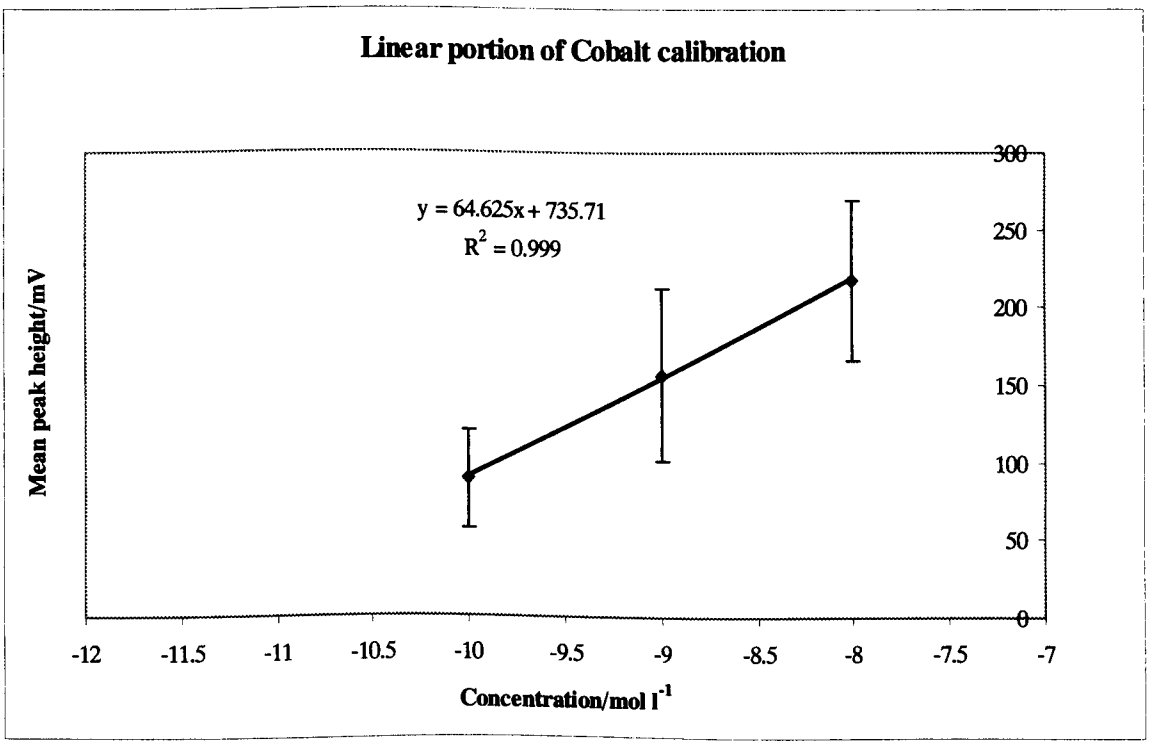

Figure 5.16 Linear portion of plot

The limit of detection was found by using the equation of the line and was determined at 95% confidence limits to be ~$4x10^{-11}$ mol l^{-1} cobalt nitrate which equates to 0.01 ng ml^{-1}. From the literature, the limit of detection quoted for cobalt (II) analysis varies depending on the reaction conditions used. Chang and Patterson[176] investigated the effect of halide

ions on the lowering of the limit of detection in the detection of Co(II), Fe(II) and Cr(III) using the luminol reaction. In the absence of halide ions, they quoted the limit of detection for Co(II) to be $1.5x10^{-9}$ mol l^{-1}, which in the presence of 0.3 mol l l^{-1} bromide was reduced to $1.1x10^{-9}$ mol l^{-1} which is equivalent to 0.32 ng ml^{-1} cobalt nitrate. Sakai *et al.*[172] quote a detection limit of 1.0pg ml^{-1} Co(II) for a sample of 100 µl, using CL detection coupled to ion chromatographic separation.

An RSD of 6.9% (n=3) was obtained for the $1x10^{-8}$ mol l^{-1} standard. The sample run time was approximately 12 minutes that resulted in an average overall throughput time of 15 minutes.

5.5. Conclusions

A miniaturised analysis system has been produced that enabled the detection of a metal ion in solution. A calibration over seven orders of magnitude with a detection limit for cobalt nitrate of 0.01 ng ml^{-1} was successfully achieved.

A suitable manifold was designed. Although this was unable to be fully implemented it has been found that the use of a larger dimension manifold, with frits placed in the channels to prevent hydrodynamic flow, improved reproducibility. The incorporation of a fibre optic directly into the channel requires further investigation, but could potentially increase sensitivity and improve the overall portability of the miniaturised analysis system device. Surfactants were again used to modify the flow characteristics and multivariate experimental design was successfully carried out to optimise the CL emission intensity.

Further improvements to this miniaturised analysis system could include a separation step to allow multi-analyte detection, either by using electrophoresis in an additional separation channel or by coupling a specific miniaturised separation system to this detection system to produce a complete miniaturised analysis system.

Use of a pre-programmed set of voltages, controlled by a software package such as Labview®, could allow voltages to be applied across various channels at specified time intervals. This would prove very useful for improving flow rate reproducibility, especially for the injection of one flowing stream into another.

6. General Conclusions and Future Work

This thesis has described the application and potential advantages of using chemiluminescence as a method of detection in miniaturised analytical systems. The main conclusions arising from the work have been discussed at the end of each chapter. Here they are outlined again in the same order in which they have been previously described, including further suggestions for future work.

6.1. The use and applications of miniaturised analytical measurement

The origins, theoretical principles, manufacture and operating procedures of miniaturised analytical systems were outlined in chapter 1. The aims of this technology are to enable the production of small, inexpensive, user-friendly sensing devices, designed to give results that are at least comparable to those obtained in a conventional laboratory, but at the same time allow rapid and remote sensing to be carried out. These devices are relatively inexpensive to fabricate and a range of substrates can be employed for manufacture.

Many miniaturised analytical systems utilise electrokinetic methods for reagent mobilisation. The factors affecting electro-osmotic and electrophoretic flow were discussed in addition to the use of manifold design in order to increase turbulence necessary to bring about mixing and separation in electrokinetically driven flow systems. Methods of surface modification, the incorporation of silica micro-porous structures (frits) and methods of detection in miniaturised analytical systems were described. The

applications of these devices in the literature were reviewed and the potential merits of using chemiluminescence as a means of detection in miniaturised analytical systems were outlined. These included the low cost, simple instrumentation requirements of chemiluminescence, coupled with the very small reagent volumes required in a one-shot, disposable miniaturised device.

6.2. A review of chemiluminescence as an analytical method of detection

The occurrence, mechanisms and current analytical applications of chemiluminescence, in particular that of the tris(2,2'-bipyridyl)ruthenium (II) (TBR) and the luminol reactions, were reviewed. A detailed review of the analysis of codeine and cobalt (II), the two analytes used in the work described in chapters 4 and 5 respectively, was also given.

The use of surfactants to help overcome pH imbalances in chemiluminescent systems and the enhancement effect of the CL emission intensity at concentrations greater than the critical micelle concentration was examined. Possible reasons for this observed enhancement are thought to be due to changes in the microenvironment of the CL system that result in lower energy transfer pathways as a consequence of high localised reagent concentrations which occur in and around the micelles. The specific use of cationic surfactants in the luminol reaction was reviewed.

Finally, the justification for using chemiluminescence as a means of detection in miniaturised analytical systems and publications citing the use of both chemiluminescence and electrogenerated chemiluminescence detection in miniaturised

systems was reported. Most of the previous publications demonstrate only the feasibility of using CL in a miniaturised system. There have been a few reports of analyte quantification although mainly using electrogenerated chemiluminescent systems.

6.3. Development of instrumentation for the miniaturised analytical system

The substrates, designs and method of fabrication of the miniaturised analytical systems used in this work were described, in addition to the instrumentation required to enable electro-osmotic flow to be used as the method of fluid mobilisation. The four detection arrangements, that were examined in order to determine the best method for optimising output from a CL reaction in a miniaturised system, were described. The use of a fibre optic coupled to a miniaturised photomultiplier tube detector was finally chosen in order to maximise the amount of light observed.

6.4. Determination of codeine in a miniaturised analytical detection system using the tris(2,2'-bipyridyl)ruthenium (II) (TBR) reaction

The tris(2,2'-bipyridyl)ruthenium (II) reaction was chosen as a feasibility study. This reaction was optimised and used to determine codeine. The effect on the emission intensity of using both lead oxide and cerium (IV) sulphate to oxidise the TBR species was examined. Lead oxide was found to produce a higher intensity of light, although this meant that filtration of the solution was required prior to use in the miniaturised analytical system.

The addition of a non-ionic surfactant, Triton X-45 (0.1g l^{-1}), to the oxidised ruthenium species and sulphuric acid mixture was found to increase the overall emission intensity by % and a dramatic increase the flow rate was also observed. Optimum flow rates of 5.0 ± 0.2 µl and 1.8 ± 0.2 µl for the oxidised ruthenium species ($1x10^{-3}$ mol l^{-1}), sulphuric acid (0.05 mol l^{-1}) and triton X-45 (0.1 mol l^{-1}) mixture and the codeine ($1x10^{-4}$ mol $^{-1}$) in acetate (0.01 mol l^{-1}) solution, respectively at a voltage of 400 V.

A calibration for codeine, linear over 3 orders of magnitude, was achieved, with a limit of detection of 8.3 $x10^{-3}$ mol l^{-1} at 95% confidence limits.

6.5. Determination of cobalt (II) nitrate in a miniaturised analytical system using the luminol reaction

The overall aim of the project was to investigate the feasibility of combining CL detection in a miniaturised analytical system and then use this set-up for a determination of metal ions. The most suitable CL reaction for metal ion analysis is the luminol reaction.

Due to the high pH requirements of this reaction (pH 10.4), surfactants were again employed to mobilise the luminol in sodium carbonate solution. The use of cationic surfactants and their enhancement effect of the luminol reaction has been well documented and they were chosen for examination.

A multivariate experimental design programme was successfully carried out in order to examine the effect of pH, buffer, buffer concentration, surfactant and surfactant

concentration on the chemiluminescent emission of the luminol reaction. It was found that the addition of surfactants increased both the initial chemiluminescence intensity and the overall lifetime of the luminescence. Overall, a mixture of the cationic surfactants CTAB (0.2800g/100 ml) and CTAC (0.1800g/100ml) was found to show the greatest enhancement effect. It was discovered that the length of time the luminol in carbonate solution remained in contact with the surfactant mixture prior to analysis also had a large effect on the emission intensity. A contact time of 120 minutes was observed to produce the greatest enhancement effect.

The results of this experimental design programme were used in the optimisation of the luminol reaction in the miniaturised analytical system.

Optimum flow rates for hydrogen peroxide (0.01 mol l^{-1}) solution of 2.32 ± 0.4, for cobalt (II) nitrate (0.01 mol l^{-1}) solution of 1.01 ± 0.22 µl min^{-1} and for the luminol ($1x10^{-3}$ mol l^{-1}) in the optimised surfactant mixture.

A calibration over seven orders of magnitude was carried out which was linear over the concentrations of 10^{-10} – 10^{-8} mol l^{-1}. The equation of the line was found to be y = 64.625x + 735.71 with R^2 = 0.999, with an RSD of 6.9% (n=3) obtained for the $1x10^{-8}$ mol l^{-1} standard. A detection limit of ~$4x10^{-11}$ mol l^{-1} cobalt nitrate (0.01 ng ml^{-1}) was determined at 95% confidence limits.

6.6. Future work

In order to enable multi-analyte determinations to be carried, a separation step would be required. This could feasibly be carried out in a number of ways. Electrophoresis in an additional separation channel could be used. Additionally, the design could be modified to allow inclusion of a separation structure that would increase the turbulence of the flowing system by dividing the channel network into smaller laminae, before subsequent recombination of these separate flowing streams produced a single mixed stream of solution. Alternatively, the miniaturised detection system demonstrated here could be coupled to a specific miniaturised separation system, such as a miniaturised isotachophoresis unit, to produce a complete miniaturised analysis system.

Use of a pre-programmed set of voltages, controlled by a software package such as Labview®, would allow voltages to be applied across various channels at specified time intervals. Such a voltage programme would be fully automated and enable "hands free" control by the user. This would prove especially useful for the injection of one flowing stream into another.

The use of clip in electrodes, possibly with a luer-type fitting would ensure exactly reproducible electrode positioning and hence reduce errors associated with flow rate measurements. Reservoirs that could be replenished, for developmental work carried out in the laboratory, without the need for electrode removal would also improve flow rate reproducibility.

7. References

1. S. Lui and P.K. Dasgupta, Anal. Chim. Acta, 1993, **283**, 739.
2. A. Manz, N. Graber and H.M. Widmer, Sens. Act. B1, 1990, 244.
3. A. Manz, J.C. Fettinger, E. Verpoorte, H. Lüdi, H.M. Widmer and D.J. Harrison, TrAC, 1991, **10**, 144.
4. C.S. Effenhauser and A. Manz, American Lab., 1994, 15.
5. A. van den Berg and P. Bergveld (editors), Micro Total Analysis Systems, Kluwer Academic Publishers, The Netherlands, 1995, pp 5.
6. A. Manz, C.S. Effenhauser, N.Burggraf, E.M.J. Verpoorte, D.E. Raymond and H.M. Widmer, Analusis Mag.,1994, **22**, M25-M28.
7. R. Bogue, Lab. Equip. Digest, 1995, 14.
8. G.T.A. Kovacs, K. Petersen and M. Albin, Anal. Chem. News and Features, 1996, July, 407A.
9. S.C. Terry, J.H. Jarman and J.B. Angell, IEEE Trans. Electron, 1979, ED-26, 1880.
10. N.P. Chopey, G. Ondrey and G. Parkinson, Chem. Eng., 1997, 30.
11. G.N.Doku and S.J. Haswell, Anal. Chim. Acta, 1999, **382**, 1.
12. G.M. Greenway, S.J. Haswell and P.H. Petsul, Anal. Chim. Acta, 1999, **387**, 1.
13. S.C. Jacobson, L.B. Koutny, R. Hergenröder, A.W. Moore Jnr. and J.M. Ramsey, Anal. Chim. Acta, 1994, **66**, 3472.
14. T. Vering, S. Adam, H. Drewer, R. Steinkuhl, A. Schultze, E.G. Siegel and M. Knoll, Analyst, 1998, **123**, 1605.
15. M. Sudoh, A. Mori, H. Fujimura, H. Katayama, Electrochim. Acta, 1999, **44**, 3839.

16. E. Demsey, D. Diamond, M.R. Smyth, G. Urban, G. Jobst, I. Moser, E.M.J. Verpoorte, A. Manz, H.M. Widmer, K. Rabenstein and R. Freaney, Anal. Chim. Acta, 1997, **346**, 341.

17. L.C. Waters, S.C. Jacobson, N. Kroutchinina, J. Khandurina, R.S. Foote and J.M. Ramsey, Anal. Chem., 1998, **70**, 158.

18. M.U. Kopp, A.J. de Mello and A. Manz, Science, 1998, **280**, 1946.

19. A.T. Woolley, D. Hadley, P. Landre, A.J. de Mello, R.A. Mathies and M.A. Northrup, Anal. Chem., 1998, **68**, 4081.

20. L.C. Waters, S.C. Jacobson, N. Kroutchinina, J. Khandurina, R.S. Foote and J.M. Ramsey, Anal. Chem., 1998, **70**, 5172.

21. S.J. Haswell, Analyst, 1997, **121**, 1R.

22. R.N.C. Daykin and S.J. Haswell, Anal. Chim. Acta, 1995, **313**, 155.

23. A. Manz, D.J. Harrison, E.M.J. Verpoorte and H.M. Widmer, Miniaturisation of Separation Systems, 1991, 1.

24. J.S. Daniel and G. Delapierre, J. Micromech. Microeng., 1991, **1**, 187.

25. Z.H. Fan and D.J. Harrison, Anal. Chem., 1994, **66**177.

26. S.C. Jacobson and J.M. Ramsey, Anal. Chem.,1996, **68**, 720.

27. D.J. Harrison, K. Fluri, N. Chiem, T. Tang and Z. Fan, Sens. Act.B, 1996, **33**, 105.

28. C.T. Culbertson, S.C. Jacobson and J.M. Ramsey, Anal. Chem., 1998, **70**, 3781.

29. E. Verpoorte, A. Manz, H. Lüdi, A.E. Bruno, F. Maystre, B. Krattiger, H.M. Widmer, B.H. van der Schoot and N.F. de Rooij, Sens. Act.B, 1992, **6**, 66.

30. D.J. Harrison, P.G. Glavina and A. Manz, Sens. Act.B, 1993, **10**, 107.

31. K. Hosokawa, T. Fujii and I. Endo, Anal. Chem., 1999, **71**, 4781.

32. E. Derhamarche, A. Bernard, H. Schmid, A. Bietsch, B. Michel and H. Biebuyck, J. Am. Chem. Soc., 1998, **120**, 500.

33. D.C. Duffy, H.L. Gillis, J. Lin, N.F. Shepard Jnr., and G.J. Kellogg, Anal. Chem.,1999, **71**, 4669.

34. M. Esashi, A. Nakano, S. Shoji and H. Hebiguchi, Sens. Act.A, 1990, **21-23**, 931.

35. M. Madou, Fundamentals of Microfabrication, 1997, CRC Press LLC, Florida, chapter 8.

36. Y-T. Hsueh, R.L. Smith and M.A. Northrup, Sens. Act.B, 1996, **33**, 110.

37. K. Fluri, G. Fitzpatrick, N. Chiem and D.J. Harrison, Anal. Chem., 1996, **68**, 4285.

38. P. Norlin, O.Öhman, B. Ekström and L. Forrsén, Sens. Act.B, 1998, **49**, 34.

39. L. Martynova, L.E. Locascio, M. Gaitan, G.W. Kramer, R.G. Christensen and W.A. MacCrehan, Anal. Chem., 1997, **69**, 4783-4789.

40. M.A. Roberts, J.S. Rossier, P. Bercier and H. Girault, Anal. Chem., 1997, **69**, 2035-2042.

41. L.E. Locascio, C.E. Perso and C.S. Lee, J. Chrom. A, 1999, **857**, 275-284.

42. D. Qin, Y. Xia, J.A. Rogers, R.J. Jackman, X-M. Zhao and G.M. Whitesides, Topics in Current Chemistry, 1998, **194**, 2., Springer-Verlag, Berlin-Heidelberg.

43. M. Madou, Fundamentals of Microfabrication, 1997, CRC Press LLC, Florida, chapter 2.

44. M. Madou, Fundamentals of Microfabrication, 1997, CRC Press LLC, Florida, chapter 6.

45. W. Ehrfeld, P. Bley, F. Götz, P. Hagmann, A. Maner, J. Mohr, H.O. Moser, D. Münchmeyer, W. Schelb, D. Schmidt and E.W. Becker, Micromaching and MEMS,

1997, Ed W.S. Trimmer,623, Institute of Electrical and Electronic Engineers Inc., New York.

46. Jenoptik Group, Jena, Germany; company brochure.

47. H. Becker, W. Dietz and P. Dannberg, Proceedings of Micro-TAS'98, Banff, Canada, October 1998, pp. 253.

48. H. Becker, U. Heim, O. Rötting, Proceedings of SPIE-Microfluidic Devices and Sytems, September 1999, Santa Clara, USA, pp. 74.

49. L. Martynova, L.E. Locascio, M. Gaitan, G.W. Kramer, R.G. Christensen and W.A. MacCrehan, Anal. Chem., 1997, **69**, 4783.

50. K.L. Mittal (Ed), Polymer Surface Modification: relevance to adhesion, 1996, 3, VSP, Utrecht, The Netherlands.

51. G.S. Feugerson, M.K. Chaudhury, H.A. Biebuyck and G.M. Whitesides, Macromolecules, 1993, **26**, 5870.

52. Surface treatment of PDMS, University of Wisconsin-Madison home page, http://www.mrsec.wisc.edu/EDETC/pdmsexp4.html

53. M. Madou, Fundamentals of Microfabrication, 1997, CRC Press LLC, Florida, chapter 9.

54. P. Gravesen, J. Branebjerg and O.S. Jensen, J. Micromech. Microeng., 1993, **3**, 168.

55. R. Zengerle, A. Richter and H. Sandmaier, Proc. MEMS'92, 19.

56. A. van den Berg and T.S.J. Lammerink, Topics in Current Chemistry, 1998, **194**, 21, Springer-Verlag, Berlin-Heidelberg

57. A. Manz, C.S. Effenhauser, N. Burggraf, D.J. Harrison, K. Seiler and K. Fluri, J. Micromech. Microeng., 1994, **4**, 257.

58. P.J.A. Kenis, R.F. Ismagilov and G.M. Whitesides, Science, 1999, **285**, 83.

59. P.D.I. Fletcher, S.J. Haswell and V.N. Paunov, Analyst, 1999, **124**, 1273.

60. N.A. Patankar and H.H. Hu, Anal. Chem., 1998, **70**, 1870.

61. E.V. Dose and G. Guiochon, J. Chrom., 1993, **652**, 263.

62. H. Poppes, A. Cifuentes and W.T. Kok, Anal. Chem., 1996, **68**, 888.

63. J. Jednacak, V. Pravdic and W. Haller, J. Coll. Inter.Sci., 1974, **49**, 16.

64. P.J. Scales, F. Grieser, T.W. Healy, L.R. White and D.Y.C. Chan, Langmuir, 1992, **8**, 965.

65. A. Vernhet, M.W. Bellon-Fontaine and A. Doren, J. Chim. Phys., 1994, **91**, 1728.

66. R.A. van Wagenen and J.D. Andrade, J. Coll. Inter. Sci., 1980, **76**, 305.

67. C.A. Lucy and R.S. Underhill, Anal. Chem., 1998, **70**, 1045.

68. C.A. Lucy and R.S. Underhill, Anal. Chem., 1996, **68**, 300.

69. C.A. Lucy and K.K.C. Yeung, J. Chrom.A, 1998, **804**, 319.

70. S.C. Jacobson, R. Hergenröder, L.B. Koutny and J.M. Ramsey, Anal. Chem., 1994, **66**, 1114.

71. S.C. Jacobson, R. Hergenröder, L.B. Koutny, R.J. Warmack, J.M. Ramsey, Anal. Chem., 1994, **66**, 1107.

72. M. McEnery, A. Tan, J. Alderman, J. Patterson, S.C. O'Mathuna and J.D. Glennon, Analyst, 2000, **125**, 25.

73. F.G. Bessoth, A. J. de Mello and A. Manz, Anal. Commun., 1999, **36** 213.

74. C. Erbacher, F.G. Bessoth, M. Busch, E. Verpoorte and A. Manz, Mikrochim. Acta 1999, **131**, 19.

75. W. Ehrfeld, K. Golbig, V. Hessel, H. Löwe, T. Richter and K. Russow, Microsystem Technol. News, 1996, **17**, 5.

76. R. Miyake, T.S.J. Lammerink, M. Elwenspök and J.H.J. Fluitman, Proc. IEEE Micro Electro Mechanical Systems, Fort Lauderdale, 1993, 248.

77. M. Elwenspök, T.S.J. Lammerink, R. Miyake and J.H.J. Fluitman, J. Micromech. Microeng., 1994, **4**, 227.

78. C.S. Effenhauser, A. Manz and H.M. Widmer, Anal. Chem., 1993, **65**, 2637.

79. D.A. Skoog and J.J. Leary, Principles of Instrumental Analysis, 4th Ed, 1992, Harcourt Brace College Publishers, Orlando.

80. S.C. Jacobson, R. Herenröder, A.W. Moore Jnr. and J.M. ramsey, Anal. Chem., 1994, **66**, 4127.

81. Q. Mao and J. Pawliszyn, Analyst, 1999, **124**, 637.

82. P.C.H. Li and D.J. Harrison, Anal. Chem., 1997, **69**, 1564.

83. A.T. Woolley and R.A. Mathies, Proc. Natl. Acad. Sci. USA, 1994, **91**, 11348.

84. N. Burggraf, B. Krattinger, A.J. de Mello, N.F. de Rooij and A. Manz, Analyst, 1998, **123**, 1443.

85. T. Kappes and P.C. Hauser, Anal. Commun., 1998, **35**, 325.

86. S.J. Baldock, N. Bektas, N.J. Goddard, L.W. Pickering, J.E. Prest, R.D. Snook, B.J. Treves Brown and D.I. Vaireanu, Proceedings of μTAS '98, Ed. D.J. Harrison and A. van den Berg, Banff, Canada, October 1998, pp 359.

87. P.R. Fielden, S.J. Baldock, N.J. Goddard, L.W. Pickering, J.E. Prest, R.D. Snook, B.J. Treves Brown and D.I. Vaireanu, Proceedings of μTAS '98, Ed. D.J. Harrison and A. van den Berg, Banff, Canada, October 1998, pp 323.

88. K.K.C. Yeung and C.A. Lucy, Anal. Chem., 1998, **70**, 3286.

89. P.D. Christensen, S.W.P. Johnson, T. McCreedy, V. Skelton and N.G. Wilson, Anal. Comm., 1998, **35**, 1.

90. A. Aoki, T. Matsue and I. Uchida, Anal. Chem., 1990, **62**, 2206.

91. P.L.H.M. Cobben, R.J.M. Egberink, J.G. Bomer, E.J.R. Sudholter, P. Bergveld and D.N. Reinhoudt, Anal. Chim. Acta, 1991, **248**, 307.

92. A. Manz, D.J. Harrison, E. Verpoorte and H.M. Widmer, Adv. Chromatogr., 1993, **33**, 1.

93. C.M. Henry, Analytical Chemistry News and Features, April 1999, 264A.

94. Miniature VIS spectrometer, MicroParts (company brochure).

95. M. Suda, T. Sakuhara and I. Karube, App. Biochem. Biotechnol., 1993, **41**, 3.

96. Z. Liang, N. Chiem, G. Ocvirk, T. Tang, K. Fluri and D.J. Harrison, Anal. Chem., 1996, **68**, 1040.

97. P. Norlin, O. Öhman, B. Ekström and L. Forssén, Sens. Actuators B, 1998, **49**, 34.

98. S. Sirichai and A.J. de Mello, Analyst, 2000, **125**, 133.

99. Z. Huang, N. Munro, A.F.R. Hühmer and J.P. Landers, Anal. Chem., 1999, **71**, 5309.

100. G. Ocvirk, T. Tang and D.J. Harrison, Analyst, 1998, **123**, 1429.

101. J.P. Lenney, N.J. Goddard, J.C. Morey, R.D. Snook and P.R. Fielden, Sens. Act.B, 1997, **38-39**, 212.

102. N.J. Goddard, K. Singh, R.J. Holmes and B. Bastani, Sens. Act.B, 1998, **51**, 131.

103. K. Swinney, J. Pennington and D.J. Bornhop, Analyst, 1999, **124**, 221.

104. N.J. Goddard, K. Singh, F. Bounaira, R.J. Holmes, S.J. Baldock, L.W. Pickering, P.R. Fielden and R.D. Snook, Proceedings of μTAS '98, Ed. D.J. Harrison and A. van den Berg, Banff, Canada, October 1998, pp 97.

105. S. Waseda, T. Shimosaka, K. Uchiyama and T. Hobo, Chem. Lett., 1999, July, 1195.

106. R.J. Cotter, C. Fancher and T.J. Cornish, J. Mass Spectrom., 1999, **34**, 1368.

107. S.Taylor, J.J. Tunstall, R.R.A. Syms, T. Tate and M.M. Ahmad, Electron. Lett., 1998, **34**, 546.

108. O. Kornienko, P.T.A. Reilly, W.B. Whitten and J.M. Ramsey, Rapid Commun. In Mass Spectrom., 1999, **13**, 50.

109. M. Hashimoto, K. Tsukagoshi, R. Nakajima, K. Kondo and A. Arai, Chem. Lett., 1999, April, 781.

110. D. Mangru and D.J. Harrison, Electrophoresis, 1998, **19**, 2301

111. G.C. Fiaccabrino, N.F. de Rooij and M. Koudelka-Hep, Anal. Chim. Acta, 1998, **359**, 263.

112. C.A. Marquette and L.J. Blum, Anal. Chim. Acta, 1999, **381**, 1.

113. G.C. Fiaccabrino, M. Koudelka-Hep, Y-T Hsueh, S.D. Collins and R.L. Smith, Anal. Chem., 1998, **70**, 4157.

114. J.P. Preston and T.A. Nieman, Anal. Chem., 1996, **68**, 966.

115. P.E. Michel, G.C. Fiaccabrino, N.F. de Rooij and M. Koudelka-Hep, Anal. Chim. Acta, 1999, **392**, 95.

116. I-STAT point-of-care diagnostic cartridge analyser system, I-STAT press releases for 3rd quarter 1999.

117. K. Robards and P.J. Worsfold, Anal. Chim. Acta, 1992, **266**, 147.

118. A. Townshend, Analyst, 1990, **115**, 495.

119. J.W. Birks (Ed), Chemiluminesence and Photochemical Reaction Detection in Chromatography, VCH, New York, 1989.

120. T. Komatsu, M. Ohira, M. Yamada and S. Suzuki, Bull. Chem. Soc. Jpn., **59**, 1986, 1849.

121. J.L. Burguera, M. Burguera and A. Townshend, Anal. Chim. Acta, **127**, 1981, 199.

122. Q.X. Lin, A. Guiraum, R. Escobar and F.F. Delarosa, Anal. Chim. Acta, 1993, **283**, 379.

123. R. Escobar, Q.X. Lin, A. Guiraum and F.F. Delarosa, Analyst, 1993, **118**, 643.

124. S. Nakano, M. Fukuda, S. Kageyama, H. Itabashi and T. Kawashima, Talanta, 1993, **40**, 75.

125. A.R. Bowie, P.R. Fielden, R.D. Lowe and R.D. Snook, Analyst, 1995, **120**, 2119.

126. K.H. Coale, K.S. Johnston, P.M. Stout and C.M. Sakamoto, Anal. Chim. Acta, 1992, **266**, 345.

127. N.M. Rao, K. Hook and T.A. Nieman, Anal. Chim. Acta, 1992, **266**, 279.

128. D. Price, P.J. Worsfold and R.F.C. Mantoura, Anal. Chim. Acta, 1994, **66**, 1766.

129. X.F. Xie, A.A. Suleiman, G.G. Guilbault, Z.M. Yang and Z.A. Sun, Anal. Chim. Acta, 1992, **266**, 325.

130. M. Katayama, H. Takeuchi and H. Taniguchi, Anal. Chim. Acta, 1993, **281**, 111.

131. Y.X. Ci, J.K. Tie, Q.W. Wang and W.B. Chang, Anal. Chim. Acta, 1992, **269**, 109.

132. A.A. Suleiman, R.L. Villarta and G.G. Guilbault, Anal. Lett., 1993, **26**, 1493.

133. R. Delavalle and M.L. Grayeski, Anal. Biochem., 1991, **197**, 340.

134. M. Tabata, M. Totani and J. Endo, Anal. Chim. Acta, 1992, **262**, 315.

135. A.A. Alwarthan, Analyst, 1993, **118**, 639.

136. A.A. Alwarthan and A.Townshend, Anal. Chim. Acta, 1986, **185**, 329.

137. K. Imai and R. Weinburger, TrAC, 1985, **4**, 170.

138. P.J.M. Kwakman, D.A. Kamminga, U.A.T. Brinkman, G.J. Dejong, J. Chrom., 1991, **553**, 345.

139. P.J.M. Kwakman, H. Koelewijin, I. Kool, U.A. Th. Brinkman and G.J. de Jong, J. Chromatogr., 1990, **511**, 155.

140. T. Kawasaki, K. Imai, T. Higuchi and O. wong, Biomed. Chromatogr., 1990, **4**, 113.

141. M. Tod, M. Prevot, J. Chalom, R. Farinotti and G. Mahuzier, J. Chromatogr., 1991, **542**, 295.

142. J.A. Holeman and N.D. Danielson, J. Chromatogr. A., 1994, **679**, 277.

143. K. Hayakawa, R. Kitamura, M. Butoh, N. Imaizumi and M. Miyazaki, Anal. Sci., 1991, **7**, 573.

144. M. Maeda, K. Tsukagoshi, M. Murata, M. Takagi and T. Yamashita, Anal. Sci., 1994, **10**, 583.

145. H. Li and R. Westerholm, J. Chromatogr. A., 1994, **664**, 177.

146. N.A. Wu and C.W. Huie, J. Chromatogr., 1993, **634**, 309.

147. T. Hara, J. Yokogi, S. Okamura, S. Kato and R. Nakajima, J. Chromatogr. A., 1993, **652**, 361.

148. R. Dadoo, A.G. Seto, L.A. Colon and R.N. Zare, Anal Chem., 1994, **66**, 303.

149. K. Tsukagoshi, T. Nakamura, M. Hashimoto and R. Nakajima, Anal. Sci., 1999, **15**, 1047.

150. K. Tsukagoshi, M. Otsuka, M. Hashimoto, R. Nakajima and K. Kondo, Anal. Sci., 1999, **15**, 1257.

151. M. Hashimoto, K. Tsukagoshi, R. Nakajima and K. Kondo, J. Chrom. A., 1999, **832,** 191-202.

152. A.L. Howard, L.T. Taylor, Anal. Chem., 1993, **65**, 724.

153. D.M. Hercules and F.E. Lytle, J. Am. Chem. Soc., 88 (1966) 4745.

154. R.D. Gerardi, N.W. Barnett and S.W. Lewis, Anal. Chim. Acta, 1999, **378**, 1.

155. J.B. Noffsinger and N.D. Danielson, Anal. Chem., 1987, **59**, 865.

156. N.W. Barnett, R.D. Gerardi, D.L. Hampson and R.A. Russell, Anal. Comm., 1996, **33**, 255.

157. N.W. Barnett, T.A. Bowser, R.D. Gerardi and B. Smith, Anal. Chim. Acta, 1996, **318**, 309.

158. N.W.Barnett, B.J. Hindson, S.W.Lewis, Anal. Chim. Acta, 1999, **384**, 151.

159. R.D. Gerardi, N.W. Barnett and P. Jones, Anal. Chim. Acta, 1999, **388**, 1.

160. I. Rubenstein and A.J. Bard, J. Am. Chem. Soc., 1981, **103**, 512.

161. N.W. Barnett, T.A. Bowser and R.A. Russell, Anal. Proc. Incl. Anal. Comm., 1995, **32**, 57.

162. G.A. Barbieri, G.B. Bonino, Rend. (Accad. Naz. Lin. Clas. Sci.. Fis., Mat. Nat., 1948, **8**, 561.

163. F.H. Burstall, J. Chem. Soc., 1936, 173.

164. Z. He, H. Gao, L. Yuan, Q. Luo and Y. Zeng, Analyst, 1997, **122**, 1343.

165. L.-S. Ling, Z.-K. He, R.-X. Cai, Chemical Journal of Chinese Universities, 1997, **18**, 1963.

166. N.W. Barnett, D.G. Rolfe, T.A. Bowser and T.W. Paton, Anal. Chim. Acta, 1993, **283**, 551.

167. R.W. Abbott, A. Townshend and R. Gill, Analyst, 1986, **111**, 635.

168. T.J. Christie, R.H. Hanway, D.A. Paulls and A. Townshend, Anal. Proc., 1995, **32**, 91.

169. N.W. Barnett, B.J. Hindson, Simon W. Lewis and Stuart D. Purcell, Anal. Commun., 1998, **35**, 321.

170. G.M. Greenway, A.W. Knight and P.J. Knight, Analyst, 1995, **120**, 2549.

171. J.L. Burguera, A. Townshend and S. Greenfield, Anal. Chim. Acta, 1980, **114**, 219.

172. H. Sakai, T. Fujiwara, M. Yamamoto and T. Kumamaru, Anal. Chim. Acta, 1989, **221**, 249.

173. B. Gammelgaard, O. Jones and B. Nielsen, Analyst, 1992, **117**, 637.

174. T.G. Burdo and W.R. Seitz, Anal. Chem., 1975, **47**, 1639.

175. A. MacDonald, K.W. Chan and T. Nieman, Anal Chem., 1993, 2077.

176. C.A. Chang and H.H. Patterson, Anal. Chem., 1980, **52**, 653.

177. B. Yan, S.W. Lewis, P.J. Worsfold, J.S. Lancaster and A. Gachanja, Anal. Chim. Acta, 1991, **250**, 145.

178. A.A. Alwarthan, A. Almuaibed and A. Townshend, Anal. Sci., 1991, **7**, 623.

179. S. Stieg and T.A. Nieman, Anal. Chem., 1977, **49**, 1322.

180. P. Jones and H.G. Beere, Anal. Proc., 1995, **32**, 169.

181. M. Ishii and M. Shirai, Bunseki Kagaku, 1992, **41**125.

182. Y.X. Ci, J.K. Tie, F.J. Yao, Z.L. Liu, S.Lin and W.Q. Zheng, Anal. Chim. Acta, 993, **277**, 67.

183. B. Naslund, P. Arner, J. Blinder, L. Hallander and A. Lundin, Anal. Biochem., 1991, **26**, 1493.

184. B.A. Petersson, Anal. Lett., 1989, **22**, 83.

185. W. Qin, Z.J. Zhang, Y.Y. Peng and B.X. Li, Anal. Comm., 1999, **36**, 337.

186. Y.M. Huang, C. Zhang and Z.J. Zhang, Anal. Sci., 1999, **15**, 867.

187. C.A. Marquette and L.J. Blum, Anal. Chim. Acta, 1999, **381**, 1.

188. H. Cui, R. Meng, H. Jiang, Y. Sun and X. Lin, Luminescence, 1999, **14**, 175.

189. H. Obata, H. Karatani, E. Nakayama, Anal. Chem., 1993, **65**, 1524.

190. V.A. Elrod, K.S. Johnson, K.H. Coale, Anal. Chem., 1991, **63**, 893.

191. M. Derbyshire, A. Lamberty and P.H.E. Gardiner, Anal. Chem., 1999, **71**, 4203.

192. T. Komatsu, M. Ohira, M. Yamada and S. Suzuki, Bull. Chem. Soc. Jpn., 1986, **59**, 1849.

193. T. Williams, P. Jones and L. Ebdon, J, Chromatogr., 1989, **482**, 361.

194. M.R. Porter, Handbook of Surfactants, 2nd Ed., Blackie, 1994.

195. J. Lasovsky and F. Grambal, Biochem. Bioenerg., 1986, **15**, 95.

196. M.S. Abdel-Latif and G. G. Guilbault, Anal. Chim. Acta, 1989, **221**, 11.

197. K. Saitoh, T. Hasebe, N. Teshima, M. Kurihara and T. Kawashima, Anal. Chim. Acta, 1998, **376**, 247.

198. J. Hadjianestis and J. Nikokavouras, J. Photochem. Photobiol. A, 1992, **67**, 237.

199. H. Hoshino and W.L. Hinze, Anal. Chem., 1997, **59**, 496.

200. S. Igarashi and W.L. Hinze, Anal. Chim. Acta, 1989, **225**, 147.

201. G-N. Chen, J-P. Duan and Q-F. Hu, Mikrochim. Acta, 1994, **116**, 227.

202. N. Dan, M.L.Lau and M.L. Grayeski, Anal. Chem., 1991, **63**, 1766.

203. R. van Wandruszka, Crit. Rev. Anal. Chem., 1992, **23**, 187.

204. M.L. Grayeski and P.A. Moritzen, Langmuir, 1997, **13**, 2675.

205. Z-H. Xie, F. Zhang and Y-S. Pan, Analyst, 1998, **123**, 273-275.

206. A. Manz, A. de Mello and A. Arora, Anal. Commun., 1997, **34**, 395.

207. R.N.C. Daykin and S.J. Haswell, Anal. Chim. Acta, 1995, **253**, 155.

208. P.D. Christensen, S.W.P. Johnson, T. McCreedy, V. Skelton and N.G. Wilson, Anal. Commun., 1998, **35**, 1.

209. W-Y. Lee, Mikrochim. Acta, 1997, **127**, 19.

210. A.W. Knight, PhD Thesis, Department of Chemistry, University of Hull, Hull, UK, 1995.

211. P.G. Rouxhet, N. Mozes, M.P. Hermesse and G. Matta-Ammouri, in Neysseland *et al.* Eds. Proc. 4th European Congress on Biotechnology, 1987, **2**, 93.

212. E.J. Kone, P. Welch, B.D. Paul, J.M. Mitchell, J. Anal.Tox., 1991, **15**, 1.

8. Publications and Presentations

The following is a list of publications and presentations resulting from the work contained in this thesis.

8.1. Publications

1. Investigation of a Chemiluminescent Micro-analytical System.

Gillian M. Greenway, Lorna J. Nelstrop and Simon N. Port. *μTAS '98 proceedings*, Banff, Canada, Ed. D.J. Harrison.

2.) Tris(2,2'-bipyridyl)ruthenium (II) Chemiluminescence in a Microflow Injection System for Codeine Determination.

Gillian Greenway, Lorna J. Nelstrop and Simon N. Port. *Analytica Chimica Acta*, 2000, **405**, 43-50.

3.) Luminol Chemiluminescence Systems for Metal Analysis by μTAS.

Gillian M. Greenway, Lorna J. Nelstrop, Tom McCreedy and Paul Greenwood. *μTAS 2000 proceedings,* Enshede, Netherlands, Ed. A. van den Berg.

8.2. Presentations

1. Investigation of chemiluminescent microflow systems.

Poster Presentation - RSC Research and Development Topics in Analytical Chemistry Meeting. University of Newcastle. April 1997.

2. Investigation of chemiluminescent micro-analytical systems.

Poster Presentation - RSC Research and Development Topics in Analytical Chemistry Meeting. University of Durham. April 1998.

3. Investigation of chemiluminescent micro-analytical systems.

Poster Presentation - μTAS '98. Banff, Canada. October 1998.

4. Investigation of chemiluminescent micro-analytical systems.

Oral Presentation – RSC Research and Development Topics in Analytical Chemistry Meeting. University of Greenwich. April 1999.